COMPARATIVE ANALYSIS OF RESERVES DETERMINATION TECHNIQUES IN OVERPRESSURED GAS RESERVOIRS

A THESIS

Presented to the Graduate Faculty

Of the African University of Science and Technology

In Partial Fulfillment of the Requirements

For the Degree of

MASTER OF SCIENCE IN PETROLEUM ENGINEERING

By

Akinyede Esther Olubunmi

Abuja, Nigeria

December 2010

COMPARATIVE ANALYSIS OF RESERVES DETERMINATION TECHNIQUES IN OVERPRESSURED GAS RESERVOIRS

By

Akinyede Esther Olubunmi

RECOMMENDED:

_____

Chair, Professor Djebbar Tiab

_____

Dr. Alpheus Igbokoyi

_____

Dr. Samuel Osisanya

APPROVED: _____

Chief Academic Officer

_____

Date

ACKNOWLEDGEMENTS

To my Creator, the giver of life and the lover of my soul, I am extremely grateful for the power YOU have given me to successfully complete another phase of life.

To my mentor and father, Dr D.K. Olukoya, thank you for teaching me those principles that have helped me achieve all that I have today.

To my supervisors, Dr. D. Tiab and Dr. A. Igbokoyi, your support and assistance is highly appreciated. Thank you for not leaving me in the dark.

To my parents, especially my Mom, thank you for always being there for me. To my siblings, I appreciate and love you.

To my friends, Bimpe, Ene, Ronke Aderibigbe, Jide, Seun,Titus, Azeb, Dorcas, Kehinde, Tunde, Parker, Nii and to mention a few, you guys are too much. I cherish and appreciate you all.

To my love, thank you for being so nice and for always understanding.

To my faculty and teachers in AUST, Dr S. Osisanya, Dr D. Ogbe, Dr W. Iledare, Dr Debamista Misra (alias Alhaji Debu), Dr G. Chukwu, Dr O. Lafe, Dr M.Prado and Prof. Z. Bassiouni, thank you all for imparting knowledge and for believing in me and bringing out the best in me throughout my stay in AUST.

To the Management of AUST, thank you for giving me this rare opportunity to get a sound education in a graduate school right on African soil.

ABSTRACT

Conventional methods used in determining initial gas-in-place and reserves for a dry gas reservoir entails the use of P/z vs cumulative production data. In a normally pressured gas reservoir, the only important production mechanism is the compressibility of the gas. Many reservoir engineering calculations take advantage of this fact to simplify analysis. However, in deep geopressured gas reservoirs, the compressibility of the gas is much smaller and does not totally dominate production performance. Using simplified approaches may lead to serious errors in these cases. In geopressured systems, the compressibility of the rock and water may be just as large as the gas. Excluding these sources of energy from performance calculations would result in very pessimistic predictions of production versus pressure. Some investigators have postulated that water will be released from shales as the reservoir compacts during depletion. This would result in an internal water drive similar to aquifer influx. Because the reservoir rock is usually highly compressible and under-compacted, the decrease in pore volume during depletion may be very non-linear. Along with the rock compressibility, the absolute permeability may also decrease with declining pressure.

Several material balance models have been proposed to calculate the initial gas-in-place for abnormally-pressured gas reservoir. The present study is concerned with analyzing the different material balance models used to estimate IGIP for abnormally pressured reservoirs, review the bases and assumptions on which these models have been developed, as well as discuss the strength and weakness of every model. In addition, the study comprises comparative analysis of calculations of the IGIP by these material balance models for some reservoir case studies in the Gulf Coast. A sensitivity analysis is also done on some of the input parameters in these material balance models to determine their effect on estimating the original gas-in-place. Moreover, the present investigation reveals that most of the material balance models analyzed in this study are sensitive to the value of the initial reservoir pressure and the early data. Unfortunately, this is the time when reliable estimate for the IGIP is vital for economic decision regarding the development of such gas reservoirs. However, accurate estimation of the IGIP plays an important role in the evaluation, analysis, prediction of future performance, and making economic decision regarding the development of gas reservoirs.

Table of Contents

List of Tables

List of Figures

CHAPTER 1 - Introduction

Gas reservoirs with abnormally-high pressures have been encountered all over the world. For these reservoirs, a straight line plot of *P/z* versus G_p for the early production data and extrapolation to zero reservoir pressure projects incorrect initial gas-in-place (IGIP). The *P/z* plot is based on the assumption that gas compressibility is the **"sole"** reservoir driving mechanism. In overpressured gas reservoirs however, grain expansion, formation water expansion and water influx from shale or small associated aquifer, in addition to gas expansion contribute significantly to gas production. In normally pressured reservoirs, the pore volume change with pressure is considered minimal, and thus the pore volume (formation) compressibility retains a very small constant value. However, in an overpressured gas reservoir, the natural compaction is incomplete, as a large portion of the overburden remains supported by high internal pore pressure. As this pressure is released, through fluid production, the pore space may reduce significantly. Thus, under overpressured conditions, c_f is relatively large and may have significant variation with pressure. This becomes important to the material-balance equation, as the pore compressibility is a significant energy term in overpressured reservoirs. In normally pressured gas reservoirs, the energy of the formation is usually negligible compared to the energy of the gas.

Overpressures are subsurface fluid pressures that are greater than the pressures expected under normal hydrostatic conditions. Overpressured reservoirs are abundant in sedimentary basins throughout the world. In the United States, abnormally-pressured gas reservoirs are concentrated in the Gulf Coast, Anardako Basin, Delaware Basin and Rocky Mountain Area. In the Middle East, overpressured gas reservoirs are found in Iraq, Iran and Saudi Arabia. These reservoirs commonly produce light oils and gases and require special evaluation techniques. Prior knowledge of the possibility of encountering overpressures at particular subsurface depths is important when exploring for oil and gas. This is because the presence of higher-than-normal pressure increases the complexity and cost of drilling, well-completions and production operations. Additionally, the effect of overpressures on reservoir behavior must be recognized when predicting performance.

Initial reservoir pressure gradients are normally 0.465 psi/ft of depth, which is the hydrostatic gradient of typical brine. In many producing areas, particularly along the Gulf Coast, reservoirs exist with pressure gradients far in excess of this normal. Gradients of almost 1.0 psi/ft of depth have been observed. Any gradient in excess of 0.465 is abnormal, but the effects of abnormal pressure on reservoir engineering calculations are often ignored unless a gradient of 0.65 psi/ft or more exists. A significant amount of gas exists in abnormally-pressured reservoirs. In the offshore Gulf Coast alone, over 300 gas reservoirs have been discovered with initial gradients in excess of 0.65 psi/ft at depths greater than 10,000 ft [Bernard (1985)].

Efficient development and operation of any hydrocarbon-bearing reservoir depends on the accuracy of the predicted performance. Reserves estimates are most critical offshore, where typical development projects require large capital investments prior to obtaining significant reservoir performance data. Hence, accurate determination of the IGIP and reserves for gas reservoirs early in their production life is necessary for predicting future production and making economic decisions regarding the development and production of such reservoirs. The industry standard method for the estimation of the IGIP for volumetric gas reservoirs, which is determined from the plot of P/z vs G_p by fitting a straight line through the early data and extrapolating to zero pressure, has the inherent assumption that gas production is exclusively due to gas expansion. Hence, the estimation of IGIP for abnormally-high pressured gas reservoirs using this method results in an overestimate. Incorrect estimate of IGIP based on early production and pressure data may result in investment that was never needed.

Analysis of geopressured gas reservoirs often times is particularly difficult. The effect of pore volume compressibility as well as the uncertain presence of water influx should usually be included in the calculation procedures. Material balance plots of P/z versus gas produced for most geopressured gas reservoirs generally exhibit a dual slope curve. Extrapolation of the early (and lesser gradient) slope will lead to an optimistic (overestimated) reserves value. Harville and Hawkins [Harville and Hawkins (1965)] felt that the initial slope was caused by the pore volume, rock crystal and water compressibility effects not being included in the pressure depletion, gas material balance equation. The effects of shale water influx, compaction or rock

failure, solution gas liberated from the connate water and the aquifer were also mentioned in the literature as possible additional influences on the shape of the plot.

The main objective of this thesis is to analyze and review the Material Balance techniques for those that have been proposed by various researchers for calculating original gas-in-place and remaining recoverable reserves from pressure and production data. A comparative analysis of these techniques was carried out and a sensitivity analysis of some of the input parameters in the material balance models was performed.

Work Outline

Chapter 2 gives a full detailed literature background on geopressured gas reservoirs. Chapter 3 discusses the various Material Balance techniques which have been proposed for determination of IGIP in geopressured gas reservoirs. Chapter 4 entails a comparative analysis of the various MB techniques discussed in chapter three, using four geopressured gas reservoirs found in the Gulf Coast as case studies. Chapter 4 also includes a sensitivity analysis of some input parameters in some of the material balance models discussed. Chapter 5 gives the summary of the results and Chapter 6 entails the conclusions and recommendations.

CHAPTER 2 - Literature Background

Overpressured reservoirs are abundant in sedimentary basins throughout the world. These reservoirs commonly produce light oils and gases and require special evaluation techniques. Many of these reservoirs are fully bounded in thick sections of shale; consequently, pressure depletion conditions should exist. In actuality, a study of the production histories of overpressured gas reservoirs indicate that water influx of varying degrees of effectiveness is a fairly common occurrence. Efficient development and operation of any hydrocarbon bearing reservoir depends on the accuracy of predicted performance. Reserve estimates are most critical in offshore, where typical development projects require large capital investments prior to obtaining significant reservoir performance data. In many cases, reserves must be estimated without the benefit of historical production trends. A number of methods are used in the industry to detect and evaluate overpressured formations. The best approach is the study of a combination of several measured parameters or "geopressured indicators".

2.1 An Overview of Overpressured Gas Reservoirs

Overpressures are subsurface fluid pressures that are greater than pressures normally expected under normal hydrostatic conditions. Prior knowledge of the possibility of encountering overpressures at particular subsurface depths is more important when exploring for oil and gas. The presence of higher than normal pressures increases the complexity and cost of drilling, well completion and production operations. Also, the effect of overpressures on reservoir behavior must be recognized when predicting performance. According to Walter and Donald (1971), geopressures are an important factor in several aspects of reservoir engineering. This includes consideration of compressibility and failure of the reservoir rock and the possibility of water influx from the overlying and underlying shale formations.

Gas reservoirs, in general, have five sources of reservoir energy: gas expansion, connate water expansion, sand grain expansion, rock compaction, and connate water solution gas liberation.

Many gas reservoirs are bounded by water-bearing rocks or aquifers. Associated aquifers contribute additional pressure support to the overall drive mechanism from aquifer water expansion, aquifer pore volume compressibility, and solution gas liberation from the aquifer water. Water influx from the shales bounding a gas reservoir and "associated aquifer" add a final source to overall reservoir energy. The relative magnitude of each of these energy sources varies with reservoir rock and fluid properties, with shale permeability, and with the ratio of initial aquifer volume to initial gas reservoir volume.

2.1.1 Geologic Occurrence & Origins of Geopressured Reservoirs

Abnormally high-pressure or geopressured reservoirs are becoming more common as exploration into deeper horizons increases. Understanding what circumstances influence their formation will give insight into predicting where they occur and how they will respond to production. The ability to detect and recognize overpressured formation is critical in conducting efficient and safe drilling operations. Observed changes in the properties of rocks, especially shale, can be used to evaluate the overpressured zones. Variations of rock properties can be detected by geophysical methods, wire-line logging techniques, surface measurements on the drilling mud and shale cuttings, and monitoring of several drilling parameters.

The best approach for the detection and evaluation of overpressured formations is the study of a combination of several measured parameters since relying on one type of data can result in misinterpretations.

In the worldwide search for oil and gas, abnormally high-pressure zones (geopressured) have been encountered in numerous countries on several continents. In our present discussion, such geopressured or abnormally high subsurface pressures are defined as any pressure which exceeds the hydrostatic pressure of a column of water containing approximately 80,000ppm total solids. The term "geopressured" is defined by Dickinson (1953) as "any pressure which exceeds the hydrostatic pressure gradient of a column of salt water". The hydrostatic pressure

gradient of salt water is 0.465 psi/ft. Geo-pressured reservoirs can now be defined as any reservoir for which the subsurface fluid pressure gradient is between 0.465 and 1 psi/ft.

According to Dickinson, fluid pressures within sediments are “dominated by two factors, the compression due to compaction on one hand, and the resistance to expulsion on the other”. The weight of overburden increases with depth of burial causing sands and shales to compact and lose porosity. Water, oil, and gas are forced out of the sands and shales as this compaction occurs. If flow passages are available, the fluids migrate towards the surface. “When sand in a sand-shale sequence exceeds 50% and sand is displaced opposite sand at faults, few geopressured reservoirs are encountered. As the relative amount of shale increases, flow channels available for fluid migration decrease. Geopressured reservoirs occur when fluids are unable to migrate. They are usually of limited areal extent and most are faulted or shaled out without development of a significant associated aquifer. The impedance of fluid flow also reduces the rate of heat flow which can cause geopressured reservoirs to become overheated.

2.1.2 Effects of Overpressures on Reservoir- Rock properties

Reservoir sandstones located in overpressured sections commonly shows increased porosity when compared with normal-pressured sections of similar rock character. Increased porosity is accompanied by changes in other reservoir properties, such as increased permeability and oil and gas volumes and decreased capillary displacement pressures. The increased porosity is largely the result of the dissolution effect of flow of formation waters over geologic time. Overpressuring of any section means that the potential for flow and the release of overpressure can take place by flow through sandstones and/or along fractures or faults. Primary porosity is a product of the deposition environment as well as of the normal compaction process and generally decreases with depth as a continuous function. The increased porosity at greater depth caused by dissolution is known as secondary porosity. Many overpressured sandstone sections contain secondary porosity. The increased pore volume is greater than would be expected if normal compaction and cementation processes had taken place. The secondary porosity can be the result of the dissolution of either grains or cements.

As average reservoir pressure declines with production, a decrease in porosity and permeability will occur. A significant reduction in permeability can substantially reduce well productivity. Declining reservoir pore pressure increases the amount of overburden supported by the reservoir rock causing the rock to compact and permanently deform. If the net pressure (weight of overburden minus pore pressure) on the formation rock is high enough, the rock grains will crush causing the pore structure to collapse. This explains high abandonment pressures common to geopressured systems. Hammerlindl[1] states that "abandonment pressures ranging from 1500 psi to 5000 psi can be expected", suggesting sands quality as the dominant factor. Although sand quality has a major influence, total pressure drop in the system is probably the controlling factor which determines abandonment pressure.

Formation Compressibility: also known as pore volume compressibility is defined as the fractional change of a unit pore volume related to a change in pressure. Formation compressibility is a combination of elastic rock-material expansion and inelastic compression and compaction of the porous medium.

$$c_f = -\frac{1}{V_p}\frac{\Delta V_p}{\Delta p} = \frac{1}{\varphi_i}\left(\frac{\varphi_i - \varphi_2}{p_i - p_2}\right) = \left(1 - \frac{\varphi_2}{\varphi_i}\right)\frac{1}{\Delta p} \qquad (2.1)$$

The normal compacting process is incomplete in overpressured reservoirs because a higher than normal portion of the overburden remains supported by fluid pressure. Production of reservoir fluids transfers some of the supporting stress to the under-indurate rock matrix. Compression occurs as micro fractures are formed when the increased stress exceeds the fracturing pressure of the rock matrix. Bulk- and pore- compressibility values are assumed to be the same for most practical petroleum engineering studies, and can be defined in similar manner as pore- compressibility. It can be easily shown that the three compressibilities are related as follows:

$$c_B = (1 - \emptyset)c_g + \emptyset c_P \qquad (2.2)$$

The general compressibility equation relates the change in a unit volume of material to a change in confining pressure when the system is assumed to remain at a constant temperature. Loss of pore pressure because of production from oil or gas reservoir causes the rock to compress in an elastic or inelastic manner. Viscous or elastic deformation implies that the compressed material will return to its original volume when the pressure differential is relieved. The inability of a rock sample to return to its original volume after compression/ decompression cycle is called a *hysteresis effect*. The deformation of a reservoir rock may be defined as changes in the rock, bulk or pore volume compressibility.

Figure 2.1 is an example of a P/z plot for an abnormally pressured reservoir.

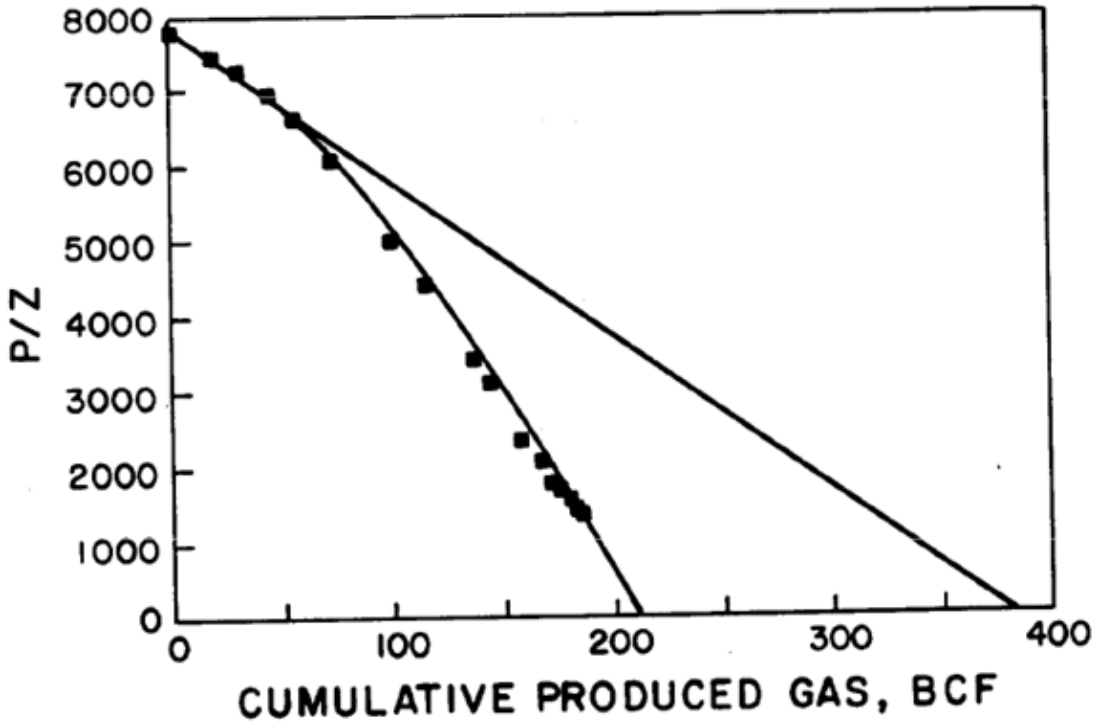

Figure 2.1 P/z plot showing severe deviation from a straight line

Formation compressibility in normally pressured sandstone reservoirs is from 3 to 6 micropsi while abnormally pressured reservoirs have an apparent formation compressibility up to 28 micropsi and possibly higher over the abnormally pressured section of the reservoir. The

apparent formation compressibility includes both the crystal expansion and formation compaction and will be referred to as **effective formation compressibility**.

In an overpressured reservoir, the sand grains are not supporting as great a portion of the overburden pressure as they would in a normally pressured reservoir. Therefore, the reservoir fluid is supporting some portion of the overburden pressure. When the pressure is reduced, three simultaneous reactions take place to reduce the hydrocarbon pore space: the reservoir contracts (which is compaction), the sand grains expand and the connate water expand. This reduction in gas pore volume acts as a drive mechanism, thus, reserve estimates using early life pressures indicates errors that have been shown to approach 100%. At approximately a normal gradient, the reservoir characteristics change to the same as a normally pressured reservoir where the effect of formation compressibility virtually ceases.

Rock-grain Compressibility

Rock-grain compressibility is an inelastic property and is defined as the volume change for a unit volume of solid rock material measured as a function of changing confining pressure. An average value for quartz, feldspar and rock fragments is approximately $c_{gr} = 0.16 \text{ X } 10^{-6} \text{ psi}^{-1}$. This term is usually at least $\frac{1}{20}$ of the formation-compressibility value. Therefore, the influence of rock-grain compressibility on reservoir performance is minimal and is usually of negligible interest when evaluating an overpressured reservoir.

Bulk Compressibility

Bulk compressibility is the fractional change of a total unit bulk volume of the rock related to a change in differential pressure. Bulk compressibility is equal to the pore compressibility divided by the porosity. Subsidence studies involve the application of the bulk-volume compressibility.

Effective Formation Compressibility

Loss of reservoir pressure during depletion of an overpressured gas reservoir causes connate water volume to expand and pore volume to compress. The net effect is a reduction of the

hydrocarbon pore volume. This is defined as the effective formation compressibility and is expressed as

$$c_e = \frac{c_w S_{wi} + c_f}{1 - S_{wi}} \qquad (2.3)$$

The effective formation compressibility expression is a measure of the effect of changing pressure on the hydrocarbon pore volume. This term is particularly important when studying overpressured gas reservoirs because of the high initial pressures and usual dramatic pressure loss during depletion. A good average value for water compressibility is $c_w = 3 \times 10^{-6}$ psi^{-1}. Pore volume compressibility (c_f) is usually unknown and is a difficult reservoir parameter to measure because its value is a function of rock type and internal (or pore) and external (or confining) pressure stresses. These subsurface stress and rock-character conditions must be replicated in the laboratory to obtain accurate measurement of the stress/compressibility relationship for a particular reservoir or field. All gas reservoirs possess the same gas- and effective formation compressibility/pressure relationships. However, effective-formation and gas compressibility values are of approximately the same magnitude at elevated pressures. Therefore, both terms are included in a material balance equation describing the performance for the overpressured reservoir case. On the other hand, the effective-formation compressibility term is not included in a material balance expression for the moderate- to low-pressure, depletion-drive case because the gas-expansion effect controls the performance history. [Poston and Berg, 1997]

2.1.3 Reservoir Fluid properties of interest

The molecular weight, compressibility and phase relations of each component in a natural gas often differ by a considerable degree. All gas volume calculations apply a specified temperature and pressure to define the reference volume. Reference or base conditions are promulgated by local governing bodies and vary according to geography and governmental edict.

Gas Deviation Factor, z

The gas deviation or z factor is a fundamental property defining the divergence of a gas volume between ideal and real conditions. The term accounts for the effect of molecular interactions

on temperature-pressure-volume measurements. These non-linear effects must be taken into account when converting gas production-volumes measured at the surface to reservoir conditions. From the ideal gas law which relates pressure, composition and volume,

$$pV = znRT \qquad (2.4a)$$

where the z term is used to relate the difference between a gas volume measured at real and ideal conditions.

$$z = \frac{v_{actual}}{v_{ideal}} \qquad (2.4b)$$

The difference in the two volumes is non-linear and is a function of the degree of interference between the gas molecules. All components are assumed to remain as gases over the pressure and temperature range of interest. [Poston and Berg, 1997]

Gas Compressibility

Gas compressibility is the isothermal coefficient of expansion of gas and should not be confused with 'z', the gas deviation factor. Gas compressibility is thought of as being of the order of 200 and 300 x 10^{-6}psi^{-1}, but in overpressured reservoirs below 10,000ft, the gas compressibility is generally in the range of 30 to 50 x 10^{-6}psi^{-1}. The gas compressibility number becomes smaller as pressure and gravity increase and temperature decreases. Gas compressibility is often related to formation and connate-water compressibility in studies of overpressured gas reservoirs. The ideal gas law is differentiated with respect to pressure to develop a compressibility/z-factor relationship for constant temperature conditions.

$$\frac{dV}{dp} = \frac{nRT}{p}\frac{dz}{dp} - \frac{znRT}{p^2} \qquad (2.5)$$

Inserting the general equation for compressibility and simplifying yields

$$c_g = \frac{1}{p} - \frac{1}{z}\frac{dz}{dp} \qquad (2.6)$$

Gas compressibility can be calculated with the $1/p$ portion of the equation for ideal conditions (z = 1, which can occur at low to moderate pressures), a condition seldom encountered in petroleum reservoirs. However, the z-factor and the slope of the pressure/z-factor line terms

expressed in the above equation must be included when evaluating the gas compressibility at high pressures. Pseudoreduced compressibility expresses gas compressibility in terms of pseudo-critical and pseudo-reduced pressure.

2.1.4 Effect of Formation Compressibility

As the pressure is reduced, the pore volume is reduced due to formation compressibility. Water saturation is an important factor in gas pore volume reduction. Increasing water saturation reduces the relative permeability to gas. Retrograde condensate reservoirs accumulate liquids especially around the wellbore, which decreases the relative permeability to gas.

All gas reservoir performance is related to effective compressibility and not to gas compressibility. When the pressure is abnormal and high, effective compressibility may equal two or more times that of gas compressibility. If effective compressibility is equal to twice the gas compressibility, then the first cubic feet of gas produced is due to 50 percent gas expansion, and 50 percent formation compressibility and water expansion. As the pressure is lowered in the reservoir, the contribution due to gas expansion becomes greater because gas compressibility is approaching effective compressibility.

2.2 Reservoir Mechanics - Flow Characteristics of Geopressured Gas Reservoirs

The primary influence on performance history of depletion-drive gas reservoirs is the value of the gas compressibility term. However, water influx must be included with the gas compressibility effect when combination or complete water drive reservoirs are studied. Overpressured gas reservoir performance histories may also be affected by three additional but subordinate drive mechanisms. These potential energies are effective formation compressibility (which is a function of rock-grain and connate-water expansion and formation compaction); possible influx of water from adjacent shales; and liberation of solution gas from connate and aquifer water. Theoretically, each of these energy potentials must be identified and their effects quantified to predict reservoir performance. In reality, this is a virtual impossibility, and these subordinate categories are often included as a basket of uncertain values in the effective

formation-compressibility expression. One would expect the influence of these subordinate drives to be of most interest at early times because gas compressibility is at its lowest value at initial conditions. The increased size of the gas-compressibility term at moderate to low pressures usually nullifies the influence of subordinate drive mechanisms.

Production of reservoir fluids reduces the pore pressure. The net effect of the pressure loss is a reduction in the hydrocarbon pore volume (HCPV) because of the expansion of the connate water and rock material. Water influx may come from an aquifer or from adjacent under-compacted shales. Solution gas may be liberated from the connate and aquifer water if a significant decline in reservoir pressure occurs. The gas-expansion effect is the primary drive mechanism for depletion gas reservoirs. These reservoirs can be divided into two types: (1) the over- or very-high pressure case where the gas-, formation- and connate water compressibility values are of similar magnitude at initial conditions but diverge with declining pressure and (2) the normal-pressured case where the gas effect is the predominant drive mechanism. **Figure 2.2** illustrates the effect of changing pressure on gas-, formation- and water- compressibility values for the Anderson "L" reservoir. Gas compressibility increased from *26 X 10^{-6}* to *232 X 10^{-6}* psi^{-1}, while water and formation compressibility remained essentially constant at $c_w \approx 3\ x\ 10^{-6}$ psi^{-1} and $c_f \approx 15\ x\ 10^{-6}$psi^{-1} respectively, over a 6,000-psi pressure range. The figure indicates that water and formation compressibility will probably play a major role in reservoir performance only at pressures > 8,000 psia. The large value of the gas-compressibility term essentially nullifies the potential for effective-formation compressibility term to alter performance behavior at moderate to low reservoir pressures. A material balance equation can mathematically account for all the major and minor potential energies in a single expression. [Poston and Berg, 1997]

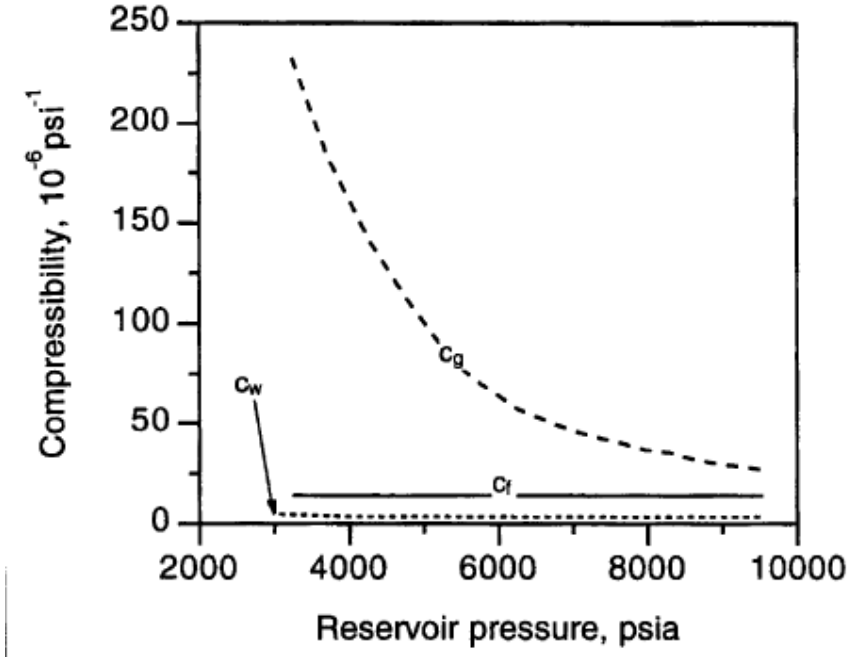

Figure 2.2 Effect of changing pressures on compressibility values

Gas Expansion: The initial gas volume is subtracted from the produced gas volume to calculate the volume of the remaining gas at the latter conditions. These volumes are evaluated at a common reservoir pressure and are related to the base conditions in units of reservoir barrels per standard cubic foot. The expansive effects of the gas remaining in the reservoir as pressure declines from $p_i \longrightarrow p$ provides an expanding effect to lessen the pressure loss caused by reservoir voidage. The remaining gas volume in terms of the ***z*** factor is

$$G_r = 0.00504(G - G_p)\frac{zT}{p} \qquad (2.7)$$

Moderate-to-Low Pressure Reservoirs

When water influx and subordinate energy terms are assumed to be absent and the initial reservoir pressure is less than 6000 psia, the following equation holds:

$$\frac{p}{z} = \frac{p_i}{z_i} - \frac{p_i}{z_i}\frac{G_p}{G} \qquad (2.8)$$

Gas compressibility is assumed to supply all the energy for producing normal-pressured depletion-type gas reservoirs. A straight line relationship results when the p/z term is plotted on the ordinate and G_p is plotted on the abscissa. The endpoint of the straight line is an estimate of the volume of gas originally in place because pressure at this point is zero. The effect of decreasing the flowing bottomhole pressure on ultimate recovery is easily visualized. The p/z plot will remain a straight line as long as the reservoir depletion drive is not affected by water influx or some other alteration of the reservoir system.

Figure 2.3 is a typical example of the concave or dual-slope nature of a p/z plot of an overpressured gas reservoir. The flat-lying slope of the early-time curve indicates that an energy source other than gas compressibility must also be influencing performance history. Rock- and water- compressibility values approach the gas compressibility value at high pressures. Therefore, these two terms must be included in a material balance equation simulating the performance of overpressured gas reservoirs, at least at early-time conditions. The standard p/z plot extrapolates to the true original gas in place (OGIP) at moderate to low pressures because gas compressibility controls performance history over this pressure range. Ramagost and Farshad (1981) showed that inclusion of the effective-formation compressibility term in the material-balance solution for the overpressured depletion-drive gas reservoir resulted in a straight line.

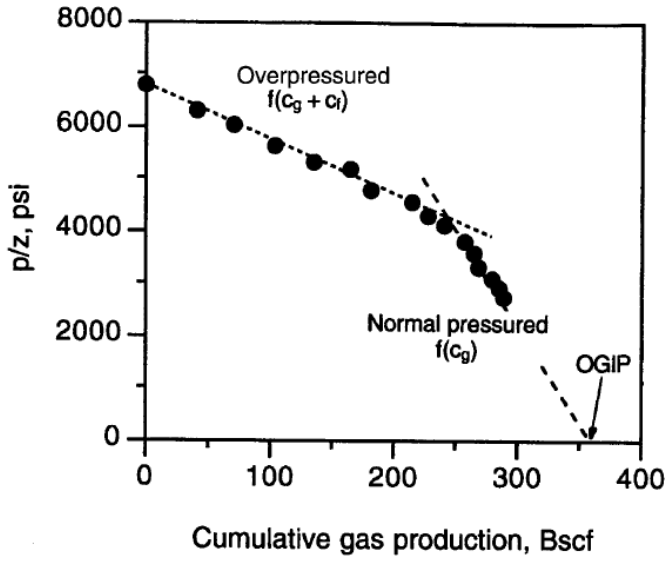

Figure 2.3 A typical dual-slope p/z plot for an overpressured gas reservoir

The work of Fetkovich et al. (1991) showed that formation compressibility can be a dual-slope function. The value can either decrease if the reservoir rock is in the compression stage or increase if the reservoir rock is in the failure stage. The reservoir-pressure range defines where a particular reservoir is operating on the compressibility curve. Unfortunately, the true stress/time relationships exerted in a reservoir can seldom be determined. The effect of the changing PV-compressibility term is most pronounced in overpressured gas reservoirs because the usual geological compaction and consolidation processed have not been completed. Therefore, average porosity is greater than and the strength of the rock matrix is less than would be found in comparable normal-pressured sections. Hammerlindl (1971) states that compaction is essentially complete when the reservoir pressure has declined to a normal gradient. PV-compressibility will become of negligible importance after this point because the value of the gas compressibility term is many times greater than the formation-compressibility value. Some past work included the effect of liberated solution gas in the reservoir water as a possible energy source when studying overpressured gas reservoirs.

2.3 Brief Overview of Normal-pressured reservoir

In a normal pressured reservoir (initial pressure gradient = 0.465 psi/ft), the majority of the overburden is supported by sand grain contacts which minimize pore volume compressibility. If there is no associated aquifer or the aquifer is small in relation to the gas pore volume, reservoir energies contributed by the aquifer become negligible. Water influx from the reservoir bounding shales can also be considered negligible. As in the reservoir rock, the majority of the overburden in the shale is supported by clay particle contacts which minimize pore volume compressibility and permeability in the shale, effectively reducing water influx to an insignificant amount. Thus, in a gas reservoir that is at or near normal pressure with a relatively small associated aquifer (as compared to the gas pore volume), gas expansion is the dominating energy source and all other factors can be considered negligible. The fractional recovery becomes the following equation which reduces to a linear relationship between P/z and G_p:

$$\frac{G_p}{G} = \frac{B_{gi} - B_{g2}}{B_{gi}} \qquad (2.9)$$

Substituting $\frac{T_{sc}P}{P_{sc}ZT}$ for B_g and rearranging yields the familiar expression:

$$\frac{P_2}{Z_2} = \frac{P_i}{Z_i} - \frac{G_p P_i}{G Z_i} \qquad (2.10)$$

This equation extrapolates to the original gas-in-place at $\frac{P_2}{z_2} = 0$ and is quite useful in predicting ultimate recovery at various abandonment pressures. As mentioned earlier, this expression accounts for gas expansion only and assumes contributions from all other energy sources are negligible. As the size of an associated aquifer increases relative to the gas pore volume, and/or the pressure gradient of the system increases, contributions from energy sources other than gas expansion also increase. [Poston and Berg, 1997]

2.4 Reserves determination in Overpressured gas reservoirs

The determination of gas reserves is a fundamental calculation in reservoir engineering. This information is crucial for the development of a production strategy, design of facilities, contracts and valuation of the reserves. Classically, reserves are estimated in three ways: volumetric, material balance and production decline (1987). The volumetric and material balance methods estimate original gas-in-place whereas production decline yields an estimate of recoverable gas. Volumetrically determined reserves can be very imprecise, because the method depends upon detailed knowledge of many reservoir characteristics that are often unknown such as the areal extent of the pool. The material balance method uses actual reservoir performance data and therefore is generally accepted as the most accurate procedure for estimating the original gas-in-place. Once determined, the original gas-in-place can be used to reliably forecast the recoverable raw gas reserves under various operating scenarios. The production decline method also uses reservoir performance data but the result is an estimate of recoverable raw gas reserves under the existing operating conditions. A change in these operations, for example, a lowering of the compressor suction pressure, can change the deliverability and the recoverable raw gas reserves. The original gas-in-place is therefore difficult to ascertain from production decline.

Overpressured gas reservoirs experiencing depletion drive typically have concave downward p/z vs Cumulative gas production plots; incorrect extrapolation of early depletion data may

result in serious overestimation of OGIP and remaining recoverable reserves. Direct and iterative-type models have been developed to study overpressured gas reservoirs. The direct-input model requires some prior knowledge of formation-rock and –fluid properties. The calculations are usually compared with the properties of a straight line to determine the quality of the answer. Iterative models generally determine a single variable that describes the depletion style of the reservoir. The value of this all-inclusive term is calculated by assuming various original-gas-in-place (OGIP) values and determining which value is the best fit to a line corresponding to a predetermined set of conditions.

2.4.1 Direct-Input Models

Hammerlindl (1971) theorizes that, for an overpressured reservoir, the sand grains are not supporting as great a portion of the overburden pressure as they would normally do in a normal-pressured reservoir. Therefore, the reservoir fluid is supporting a portion of the overburden pressure. The contraction of the reservoir, in conjunction with sand grain and connate water expansion, therefore acts as a reservoir driving mechanism. Hammerlindl developed techniques for the determination of gas reserves in an overpressured gas reservoir, based on material balance, using formation/fluid compressibilities and fluid saturations. The techniques assume a previous knowledge of formation compressibility, and formation compressibility is assumed to be constant, i.e. not a function of reservoir pressure. Hammerlindl[1] developed two methods for comparing the compressibility effects for an overpressured, depletion-drive reservoir with those for a normal pressure situation. The coefficient calculated by either method provides a factor for relating the apparent OGIP determined from the incorrect, early-time extrapolation of the *p/z* curve to the true value.

The first method, which he referred to as p/z corrections, uses the apparent OGIP as determined from the early-time portion of the p/z vs cumulative production plot. The apparent OGIP is corrected to the actual OGIP by dividing it by an average effective compressibility to gas compressibility ratio (c_e/c_g). The second, which is referred to as the material balance solution, uses an equation which solves for the ratio of actual OGIP to apparent OGIP. Accuracy of both methods hinges on the knowledge or determination of formation compressibility, which is

assumed to be constant for the life of the reservoir. Hammerlindl concluded that reserve estimates using early-life p/z cumulative gas production should be adjusted to allow for pore volume change and water expansion in overpressured gas reservoir.

The concave downward shape of material balance plots of P/z vs Gp was first reported in literature by Harville and Hawkins (1969). The authors analyzed the behavior of an abnormally pressured reservoir in the North Ossun Field of South Louisiana. In order to match the reservoir performance, they utilize a high rock compressibility value of 28 x 10^{-6} psi^{-1} when the pressure was above the hydrostatic gradient and a reduced, more normal value of about 6 x 10^{-6} psi^{-1} when the reservoir pressure fell below the hydrostatic gradient. Harville and Hawkins attributed the downward curvature to formation compaction and pore collapse.

Duggan (1971) presented a detailed study of the Anderson "L" reservoir. This reservoir is perhaps the best recognized example of an abnormally pressured gas reservoir with concave downward p/z vs. G_p behavior. Duggan concluded that the p/z vs. G_p curve is caused mainly by water extruded from the under-compacted shales that surround or are interbedded with the reservoir.

Ramagost and Farshad (1981) rewrote the material balance equation to include the effect of formation and connate-water compressibility for an overpressured depletion-drive reservoir. They included the pore volume and water compressibility effects in a material balance equation using a constant c_e defined by $c_e = {(c_w S_{wi} + c_f)}/{S_{gi}}$. The procedure takes into account all the expected compressibility effects and was applied to three case histories. This method involves an extrapolation of a straight line obtained on a graph of $p/z(1 - c_e \Delta p)$ vs G_p to estimate initial gas-in-place. The authors do not state the source(s) of the pore compressibility values used in their examples. Formation and water compressibility were assumed to remain constant. Most rock mechanics papers indicate this is not correct.

Wang and Teasdale (1987) coupled a material balance model for an overpressured gas reservoir with a water-influx model to study pressure-depleting and water drive reservoirs. They developed a computer program (GASWAT-PC) to calculate OGIP from production history for reservoirs with or without water influx. They reported accurate results when applied to the

Anderson “L” sand. Although this concept is useful, the program is not available, it must be installed in a personal computer and the operator must have knowledge of its operation.

Begland and Whitehead (1989) used a pressure-depletion, material-balance model to study the pressure-dependent effects of formation compressibility and water solution gas compressibility on the calculated OGIP. They applied the material balance equation incrementally over 100 psia drops in reservoir pressure to match production history and to infer initial gas in place. They concluded that OGIP could be overestimated by 25% if these effects were not taken into account.

The most readily usable procedure for evaluating geopressured gas reservoirs is the method first described by Roach. Roach (1981) initially developed the most practical method for studying overpressured, pressure-depleting gas reservoirs. The material-balance equation was rearranged in the form of an equation of a straight line. The input variables are production/pressure/gas-deviation-factor relationships while the outcome variables are OGIP and a single-valued expression for the formation compressibility. The utility of the method was not appreciated until Poston et al.(1994) showed that the curvature of the data plot reflects the type, strength and time frame over which transient, steady-state, and water-influx conditions occurred. Given enough p/z vs Cumulative production data, the Roach method may be used to calculate average formation compressibility during production, which is projected to be constant for the remaining life of the reservoir. Poston and Chen used the method to analyze two published case histories. They also showed the utility of a “solution plot” technique to quantify water influx effects and gas in place.

2.4.2 Iterative or Curve-fitting Models

Bernard (1985) presented a model based on a least-squares approximation for estimating a coefficient accounting for the effects of rock and water compressibility. He defined the parameter ‘C’ as a “catch-all” approximation accounting for water and rock compressibility effects. Bernard’s paper includes a plot to estimate “pseudo” rock compressibility values. Analysis of 13 overpressured gas reservoirs in Louisiana indicated that the true OGIP could be overestimated by 70% when a straight line extrapolation of the early-

time data was used. He felt all these so-called pressure-depleting reservoirs experienced either shale-water or minor aquifer-water influx. He concluded that it is virtually impossible to quantify 'C' in terms of reservoir properties.

Prasad and Rogers (1987) presented reservoir simulation studies of real and hypothetical gas reservoirs. The authors used linear compressibilities for the rock, porosity and water in the reservoir. Their model was able to include the effects of water and solution gas in the water. They concluded that not all abnormally pressured gas reservoirs exhibit downwards curving p/z vs G_p plots. No method to estimate gas in place during the initial stages of production was presented.

Ambastha (1990) applied a type-curve matching approach to determine reserves in overpressured, depletion-drive gas reservoirs. The procedure is based on a form of the material balance equation, containing a p^2/z term to correct for the non linearity of a p/z vs Cumulative Gas Production plot in an overpressured gas reservoir. His method is analogous to the dimensionless type curve approach used in well testing practices. He applied this method to the Cajun reservoir and showed that obtaining unique estimates of effective compressibility and gas-in-place was not possible using early production data.

Fetkovich et al. (1991) modified the material balance equation to calculate the variable-effective formation-compressibility vs pressure curve for various assumed values of OGIP. An alternative apparent-formation compressibility vs pressure term (c_e vs p) is also calculated for various aquifer sizes. Similarity of the two curves indicates an acceptable answer for OGIP and aquifer size. The form of material balance equation used by Fetkovich et al. contained a pressure-dependent cumulative effective compressibility term, c_e that is defined in terms of pore compressibility, water compressibility, gas solubility and total water associated with the gas reservoir volume. The total associated water includes connate water, water within interbedded shales and non-pay reservoir rock, and any limited aquifer volume. This cumulative effective compressibility term physically represents the cumulative change in hydrocarbon pore volume caused by compressibility effects and encroaching water. They concluded that the effects of pore collapse do not tend to bend the p/z vs G_p plot. They also concluded that pore collapse does not contribute significantly to pressure support in overpressured gas reservoirs.

The vast majority of industry does not have the time or the expertise to use the specialized iterative techniques to determine OGIP and predict future performance. Hence, the direct-input models are usually preferred as they can be easily arranged for solution with a spreadsheet program. All the previous methods require static reservoir pressure and cumulative gas production. Static reservoir pressures are obtained by shutting in the well to permit the pressure to build-up to stable conditions, or they can be estimated from transient pressure tests.

Literature Review Conclusions

Research of previous work conducted concerning reserve determination in overpressured, dry-gas volumetric reservoirs, in conjunction with pressure transient testing techniques reveals four important facts:

- Knowledge of formation compressibility is critical to reserve determination in overpressured dry-gas volumetric reservoirs.
- Though it is often assumed constant, formation compressibility is actually a function of pressure in an overpressured gas reservoir.
- A good estimate of formation compressibility will allow a good estimate of reserves for an overpressured, volumetric dry gas reservoir.
- Full development and operation of an overpressured gas reservoir depends on the predicted future performance of the reservoir

CHAPTER 3 - Material Balance Techniques for Reserves Determination in Overpressured Gas Reservoirs

3.1 P/z Plots for Abnormally-Pressured Gas Reservoirs

The classic method for analyzing depletion drive gas reservoirs is to plot the average reservoir pressure divided by the gas deviation factor (P/z) versus the cumulative gas production, G_p. If there is no appreciable influence from the water and rock compressibility, the plot is a straight line which can be extrapolated to a P/z of zero to obtain an estimate of the initial gas-in-place. The straight line can also be extrapolated to a P/z corresponding to abandonment conditions to obtain an estimate of ultimate recovery. The extrapolation of the P/z versus G_p is a commonly accepted method that is used to estimate original gas-in-place in volumetric gas reservoirs. However, abnormally-pressured reservoirs usually exhibit initial pressure gradients in excess of 0.65psi/ft at depths greater than 10,000ft. As a result, in addition to gas expansion, gas is produced by sand grain expansion, rock compaction and water expansion. As formation compressibility approaches gas compressibility, the standard P/z curve tends to bend downwards, making “straight line extrapolation” questionable.

If the reservoir is under the influence of a fairly strong water drive, the P/z plot may be straight during the early life, but a non-linear flattening of the plot may ultimately develop. Extrapolations are of little value. If an abnormally-pressured reservoir is undergoing depletion drive, the P/z plot will be straight during the early life, but will unusually curve downward during the later stages of depletion. Extrapolation of the early-life straight P/z line will always yield inflated estimates of initial gas-in-place and ultimate recovery. Bernard (1985) showed that most abnormally-pressured, thought-to-be depletion drive gas reservoirs in the Gulf Coast are not entirely depletion drive. Rather, they are subject to water influx from shales or small aquifers. This water influx causes the P/z plots to deviate from a straight line, therefore standard P/z analysis will almost always result in error.

3.2 Reasons for the Non-Linear P/z Behavior

A typical P/z vs G_p plot for an abnormally-pressured gas reservoir will exhibit two distinct straight lines – the first straight line corresponds to the "apparent" gas reservoir behavior (i.e. the abnormal pressure behavior) and the second straight line corresponds to the "normal pressure" behavior. The first slope is less than the second and occurs in the abnormally pressured region of the P/z curve. Several investigators have suggested reasons for the non-linear behavior of the P/z plot for the abnormally-pressured reservoirs. Two major independent theories have been proposed to explain the non-linear behavior of P/z versus G_p plot for abnormally-pressured gas reservoir systems.

(1) **Rock Collapse theory**: Harville and Hawkins (1969) attributed the non-linear P/z versus G_p behavior to "pore collapse" and formation compaction. They recommended that rock and water compressibilities should be included in the material balance calculations in order to account for these effects. A study of an abnormally-pressured reservoir in the N. Ossun Field of South Louisiana reveals that as reservoir pressure is depleted, the increase in net overburden pressure initially causes rock failure, and as failure continues with decreasing pore pressure, rock compressibility decreases until eventually it reaches a "normal" value. Due to lower rock and higher gas compressibilities at lower reservoir pressures, the reservoir performance becomes similar to that for a constant volume (i.e., normally pressured) gas reservoir system. This yields the second apparent straight line trend – extrapolation of the second P/z trend (i.e., the "normal pressure" trend) will be shown to yield accurate estimates of IGIP. Hammerlindl (1971) presented a simple method to correct the erroneous extrapolation of early-life P/z plot, the correction was also based on the "rock collapse" theory. He also presented a correlation for estimating the value of rock compressibility to use in the correction but the correlation was based on only three calculated points.

(2) **Shale Water Influx Theory**: Bourgoyne (1990) demonstrated that reasonable estimates of shale permeability and compressibility, taken as functions of pressure, can serve as significant mechanism for water influx into the reservoir—and these variables can be

used to match the “abnormal pressure” behavior of the gas reservoir. The second straight line develops because of a decrease in pressure support from the surrounding shales as the gas reservoir is depleted. Bourgoyne derived a gas material balance that utilizes a constant effective compressibility term to account for the effect of water influx from shale (and/or a small steady-state aquifer). He suggested that shales are capable of supplying sufficient water to at least partially account for the curvature of P/z plots.

3.3 Material Balance Calculations –Basic Concepts

Material Balance calculations can be used to calculate original gas-in-place and reserves for overpressured gas reservoirs. Data is always required for fluid and rock properties, pressure and production data are needed for OGIP calculations, and knowledge of all active production mechanisms is essential for reserves predictions. Several investigators have applied corrections to the traditional P/z versus G_p analysis for gas reservoirs to correct it for non-traditional production mechanisms. They are crucial for calculating reserves but during production tests they would not have much time to act and alter OGIP calculations.

The primary influence on performance history of depletion-drive gas reservoirs is the value of the gas-compressibility term. However, water influx must be included with the gas-compressibility effect when combination or complete water-drive reservoirs are studied. Overpressured gas reservoir performance histories also may be affected by **three additional but subordinate drive mechanisms**, which are

(a) effective formation compressibility --which is a function of connate water expansion and rock-grain formation compaction,

(b) possible influx of water from adjacent shale, and

(c) liberation of solution gas from connate and aquifer water.

Theoretically, each of these energy potentials must be identified and their effects quantified to predict reservoir performance. However in reality, this is a virtual impossibility hence these subordinate categories are often included as a basket of uncertain values in the effective-formation-compressibility expression. [Poston and Berg, 1997]

3.3.1 General Material Balance Equation

The changes in rock and water compressibility are significant sources of reservoir energy at early production performance for an abnormally pressured volumetric gas reservoir. Hence, the material balance analysis for abnormally-pressured gas reservoir is complicated because of water and rock compressibility effects in addition to gas compressibility effects.

The general material balance equation for a gas reservoir is:

$$G\left(B_g - B_{gi}\right) + GB_{gi}\left[\frac{c_w S_{wi} + c_f}{1 - S_{wi}}\right]\Delta p + W_e = G_p B_g + B_w W_p \qquad (3.1)$$

For most gas reservoirs, c_g is far greater than c_f and c_w, hence c_f and c_w terms are neglected. However, for abnormally high pressured reservoirs, these terms cannot be neglected. Equation (3.1) can be written in another form, considering a volumetric overpressured gas reservoir when the effects of water influx are excluded as:

$$GB_{gi} = \left(G - G_p\right)B_g + \Delta V_w + \Delta V_p \qquad (3.1b)$$

Where

GB_{gi} = initial gas volume

$\left(G - G_p\right)B_g$ = current gas volume after gas production

ΔV_w = change in connate water volume

ΔV_p = change in pore volume

This implies that

$$\Delta V_w + \Delta V_p = GB_{gi}\left[\frac{c_w S_{wi} + c_f}{1 - S_{wi}}\right]\Delta p \qquad (3.1c)$$

Gas Expansion

(Volume of gas remaining at later conditions) = (Initial gas volume) – (Produced gas volume)

$$G_r = \left(G - G_p\right)B_g \qquad (3.2a)$$

where $$B_g = 0.00504\frac{zT}{P} \qquad (3.2b)$$

Therefore,

$$G_r = 0.00504\left(G - G_p\right)\frac{zT}{P} \qquad (3.2c)$$

Net Water Influx

Net water influx = (volume of water that has encroached) – (volume of produced water)

$$W_{en} = (W_e - W_p)B_w \quad (3.3)$$

The effect of shale-water influx encroachment is generally not included even though the effects of the two are virtually indistinguishable.

Effective Formation Compressibility: An equation reflecting the changes in HCPV caused by declining reservoir pressure is developed by combining the general expression for compressibility with definitions for connate water and pore volumes (PVs)

$$\Delta V_w = -c_w V_{wi} \Delta p = 0.00504 c_w (p_i - p) \left(\frac{GS_{wi}}{1-S_{wi}}\right)\left(\frac{Tz_i}{p_i}\right) \quad (3.4)$$

The decrease in PV caused by the incremental pressure decline is equated in the same manner

$$\Delta V_p = -c_f V_p \Delta p = 0.00504 c_f (p_i - p) \left(\frac{G}{1-S_{wi}}\right)\left(\frac{Tz_i}{p_i}\right) \quad (3.5)$$

The total loss in HCPV caused by the increased connate-water volume and decreased PV is

$$\Delta V_w + \Delta V_p = 0.00504 \frac{G(p_i-p)}{1-S_{wi}}\left(c_w S_{wi} + c_f\right)\left(\frac{Tz_i}{p_i}\right) \quad (3.6)$$

Pressure- and Time-Dependent Potential Function

The basket of pressure- and time-dependent shale-water influx, $W_{e(sh)}$; connate-water solution-gas/oil ratio, $R_{s(cw)}$; and aquifer-water solution-gas/-oil ratio, $R_{s(aq)}$ subordinate energy terms are included in the pressure- and time-dependent basket of terms, the f(p,t) expression. These terms are extremely difficult to quantify and are often included in the effective-formation compressibility expression simply because of their vagueness and uncertain effects on reservoir performance history for most case history studies.

Summing and rearranging the four major energy categories gives

$$\frac{p}{z}\left[1-\frac{198.4(W_e-W_p)B_w p_i}{(p_i-p)Gz_iT}-\left(\frac{c_w S_{wi}+c_f}{1-S_{wi}}\right)(p_i-p)-f(p,t)\right]=\frac{p_i}{z_i}-\frac{p_i G_p}{z_i G}$$

(3.7)

Application of the following reservoir energy definitions shortens the above equation to a more readable expression. Net water influx is

$$W_{en}=\frac{198.4(W_e-W_p)B_w p_i}{(p_i-p)Gz_iT} \quad (3.8)$$

and effective formation compressibility is

$$c_e=\frac{c_w S_{wi}+c_f}{1-S_{wi}} \quad (3.9)$$

And the pressure-time dependent potential function is

$$f(p,t)=f[W_{e(sh)}+R_{s(cw)}+R_{s(aq)}] \quad (3.10)$$

Hence equation (3.7) can be expressed as

$$\frac{p}{z}[1-W_{en}-c_e(p_i-p)-f(p,t)]=\frac{p_i}{z_i}-\frac{p_i G_p}{z_i G} \quad (3.11)$$

The f(p,t) term is included for completeness. However, it is usually ignored because of the general uncertainties of quantifying these usually minor energy effects. Some combination of these components listed in the material balance equation influences the performance history of all gas reservoirs. [Poston and Berg, 1997]

3.4 Volumetric Geopressured Gas Reservoirs

In overpressured gas reservoirs, c_g, c_f and c_w values are of similar magnitude at initial conditions but diverge with declining pressure. Gas compressibility is assumed to supply all the energy for producing normal-pressured depletion-type gas reservoirs. For a volumetric abnormally-pressured gas reservoir, a P/z vs G_p graph shows two straight lines of distinctly different slopes. The flat-lying slope of the early-time curve indicates that an energy source other than gas compressibility must also be influencing performance history. The material balance equation

for a volumetric geopressured gas reservoir when the effects of water influx are excluded is given by

$$\frac{p}{z}[1 - c_e(p_i - p)] = \frac{p_i}{z_i} - \frac{p_i G_p}{z_i G} \quad (3.12)$$

The next section discusses and evaluates several material balance analysis methods proposed for abnormally pressured gas reservoirs to obtain reasonably accurate estimates of IGIP.

3.5 REVIEW AND DISCUSSION OF THE MATERIAL BALANCE SOLUTIONS

The present study is concerned with analyzing the different material balance models used to estimate IGIP for abnormally pressured reservoirs, review the bases and assumptions on which these models have been developed, as well as discuss the strength and weakness of every model. In addition, the study comprises calculations of the IGIP by analytical and numerical models of the material balance equations for some case histories. The study shows that solution plot of Havlena and Odeh can be used to estimate the IGIP for abnormal pressure gas reservoirs without prior knowledge of the aquifer size or formation compressibility. Moreover, the present investigation reveals that most of the material balance models analyzed in this study are sensitive to the value of the initial reservoir pressure and the early data. Unfortunately, this is the time when reliable estimate for the IGIP is vital for economic decision regarding the development of such gas reservoirs. [Elsharkawy, 1995]

3.5.1 ANALYTICAL METHODS

These are the models proposed by Hammerlindl, Havlena and Odeh, Ramagost and Farshad, Roach, Bernard, Fetkovich et al, and Ambashtha.

Hammerlindl's method

Hammerlindl proposed that the apparent gas-in-place, from P/z versus G_p plot of early data, be corrected to the effect of rock and water expansion. He proposed two methods to achieve this.

Method I – Average System Compressibility Method

This method estimates the apparent gas-in-place using the conventional P/z extrapolation of early reservoir performance and then "corrects" this estimate using an average value of the ratio of effective compressibility to the gas compressibility $(c_e/c_g)_{avg}$

$$Actual\ GIP, G = \frac{apparent\ GIP, G_a}{F_c} \quad (3.13)$$

$$F_c = \frac{\bar{c}_e}{\bar{c}_g} = \frac{\left[\frac{c_{ei}}{c_{gi}} + \frac{c_{en}}{c_{gn}}\right]}{2} \quad (3.14)$$

$$\text{And } c_e = \frac{c_{gi}S_{gi} + c_w S_{wi} + c_f}{1 - S_{wi}} \quad (3.15)$$

Where G_a= OGIP estimated from extrapolating the early-time P/z data

The subscripts i and n attached to the compressibility terms indicate initial overpressured conditions (early straight line) and normal-pressured conditions (2nd straight line) respectively.

F_c = correction factor (always $F_c \geq 1$), used to correct the overestimated OGIP obtained from early-time P/z plot.

Method II—Change in Reservoir Volume Method

This method utilizes a correction factor (G_{pr}) derived from the material balance equation for a normally pressured gas reservoir divided by the material balance relation for an abnormally pressured gas reservoir.

$$Actual\ GIP = Apparent\ GIP\ X\ G_{pr} \quad (3.16)$$

$$G = G_a G_{pr} \quad (3.17)$$

$$G_{pr} = \frac{B_{gi} - B_{gn}}{B_{gi} - B_{gn} + \frac{B_{gn}(P_i - P_n)(c_f + c_w S_{wi})}{1 - S_{wi}}} \quad (3.18)$$

Where B_{gi} = gas formation volume factor at initial overpressured conditions, P_i (scf/cuft)

B_{gn} = gas formation volume factor at normal-pressured conditions, P_n (scf/cuft)

G_a = OGIP estimate obtained from extrapolating the early-time P/z data

G_{pr} = correction factor (always ≤ 1)

This method is limited for volumetric reservoir that has no water influx from shale or limited aquifer. It assumes that rock and water compressibility are pressure independent. Rock compressibility is estimated from Hammerlindl correlation and water compressibility is calculated from Donson and Standing correlation. Both methods require a presumed value of the constant "effective" compressibility.

Havlena and Odeh Method

Havlena and Odeh arranged the material balance equation on a straight line form for water-drive gas reservoirs. The same technique can be used for abnormally-pressured gas reservoirs. Starting with the general material balance equation that accounts for formation water and rock expansion, water influx from limited aquifer and/or shale, and exclusion of gas from formation water in addition to gas expansion

$$G\left(B_g - B_{gi}\right) + GB_{gi}c_e(P_i - P) + W_e + W_{sh} = G_pB_g - W_pB_w - W_pR_{sw}B_g \quad (3.19)$$

Assuming that the aquifer or shale can be modeled by pot aquifer,

$$W_e = \alpha(P_i - P) \quad (3.20)$$

$$W_{sh} = \beta(P_i - P) \quad (3.21)$$

If
$$E_g = B_g - B_{gi} \quad (3.22)$$

$$F = G_pB_g - W_pB_w - W_pR_{sw}B_g \quad (3.23)$$

Substituting the last four equations and dividing by E_g yields

$$\frac{F}{E_g} = G + \left(GB_{gi}c_e + \alpha + \beta\right)\frac{P_i - P}{E_g} \quad (3.24)$$

A plot of F/E_g versus $\Delta P/E_g$ results in a straight line with intercept equal G and "catch-all" slope of$(GB_{gi}c_e + \alpha + \beta)$. If the method works, it has the advantage of calculating IGIP without prior assumption of the aquifer size or the formation compressibility.

Ramagost and Farshad, Roach, Bernard, Fetkovich et al. and Ambashta Methods

The material balance equations proposed by Ramagost and Farshad, Roach, Bernard, Fetkovich et al., and Ambastha for abnormal pressured gas reservoirs can be written in one generalized form as:

$$\frac{P}{Z}[1 - X(P_i - P)] = \frac{P_i}{Z_i} - \frac{P_i}{Z_i}\frac{G_p}{G} \quad (3.25)$$

Ramagost and Farshad, and Roach defined X as a single term independent of pressure $\left(X = \frac{c_w S_w + c_f}{1 - S_w}\right)$ (3.26)

Ramagost and Farshad Method

Ramagost and Farshad proposed plotting of $\frac{P}{Z}[1 - X(P_i - P)]$ versus G_p to calculate the IGIP, thus a prior knowledge of X is required. The value of X can be obtained from equation (3.26). The slope of the resulting plot is $-\frac{P_i}{Z_i G}$ and the intercept is $\frac{P_i}{Z_i}$. Water compressibility, c_w is calculated from Donson and Standing correlation at initial pressure and formation compressibility, c_f from Hammerlindl correlation.

Roach's Method (Solution Plot Technique)

$$\frac{1}{\Delta p}\left[\frac{p_i z}{p z_i} - 1\right] = -X + \frac{1}{\Delta p}\left(\frac{G_p}{G}\right)\left(\frac{p_i z}{p z_i}\right) \quad (3.27)$$

Roach proposed a rearrangement of equation (3.25) which yields equation (3.27) such that the plot of

$\alpha = \frac{[(P_i/Z_i)/(P/Z)]-1}{P_i-P}$ versus $\beta = \frac{[(P_i/Z_i)/(P/Z)]G_p}{P_i-P}$ yields simultaneously a slope of 1/G and an intercept of (–X).

This graphical technique provides for the simultaneous determination of gas-in-place and a constant effective compressibility. The gas-in-place is determined from the slope while the effective compressibility is calculated from the value of the intercept (X).

Bernard's Method

Bernard defined the parameter X as a single pressure independent, "lump-up term" that includes any source of expansion other than gas expansion and hence accounts for all the effects of rock and water compressibility, a small steady-state aquifer, and/or steady-state shale water influx. He proposed solving equation (3.25) using least squares technique. For n data points, the IGIP and the lump-up compressibility factor, C are calculated from:

$$G = \frac{\sum B \sum(\frac{B}{n})-\sum(B^2)}{\sum(AB)-\sum A \sum(\frac{B}{n})} \quad (3.28)$$

$$C = \sum \frac{A}{n} + \left(\frac{1}{G}\right) \sum \frac{B}{n} \quad (3.29)$$

$$A = \frac{\frac{P}{Z}-\frac{P_i}{Z_i}}{\Delta p(P/Z)} \quad (3.30a)$$

$$B = \frac{\frac{P_i}{Z_i}G_p}{\Delta p(P/Z)} \quad (3.30b)$$

Note that $\Delta p = p_i - p$

The difference between Roach and Bernard method is the solution technique and definition of the term X, which Bernard defined as C.

Fetkovich et al. Method

Fetkovich et al defined the parameter X as a pressure dependent term that takes into account the cumulative effects of pore compressibility, water compressibility, gas solubility, and total water associated with the gas reservoir volume. He equated X to be equal to $\overline{c_e}$ and this physically represents the cumulative change in hydrocarbon pore volume caused by compressibility effects and steady-state water influx.

$$c_e(p) = \frac{S_w c_{tw} + c_f + M[c_{tw} + c_f)]}{1 - S_w} \tag{3.31}$$

$c_{tw}\ and\ c_f$ are functions of pressure. Also, M is the total associated water volume ratio in aquifer or non-pay. Using reservoir rock and fluid properties, Fetkovich et al. proposed that a family of $\overline{c_e}$ curves at various M values (ratio of aquifer to reservoir volume) can be generated independently to match against $\overline{c_e}$ values which are "backcalculated" from pressure/cumulative production data. The total compressibility of water is expressed as:

$$c_{tw} = \frac{1}{B_{twi}}\left[\frac{B_{tw} - B_{twi}}{P_i - P}\right] \tag{3.32}$$

The total formation volume factor is:

$$B_{tw} = B_w + B_g(R_{swi} - R_{sw}) \tag{3.33}$$

And the solution of gas in formation water is calculated from the equation of state or Price and Blount correlation as:

$$R_{sw} = 3.3544 - 0.002277T + 6.27x10^{-6}T^2 - 0.004042S + 0.9904 \ln P - 0.0311 \mathrm{l}(\ln P)^2 + 3.304x10^{-4}T(\ln P) \tag{3.34}$$

Fetkovich et al proposed back calculating $c_e(p)$ from the material balance equation, equation (3.35) below, for different assumed values of the IGIP and plotting $c_e(p)$ versus pressure for various values of IGIP.

$$\bar{c_e}(p) = \left[1 - \frac{(P/Z)_i}{(P/Z)}\left(1 - \frac{G_p}{G}\right)\right]^{\frac{1}{P-P_i}} \quad (3.35)$$

Using reservoir rock and water compressibility, $c_{tw}(p)$ and $c_f(p)$ as functions of pressure, another plot of $\bar{c_e}\ (p)$ versus pressure is constructed for various assumed values of M using equation (3.31). The match of $\bar{c_e}$ data and the $\bar{c_e}$ "type curves" should yield IGIP (G) and the ratio of aquifer to reservoir (M), as well as validate the $\bar{c_e}$ function. However Fetkovich et al in their paper used constant value for $c_f(p)$ from Hall correlation. Fetkovich et al. work is a significant contribution – however, the practical application is somewhat difficult due to the requirement of compressibility data functions coupled with the proposed "data matching" approach.

Ambastha's Method

Ambastha developed a type-curve matching technique to calculate IGIP for abnormal pressure gas reservoirs based on material balance equation derived by Bourgoyne et al as:

$$G_p = G - \frac{Gz_i}{P_i}[1 - c_e P_i] - \frac{Gz_i}{P_i} c_e \frac{P^2}{Z} \quad (3.36)$$

This equation can be arranged in the form of equation (3.25). In this equation, c_e is a pressure independent term that accounts for expansion of water and rock in reservoir, associated aquifer and non-pay shales as :

$$c_e = \frac{c_f(1+R) + c_w(S_{wi}+R) + c_s(1+R)f/\emptyset}{1-S_w} \quad (3.37)$$

Ambastha proposed a dimensionless form for the above equation as

$$G_{PD} = 1 - (1 - C_D)P_D - C_D \frac{z}{z_i} P^2{}_D \quad (3.38)$$

Where $G_{PD} = {}^{G_P}/_{G}$ (3.39)

$$P_D = \frac{({}^{P}/_{Z})}{({}^{P}/_{Z})_i} \quad (3.40)$$

And $C_D = C_e P_i$ (3.41)

In order to prepare the type curve, the reservoir gas gravity is used to calculate the pseudo-critical properties from Suttan correlation. The pseudo critical properties, reservoir pressure, and temperature are used to calculate Z from Dranchuk and Abou Kaseem correlation. A type curve of P_D versus G_{PD} for various values of C_D is constructed using equation (3.38). The reservoir pressure and production data are used to plot P_D vs G_{PD} assuming different values of C_D. A type curve matching yields G, the initial gas-in-place and C_D.

3.5.2 NUMERICAL METHODS

These are the models presented by Begland and Whitehead, Prasad and Rogers, and Wang and Teasadale.

Begland and Whitehead method

Begland and Whitehead (1989) proposed a reservoir depletion model for volumetric gas reservoirs based on the following equation:

$$r = \frac{G_p}{G} = \frac{B_g - B_{gi} + \frac{B_{gi} - S_{wi}}{1 - S_{wi}}\left[\frac{B_{tw}}{B_{twi}} - 1 + c_f \frac{p_i - p}{S_w}\right]}{B_g} \quad (3.42)$$

In this model formation water compressibility, gas in solution in water, and rock compressibility are pressure dependent terms. The rock compressibility is estimated from Van Goten et al correlation. The above equation is solved numerically in an incremental manner as :

$$r_n' = \frac{B_{gn} - B_{gm} + \frac{B_{gm} - S_{wm}}{1 - S_{wm}}\left[\frac{B_{twn}}{B_{twm}} - 1 + c_{fn} \frac{p_m - p_n}{S_{wm}}\right]}{B_{gn}} \quad (3.43)$$

Where m,n denote old and current pressure levels respectively.

The fractional recovery at the end of the nth step is:

$$r_n = r_m + r_n'(1 - r_m) \quad (3.44)$$

An estimate of G can be made if cumulative gas production, Gp is divided by the fractional recovery.

Prasad and Rogers Method

Prasad and Rogers (1987) proposed a general material balance model for abnormal pressure gas reservoirs that treat the reservoir and its associated aquifer together as a sealed tank. This should be generally true for geopressured reservoirs since they are initially at pressures above hydrostatic and the reservoir must be effectively sealed to maintain the pressure. This generalized model adds two correction terms to the basic P/z model. One correction term is to collect the non-ideal factors related to the reservoir volume, and the other term is to collect the non-ideal factors related to the mass balance. The generalized tank model has the form:

$$P[X\ V] = (Y\ G)(Z\ R)T \tag{3.45a}$$

$$P\left[\frac{X\ V}{Y\ Z}\right] = \left[\frac{P_i V_i}{Y_i Z_i}\right] - (RT)G_p \tag{3.45b}$$

The “X” term= correction to reservoir pore space volume (V), includes the rock or pore volume compressibility and the fluids compressibility.

The “Y” term= correction to amount of gas in reservoir (G), accounts for gas evolved from oil and formation water in the reservoir. In this model, Prasad and Rogers assumed pore compressibility to be a linear function of pressure. Since gas compressibility and solubility of gas in water are described by non-linear equations, Prasad and Rogers solved their material balance equation numerically to model the reservoir drawdown.

Wang and Teasadle Method

$$\frac{P}{Z} = \frac{P_i}{Z_i}\left[\frac{G - G_p}{G(1 - c_e(p_i - p) - Y}\right] \tag{3.46}$$

where

$$Y = \frac{P_i}{T_i Z}\frac{T_{sc}}{P_{sc}}\left(W_e - W_p B_w\right) \tag{3.47}$$

$$W_e = Ux\ S(P,t) \qquad (3.48)$$

In this equation, a pressure independent term C_e is included. Wang reported that equation (3.46) can be used in an iteration method to obtain accurate pressure match to all kinds of reservoirs. In this method, the amount of water influx required to match the reservoir pressure to the model is calculated. They used their equation to history match the reservoir pressure for Anderson "L" gas reservoir using U=0 and formation compressibility of 15 x 10^{-6} psi^{-1}. It is important to note that if Y=0 in equation (3.46), the equation reduces to the general form expressed by equation (3.25).

3.5.3 BECERRA ARTEAGA METHOD—Pressure Plot Method

Becerra-Arteaga based the pressure-plot method on the observation that a pressure vs z-factor forms a straight line at high pressures. Becerra-Arteaga developed figure 3.1 to provide a temperature/pressure correlation for estimating the onset of the linear relationship boundaries for 0.6-, 0.7-, and 0.8- gravity gases.

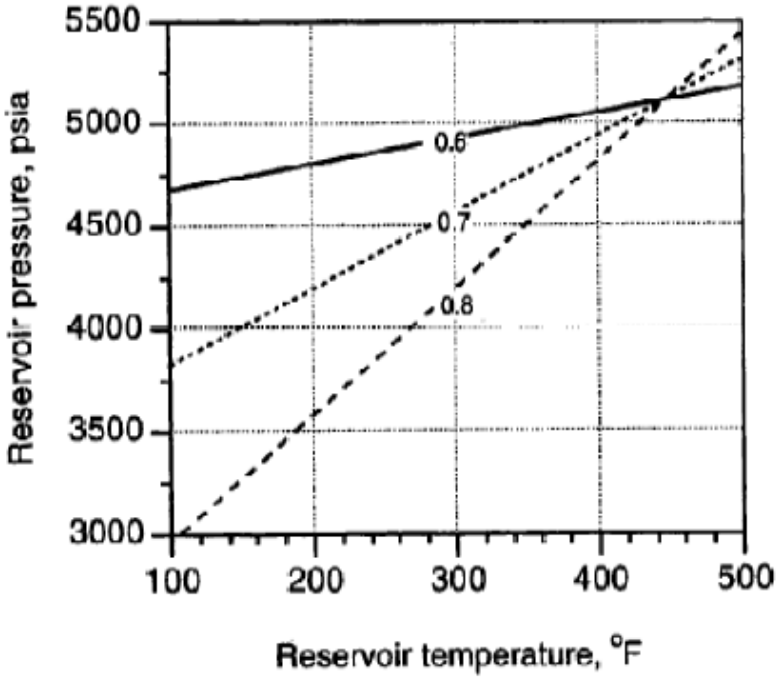

Figure 3.1: Correlation for estimating the presence of a straight line z-factor for 0.6-, 0.7- and 0.8- gravity gases

The constant-$(dz/dp)_T$- slope relationship observed at high pressure forms the basis for deriving a material balance equation for overpressured, depletion-drive gas reservoirs. The temperature- and pressure-dependent z factor is not included in the derivation; therefore, the usual $(p/z)/G_p$ straight line plot is replaced with p/G_p straight line plot. The assumptions forming the principles of the pressure-plot method are that the $(dz/dp)_T$ slope of the z-factor plot will remain constant and that water influx does not materially affect reservoir performance.

The equation describing the slope of the straight-line relation between pressure and z factor may be written as

$$z = z_i - \frac{\partial z}{\partial p}(p_i - p) \tag{3.49}$$

A relationship between the z-factor and gas compressibility c_g is:

$$c_{gi} = \frac{1}{p_i} - \frac{1}{z_i}\frac{\partial z}{\partial p} \tag{3.50}$$

Combining these two equations yields

$$z = z_i\left[p_i c_{gi} + \left(\frac{1}{p_i} - c_{gi}\right)p\right] \tag{3.51}$$

The above equation expresses the straight-line relationship for the high-pressure and straight-line portion of the Standing and Katz pressure/temperature, z-factor chart. Substituting equation (3.51) into the general material balance equation for an overpressured depletion-drive gas reservoirs results in:

$$\frac{G_p}{G} = \left[\frac{(p_i - p)(p_i c_{gi} + c_e p)}{p_i c_{gi}(p_i - p)}\right] \tag{3.52}$$

This material balance equation relates cumulative gas production to OGIP. Note that the z-factor term is not included in the equation. All previously developed gas reservoir material-balance relationships include either the gas formation-volume factor or the z factor term to account for the changing gas volume measured at reservoir conditions. The equation will be valid as long as the reservoir pressure remains in the straight-line region of the z-factor curve.

Figure (3.2) illustrates the pressure and p/z plots for an overpressured reservoir depleting to abandonment conditions. Extrapolation of the **early-time p/z data** results in an incorrect overestimate, G_o, of the OGIP, while extrapolation of the **early-time pressure data** will result in an incorrect underestimate, G_u, of the OGIP.

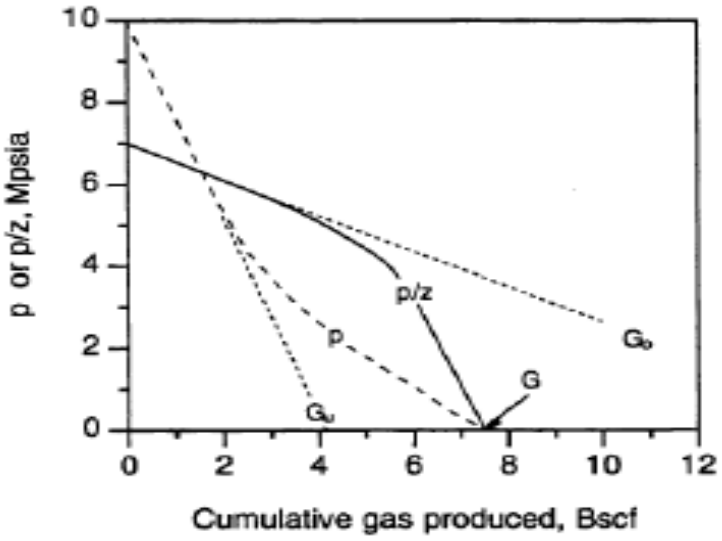

Figure 3.2: Comparison of p/z and pressure plots for an overpressured depletion drive gas reservoir

The slopes of both curves change to reflect the influence of the increasing gas-compressibility term at moderate to low pressures. Both curves ultimately converge to the true OGIP, G at atmospheric pressure.

A relationship expressing the underestimate of the early-time extrapolation of the pressure data is

$$G_u = G_p\left(1 + \frac{p}{p_i - p}\right) \tag{3.53}$$

and a relationship expressing the overestimate of the early-time extrapolation of the p/z data is

$$G_o = G_p\left[1 + \frac{\frac{p}{z}}{\left(\frac{p_i}{z_i}\right) - \left(\frac{p}{z}\right)}\right] \tag{3.54}$$

The true value of the OGIP estimated at any time must lie in the region between the G_u and G_o boundaries. Therefore,

$$G = G_p + \gamma(G_o - G_u) \tag{3.55a}$$

$$G = G_p + \gamma\left\{G_p\left[1 + \frac{\frac{p}{z}}{\left(\frac{p_i}{z_i}\right) - \left(\frac{p}{z}\right)}\right] - G_p\left(1 + \frac{p}{p_i - p}\right)\right\} \tag{3.55b}$$

where γ is the percentage of the difference between the two extrapolations.

Rearranging equation (3.51) to provide an approximation of the p/z plot for the linear portion of the z-factor curve

$$\frac{p}{z} \approx \frac{p_i}{z_i} - c_{gi}p_i(p_i - p) \tag{3.56}$$

Substituting equation (3.56) into (3.55) yields

$$\frac{p_i}{z_i}\left(1 - \frac{G_p}{G}\right) = \frac{p_i}{z_i}\left[\frac{\alpha p}{\alpha p + (p_i - p)}\right] \tag{3.57}$$

Where α = average parameter accounting for the linear variation of the z factor lying between the threshold and initial pressure boundaries. Becerra-Arteaga showed that the α term can be estimated empirically from figure (3.3), if the p_i/z_i and the p_i/D terms are known, where D= reservoir depth, ft.

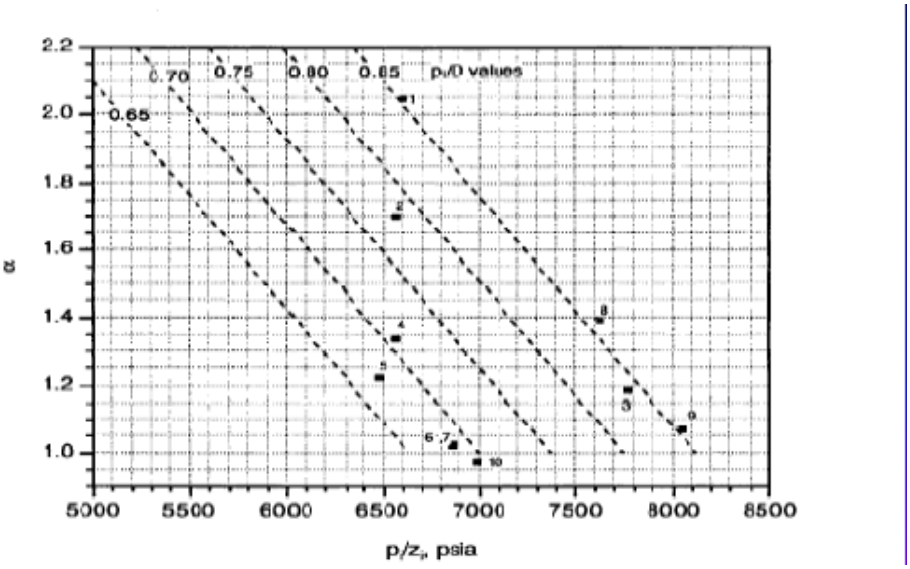

Figure 3.3: The α correlation

The table below presents the characteristics of the field case histories and references applied to generate the above figure.

TABLE 3.1: RESERVOIR DATA FOR THE α CORRELATION FIGURE

	Field or Reservoir	Reference	p_i (psia)	Depth (ft)	Gradient (psi/ft)	Gravity	z_i	α
1	Anderson L	14	9,507	11,167	0.85	0.94	1.44	2.05
2	Field 117	*	8,865	11,488	0.77	—	1.35	1.69
3	Field 33	*	12,000	14,242	0.84	0.60	1.54	1.22
4	Field 38	*,25	8,320	11,800	0.71	0.83	1.27	1.33
5	Field 41	*,25	7,784	11,650	0.67	0.83	1.20	1.24
6	Field 195	*,25	9,260	13,700	0.68	0.60	1.35	1.00
7	Field 268	*,25	9,116	13,503	0.68	0.62	1.33	1.00
8	Cajun	4	11,444	13,300	0.86	0.60	1.50	1.33
9	Rob 43-1	6	14,015	16,488	0.85	—	1.74	1.09
10	Field 70	*,25	10,144	15,000	0.68	0.64	1.45	1.77

*Personal communication with W.J. Bernhard, Louisiana State U., Baton Rouge, Louisiana (October 1987).

Rewriting equation (3.57) as an equation of a straight line yields

$$\frac{p_i}{z_i}\left(1-\frac{G_p}{G}\right)=\frac{p_i}{z_i}\left[\frac{\alpha p}{\alpha p+(p_i-p)}\right] \tag{3.58}$$

$$\frac{p_i}{z_i}\left[\frac{\alpha p}{\alpha p+(p_i-p)}\right] = -\left(\frac{p_i}{z_i G}\right) G_p + \frac{p_i}{z_i} \quad (3.58b)$$

is of the form Y = aX + b

Where X = G_p, Y = $\frac{p_i}{z_i}\left[\frac{\alpha p}{\alpha p+(p_i-p)}\right]$, a = slope = $= -\left(\frac{p_i}{z_i G}\right)$

Analysis Procedure

Step 1 – calculate the p_i/z_i and p_i/D terms from the field performance history and reservoir characteristics, where D is the total vertical depth of the reservoir.

Step 2-- Apply these correlation parameters to figure (3.3) to determine the proper α term.

Step 3 – Determine OGIP from plot, two plotting methods can be used to calculate the OGIP.

The first method involves calculating the plotting components for each data point as seen in equation (3.58b) and using the intercept on the x-axes and slope of the plot to obtain the OGIP.

The second method involves calculating G from the following equation for each data point and plotting the calculated OGIP against G_p. The best average value is selected for the OGIP estimate.

$$G = G_p\left[1 + \frac{\alpha p}{(p_i-p)}\right] \quad (3.59)$$

Elsharkawy's Method

Elsharkawy developed an easy material balance solution that incorporates all possible sources of expansion in an overpressured gas reservoir. This includes water influx from aquifer, shale water influx, formation expansion, connate water expansion and the formation of condensate. He applied his proposed solution to four case histories to estimate the IGIP, predict the production mechanism and calculate the volume of the aquifer or non-pay sands associated with the gas reservoir. The proposed material balance is of the following form:

$$G\left(B_g - B_{gi}\right) + W_e + W_s + \Delta V_w + \Delta V_p = \left(G_p + G_{LP}K_C\right)B_{\ g} + W_p B_w \quad (3.60)$$

$$G\left(B_g - B_{gi}\right) + C_a V_a (p_i - p) + C_s V_s (p_i - p) + \frac{GB_{gi}}{1 - S_w} c_w S_w (p_i - p) + \left(\frac{GB_{gi}}{1 - S_w}\right) c_f (p_i - p)$$
$$= \left(G_p + G_{LP} K_C\right) B_{\ g} + W_p B_w \qquad (3.61)$$

Collecting the pressure drop terms together and defining $c_e = c_w S_w + c_f$ results in

$$G\left(B_g - B_{gi}\right) + \{(\frac{GB_{gi}}{1-S_w})c_e + c_a V_a + c_s V_s\}(p_i - p) = \left(G_p + G_{LP} K_C\right) B_{\ g} + W_p B_w \qquad (3.62)$$

Dividing through by $\left(B_g - B_{gi}\right)$ yields

$$G + \sigma\left(\frac{p_i - p}{B_g - B_{gi}}\right) = \frac{\left(G_p + G_{LP} K_C\right) B_g + W_p B_w}{\left(B_g - B_{gi}\right)} \qquad (3.63)$$

where $\sigma = \left(\frac{GB_{gi}}{1-S_w}\right) c_e + c_a V_a + c_s V_s\Big\}$ (3.64)

$c_s V_s$ is a function of the pore volume and compressibility of the shale

c_a is the effective compressibility of the aquifer while V_a is the aquifer volume.

The above equation (3.63) can be solved graphically or using least square. However, initial scatter in the pressure-production data might affect the answer from least square. The solution plot is $Y = \frac{\left(G_p + G_{LP}\right) B_g + W_p B_w}{\left(B_g - B_{gi}\right)}$ versus $X = \left(\frac{p_i - p}{B_g - B_{gi}}\right)$ will result on a straight line with slope = σ and intercept equal to initial gas-in-place, G. Thus, the IGIP can be estimated from the intercept without prior assumptions about value of the aquifer size, shale volume, or formation compressibility. In addition, the slope can be used as an indication of the reservoir driving mechanism. The solution plot of equation above results in simultaneous estimation of the IGIP and prediction of the production mechanism. This solution technique was applied to NS2B reservoir in North Ossun field, Anderson "L" reservoir, Cajun field and Miocene reservoir.

3.6 CASE HISTORY STUDIES AND EXAMPLE CALCULATIONS

Three overpressured gas reservoirs found in the Gulf Coast will be examined and the IGIP will be calculated using the Material Balance solutions discussed above.

For the Anderson “L” Reservoir with Data below:

ANDERSON "L" RESERVOIR DATA		
Depth	11,167ft	
Porosity	24%	
Water Saturation	35%	
Dew point	6118psia	
Gas-in-Place	2240MCF/Ac-ft	
Initial BHP	9507psia	
Pressure Gradient	0.843psi/ft	
BHT	2660F	
c_w	3.4×10^{-6}	psi

The formation compressibility c_f for this reservoir is estimated from Hammerlindl correlation using figure (3.4). This yielded a value of c_f = 19.5 x 10^{-6} psi-1. Hence, effective formation compressibility is calculated thus:

$$c_e = \frac{c_w S_{wi} + c_f}{1 - S_{wi}} = \frac{(3.4\ x\ 10^{-6} x 0.35) + (19.5\ x\ 10^{-6})}{1 - 0.35} = 31.9\ x\ 10^{-6} psi^{-1}$$

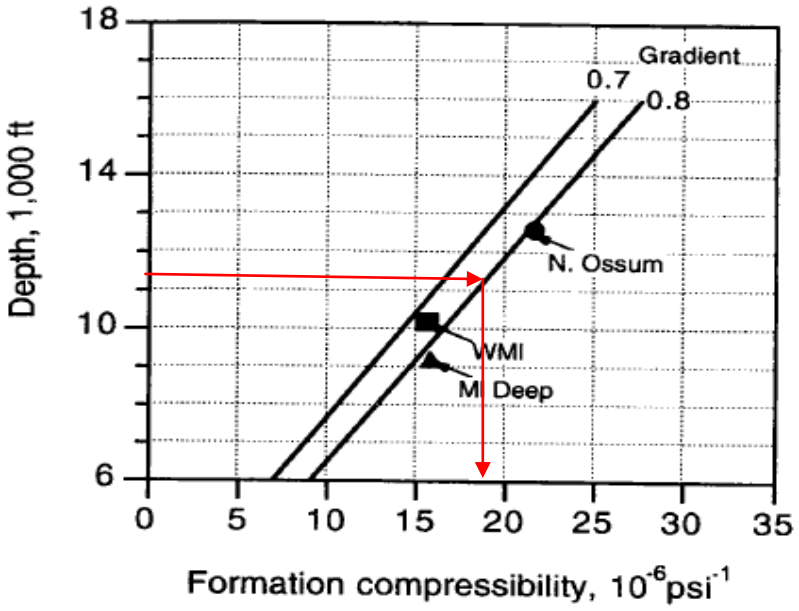

Figure 3.4: Hammerlindl formation compressibility correlation for 0.7- and 0.8-psi/ft-gradient gas reservoirs

ANDERSON "L" PRESSURE-PRODUCTION HISTORY				
BHP	**Z Factor**	**P/Z**	**CUM. GAS**	**CONDENSATE**
(psia)			**MMCF**	**MBBL**
9507	1.44	6602	0	0
9292	1.418	6553	392.5	29.9
8970	1.387	6467	1642.2	122.9
8595	1.344	6395	3225.8	240.9
8332	1.316	6331	4260.3	317.1
8009	1.282	6247	5503.5	406.9
7603	1.239	6136	7538.1	561.2
7406	1.218	6080	8749.2	650.8
7002	1.176	5954	10509.3	776.7
6721	1.147	5860	11758.9	864.3
6535	1.127	5799	12789.2	939.5
5764	1.048	5500	17262.5	1255.3
4766	0.977	4878	22890.8	1615.8
4295	0.928	4628	28144.6	1913.4
3750	0.891	4209	32566.7	2136
3247	0.854	3802	36819.9	2307.8

Using the **Ramagost and Farshad method**, the y- variable for different values of pressure is calculated thus:

$$\underbrace{\frac{P}{Z}[1 - c_e(P_i - P)]}_{Y} = \underbrace{\frac{P_i}{Z_i}}_{b} - \underbrace{\frac{P_i}{Z_i}\frac{G_p}{G}}_{mX}$$

Where X = G_p

For example, for the 8970-psia time-step,

$$\frac{P}{z}(1 - c_e(p_i - p) = \frac{8970}{1.387}(1 - (31.9x10^{-6})(9507 - 8970) = 6356psia$$

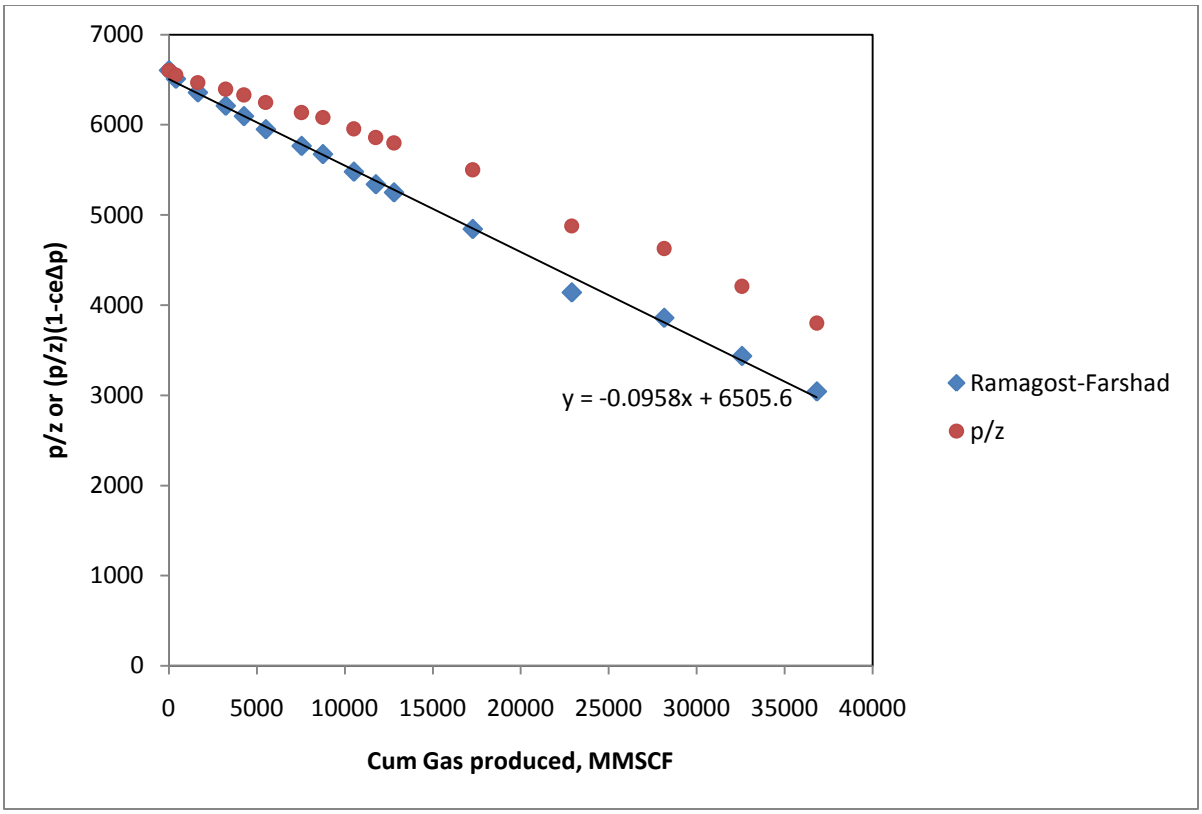

Figure 3.5: Ramagost-Farshad plot and p/z plot for Anderson "L" Reservoir

The equation of the straight line is $y = -0.0958x + 6505.6$

The slope = $-\frac{P_i}{z_i G} = -0.0958 = -(6505.6)x\frac{1}{G}$

This yields a value of **G = 70 BSCF**.

The Ramagost-Farshad method is useful for analyzing overpressured gas reservoirs when the pressure- and time- dependent formation compressibility values are known.

Using the **Roach solution plot technique**, the y-variable which is given by

$$Y = \frac{1}{p_i - p}\left(\frac{p_i z}{p z_i} - 1\right)$$

is calculated for different values of pressure and plotted against x-variable which is defined by

$$X = \frac{G_p}{p_i - p}\left(\frac{p_i z}{p z_i}\right)$$

To yield slope = 1/G and intercept = -(c_e +W_{en})

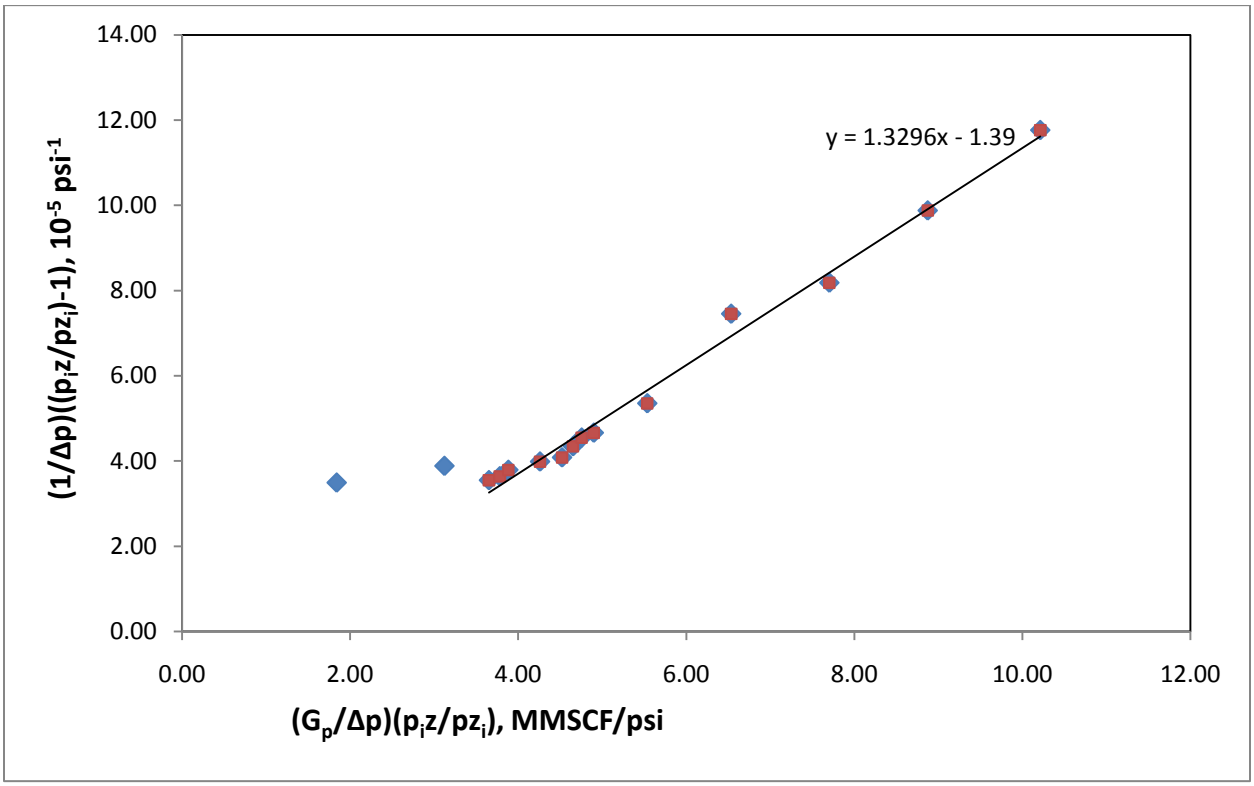

Figure 3.6: Roach Solution plot for Anderson "L" reservoir

The slope = 1/G.

$$\frac{1}{G} = 1.3296x10^{-11}$$

G = 75.2 BSCF

The intercept = - (c_e +W_{en}) and for an overpressured depletion drive gas reservoir, W_{en} = 0

Hence intercept = - c_e = -1.39 x10^{-5}

This implies that the effective formation compressibility, c_e = 13.9 x 10^{-6} psi^{-1}

The formation compressibility is calculated thus:

$$c_f = -y_{intercept}(1 - S_{wi}) - (S_{wi}c_w) = [-(-1.39x10^{-5})(1 - 0.35)] - (0.35x3.4x10^{-6})$$

$=14.85\ x\ 10^{-6}$psi^{-1}

Becerra- Arteaga Method

Step 1 – calculate the p_i/z_i and p_i/D terms from the field performance history and reservoir characteristics.

P_i = 9507psia, D = 11,167ft, S.G =0.94, z_i=1.55

$$\frac{p_i}{z_i} = \frac{9507}{1.55} = 6602\ psia$$

$$\frac{p_i}{D} = \frac{9507}{11167} = 0.85\frac{psia}{ft}$$

Step 2- Applying these correlation parameters to figure (3.3) to determine the proper α term. α=2.04

Step 3 – Determine OGIP from plot

Method A

Using equation (3.58b), the y-axis variable is calculated thus:

$$y_{variable} = \frac{p_i}{z_i}\left[\frac{\alpha p}{\alpha p + (p_i - p)}\right]$$

For the 8970-psia time step,

$$y_{variable} = \frac{9507}{1.55}\left[\frac{(2.04)(8970)}{(2.04)(8970) + (9507 - 8970)}\right] = 6414psia$$

The y-axis variable is calculated in similar ways for other values of pressure and is plotted against X (=G_p).

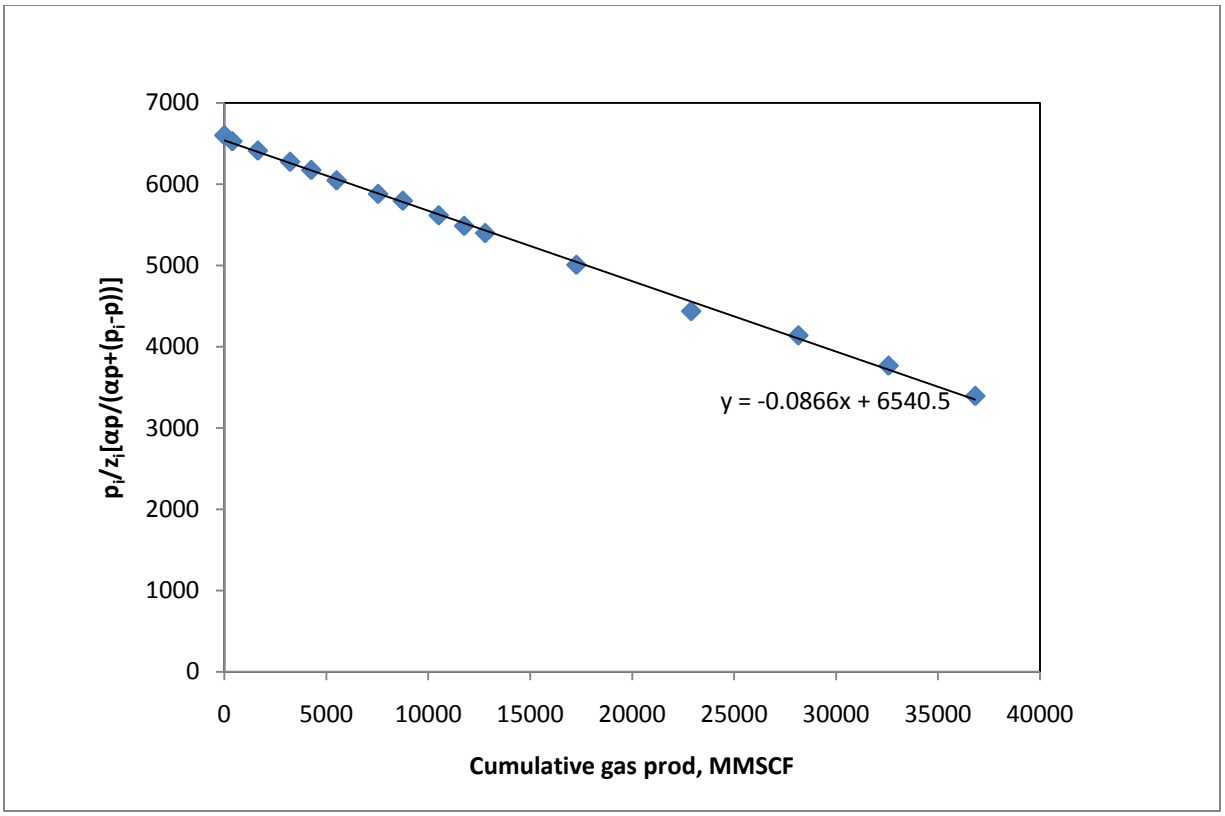

Figure 3.7: Becerra-Arteaga first pressure plot for Anderson "L" reservoir

The slope = $-\left(\frac{p_i}{z_i G}\right) = -0.0866$

This implies that $G = \frac{6540.5}{0.0866} = 75.5 BSCF$

G= 75.5 BSCF.

Method B

This entails calculating OGIP for each data point using the following equation:

$$G = G_p\left[1 + \frac{\alpha p}{p_i - p}\right]$$

An example calculation for the 8970 psia time-step is:

$$G = G_p\left[1 + \frac{\alpha p}{p_i - p}\right] = 1.642\left[1 + \frac{(2.04)(8970)}{9507 - 8970}\right] = 57.59\ Bscf$$

The plot of the calculated values of OGIP and cumulative gas produced is shown below

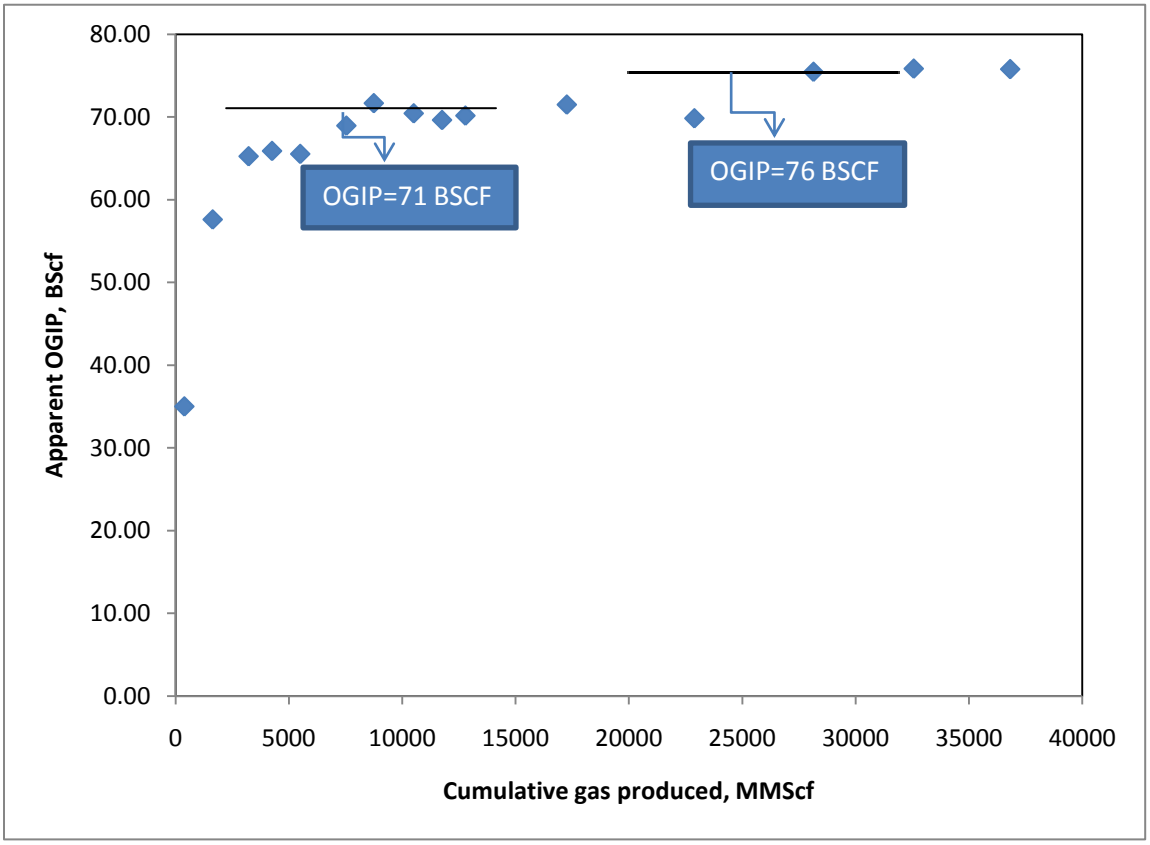

Figure 3.8: Becerra-Arteaga second pressure plot for Anderson "L" reservoir

There appears to be two average values, 71≤ G≤ 76. The average value is (71+76)/2 = **74.5 BSCF**

Note the effectiveness of the correlation.

Elsharkawy's Method

Using Elsharkawy's method for the Anderson "L" reservoir, the values of the 'X' and 'Y' variables are calculated and plotted.

For example, at the 8009 psia time-step

$$B_g = \frac{5.04\ z\ T}{P} = \frac{5.04x1.282x762}{8009} = 0.5857 bbl/MMScf$$

$$Y = \frac{(G_p + G_{LP})B_g + W_p B_w}{(B_g - B_{gi})} = \frac{(5503.5 + 0.4069)0.5857 + 0}{(0.5857 - 0.5542)} = 102{,}412.3MMSCF$$

And $X = \left(\frac{p_i - p}{B_g - B_{gi}}\right) = \frac{9507-8009}{0.5857-0.5542} = 47590.17$psi/bbl/MMscf

The plot is as shown below:

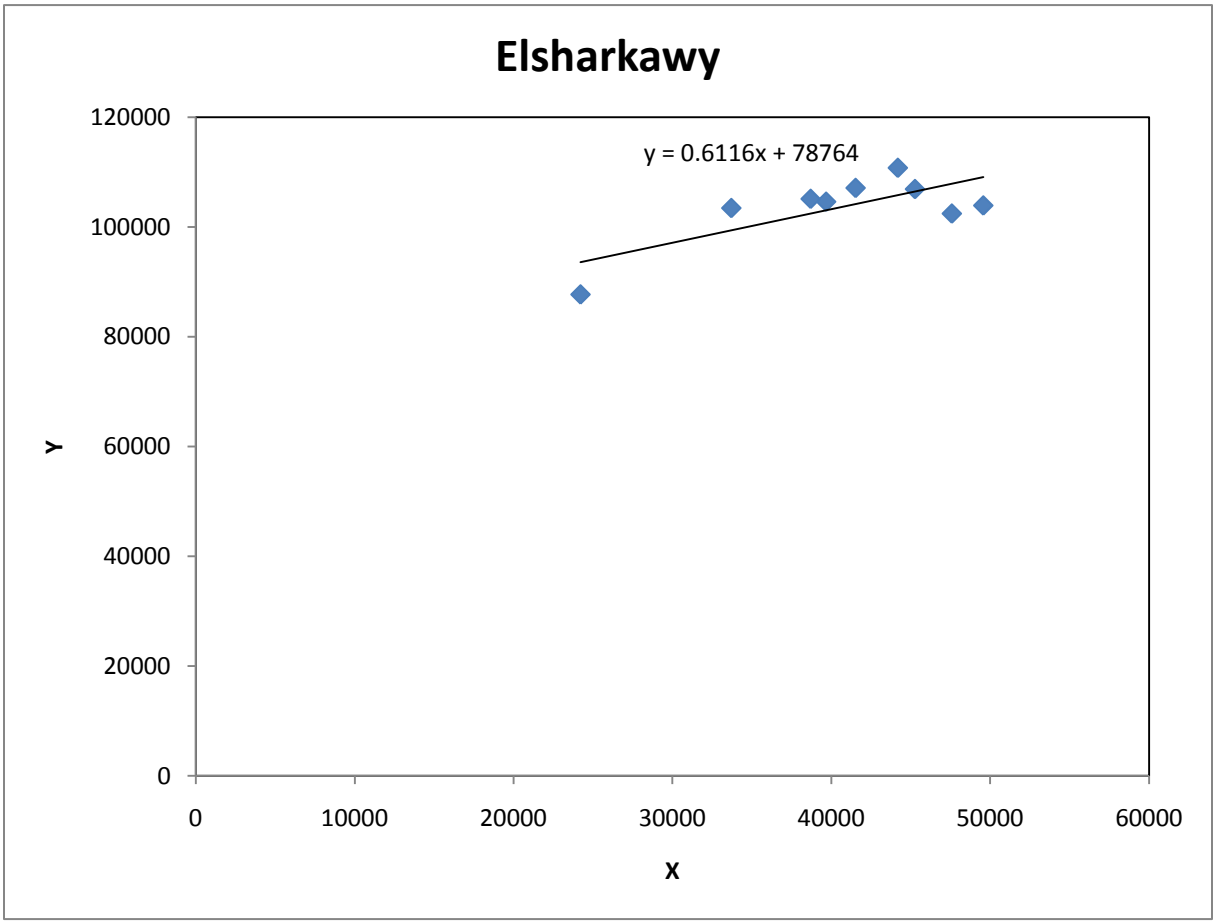

Figure 3.9: Elsharkawy's solution plot for Anderson "L" Reservoir

The intercept yields the value of **G = 78.76 BSCF**

3.7 Water-drive overpressured dry-gas reservoirs

The effect of water influx adds an additional displacement process and pressure-supplement source to the reservoir. Residual gas saturation is reduced but abandonment pressure is increased in the presence of water influx. Generally, the net effect is to reduce ultimate

recovery. Formation compressibility for most normal-pressured aquifers is assumed to range from $3x10^{-6}$ to $4x10^{-6}$ psi^{-1}. Undercompacted, overpressured aquifers should somewhat display a somewhat larger value. The effect of increasing the formation compressibility would be to decrease the apparent size of the aquifer. A study by Bourgoyne et al. indicated that the transmissibility of shales with a permeability of 10^{-5} mD could be sufficient to affect the reservoir performance history. However, the shale-water effect would be insignificant if the shale permeability was reduced to 10^{-7}mD. The pressure profile across a sand/shale interface would be quite steep. Only the first few feet of the shale layer would be able to release the connate water before loss in permeability by compaction reduces the ability of the shale water to migrate in significant volume. Shale layers can cover extensive area. However, water influx would be appreciable only in the areas of greatest pressure drawdown. Water influx is a function of shale permeability as well as the degree and net thickness of the shale layers incorporated within or adjacent to the producing interval.

Bourgoyne et al used two geopressured gas reservoirs in the Gulf of Mexico, which are the Miocene reservoir and the NS2B reservoir to confirm his findings. The water influx calculations that he made indicated that significant quantities of shale water can move into producing superpressure gas reservoirs. The use of shale permeability on the order of 10-^{5} mD and shale bulk compressibilities on the order of 40 x 10^{-6} psi^{-1} would account for all of the pressure support observed in those two South Louisiana reservoirs. These values are in line with experimentally determined values of shale permeability and compressibility. He developed a technique for calculating unsteady state water influx when permeability and compressibility is a function of pressure. He concluded that shale water influx is approximately proportional to the square root of the permeability-compressibility product. Shale permeability and/or compressibility must decrease with effective overburden pressure if the calculated reservoir behavior is to closely match the observed reservoir behavior.

CHAPTER 4 - Comparative Analysis of the Material Balance models used in determining IGIP and Reserves

The previous chapter reviewed the various material balance methods available in determining reserves and IGIP for overpressured gas reservoirs. Several researchers have presented material balance analysis methods to obtain reasonably accurate estimates of the initial gas-in-place for abnormally-pressured gas reservoirs. For this to be achieved, material balance analysis of production performance data for an abnormally-pressured gas reservoir should include water, rock and gas compressibility effects.

In this chapter, a comparative analysis will be done on the values of IGIP obtained through the material balance techniques that have been discussed in chapter three and also a sensitivity analysis of the input parameters affecting the values of IGIP being calculated. Four geopressured gas reservoirs found in the Gulf Coast will be used as case studies to demonstrate this.

ANDERSON 'L' RESERVOIR EXAMPLE

The Anderson "L" reservoir is an abnormally high-pressured reservoir discovered in 1965, with an initial pressure of 9507 psi at 11,100 ft (pressure gradient of 0.856psi/ft). The reservoir data and history were presented by Duggan[16]. It was assumed that the reservoir was depletion drive because the reservoir is separated from other blocks by faults and analysis of the fluids from surrounding blocks showed different fluids. The reservoir has 1,000 feet or more of uncompacted shales. It contains retrograde gas that has a dew point pressure of 6700 psi. The reservoir was completely abandoned after production of 55 BSCF because of excessive water production. The pressure-production history of the reservoir has been analyzed by many authors. The production mechanism of this reservoir is very controversial. Begland & Whitehead matched the production history using IGIP of 70 BSCF and assuming changing formation compressibility. Poston & Chen, Ramagost & Farshad, and Ambastha estimated the IGIP in the range of 65 to 75 BSCF and reservoir compressibility of 14×10^{-6} psi^{-1}, but they gave no explanation for the high compressibility.

Table 4.1 Anderson "L" reservoir data and Pressure-production history

ANDERSON "L" RESERVOIR DATA				
Depth	11,167ft			
Porosity	24%			
Water Saturation	35%			
Dew point	6118 psia			
Gas-in-Place	2240 MCF/Ac-ft			
Initial BHP	9507 psia			
Pressure Gradient	0.843 psi/ft			
BHT	266^0F			
c_w	3.4×10^{-6}psi^{-1}			
BHP	**z Factor**	**P/z**	**CUM. GAS**	**CONDENSATE**
(psia)			**MMCF**	**MBBL**
9507	1.44	6602	0	0
9292	1.418	6553	392.5	29.9
8970	1.387	6467	1642.2	122.9
8595	1.344	6395	3225.8	240.9
8332	1.316	6331	4260.3	317.1
8009	1.282	6247	5503.5	406.9
7603	1.239	6136	7538.1	561.2
7406	1.218	6080	8749.2	650.8
7002	1.176	5954	10509.3	776.7
6721	1.147	5860	11758.9	864.3
6535	1.127	5799	12789.2	939.5
5764	1.048	5500	17262.5	1255.3
4766	0.977	4878	22890.8	1615.8
4295	0.928	4628	28144.6	1913.4
3750	0.891	4209	32566.7	2136
3247	0.854	3802	36819.9	2307.8

According to studies made by Duggan, the Anderson "L" reservoir is 414 acres by 75 net ft of sand, or 31,050 acre-ft. The volumetric calculation of the IGIP using the above reservoir data is as follows:

$$G = 7758\, Ah\emptyset\, S_{gi}/B_{gi}$$

where $B_{gi} = \frac{0.00504zT}{P} = \frac{0.00504(1.44)(266+460)}{9507} = 5.542x10^{-4} bbl/scf$

$$\text{and } G = \frac{7758(414)(75)(0.24)(0.65)}{5.542x10^{-4}} = 69.55x10^{9}Scf \cong \mathbf{70\ BSCF}$$

The plot of P/z vs Gp of the production data for the Anderson "L" reservoir as shown in figure **4.1** yields an apparent gas-in-place of **112 BSCF**, when the early straight-line data was extrapolated to the x-axis. The early time P/z GIP volume (also called the apparent GIP) is about 1.61 times the volumetric GIP calculated.

The pressure-production history of this reservoir shows downward curvature as shown in figure **4.1**. The curvature started at 5764 psi after production of 25% of the IGIP. Water influx from non-pay sand (shale) in addition to the formation of condensate below the dew point have reduced the gas permeability and caused the downward curvature of the P/z vs Gp.

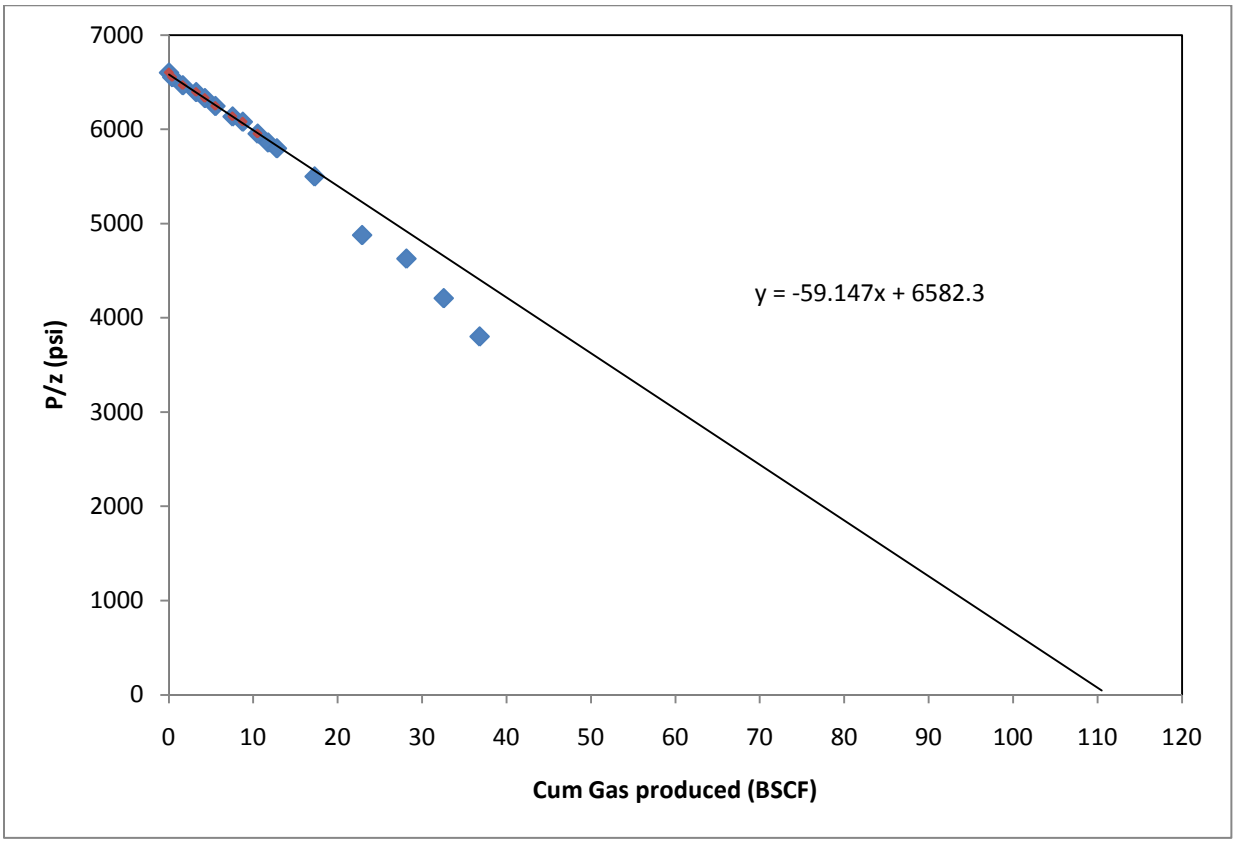

Figure 4.1 P/z vs Gp for the Anderson "L" reservoir showing extrapolation of early data

Using Hammerlindl's methods to calculate the IGIP, by correcting the apparent GIP of 112 BSCF to obtain the actual GIP, yields **67 BSCF** and **69 BSCF** for both methods respectively. In chapter 3, the calculation of IGIP using Roach's, Ramagost and Farshad's, Becerra-Arteaga's, and Elsharkawy's methods have been fully illustrated for the Anderson "L" reservoir. The table below gives a summary of the IGIP values obtained using different Material Balance techniques and their inherent assumptions. The details of the calculations can be found in Appendix A.

Table 4.2 Material Balance Results for the Anderson "L" reservoir (Volumetric estimate = 70BSCF)

Authors	IGIP (BSCF)	Assumptions	Production Mechanism
Ramagost & Farshad	70	$c_f = 15 \times 10^{-6}$ psi^{-1}	assume rock collapse
Roach	75.2		
Hammerlindl (2 methods)	67 & 69		
Bernard	91		
Fetkovich et al	76	water-to-reservoir volume = 2.25, $c_f = 3.2 \times 10^{-6}$ psi^{-1}	water influx
Ambastha	57 to 103	volumetric reservoir	
Becerra-Arteaga	75.5		
Elsharkawy	78.76		water-to-reservoir volume= 1.92
Havlena & Odeh	92		
Begland and Whitehead	70	variable water & rock compressibilities	assume rock collapse

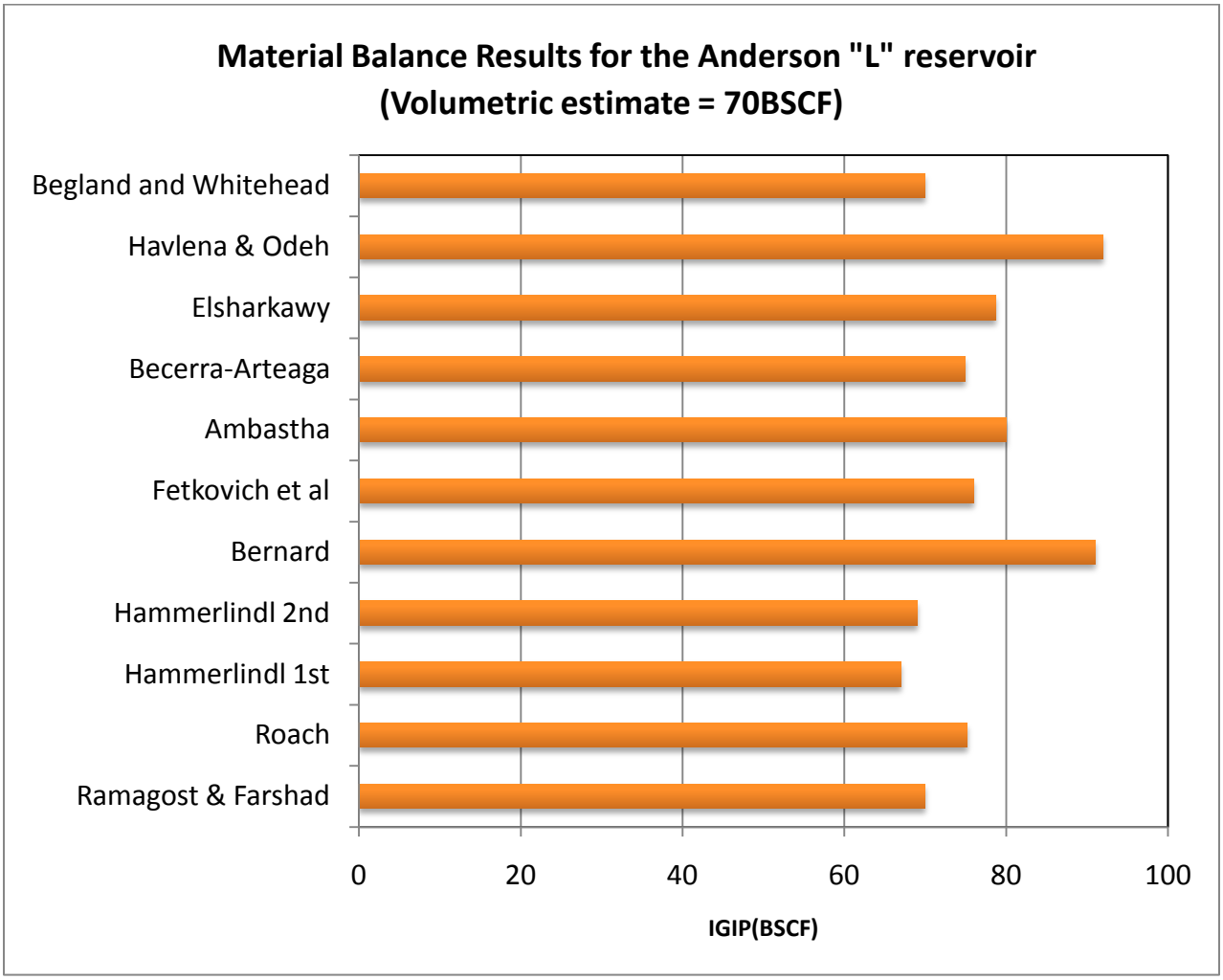

Figure 4.2 Comparative Analysis of different MB models for the Anderson "L" reservoir case

MIOCENE RESERVOIR

Miocene reservoir is abnormally high pressure with an initial pressure of 10,984 psi. The reservoir is located in South Louisiana. Pressure-production data for this reservoir is reported by Bourgoyne et al[12] and Hubble. The reservoir has a dew point pressure of 7000 psi. Porosity and water saturation are not reported but assumed to be 24 % and 34% respectively, as typical of values for Gulf Coast Reservoirs. IGIP from volumetric data is estimated to be 16 BSCF.

P/z vs G_p plot for this reservoir shows downward curvature. Extrapolation of early-time pressure production data above 8789 psi projects IGIP of 47 BSCF which is overestimated by a factor of 3 when compared to the volumetric estimate. Extrapolation of the late production data (between 7064 and 2723 psi) yields IGIP of 16.2 BSCF. Thus the correct IGIP could not be estimated from the pressure versus production plot until 40% of the IGIP was produced. The value of IGIP is also obtained using the various material balance techniques and the results tabulated as shown in Table 4.4. The details of the calculations can be found in the Appendix.

Table 4.3 Pressure-production history for Miocene Reservoir

Pressure	z	G_p	P/z
psi		BScf	
10984	1.65	0	6657
10156	1.58	0.482	6428
9924	1.56	0.648	6362
9703	1.54	0.85	6301
8936	1.49	2.505	5997
9222	1.46	2.634	6316
8789	1.44	3.366	6103
8313	1.39	3.957	5981
7064	1.25	5.251	5651
6250	1.15	6.086	5435
4928	0.96	7.608	5133
2723	0.88	10.589	3094

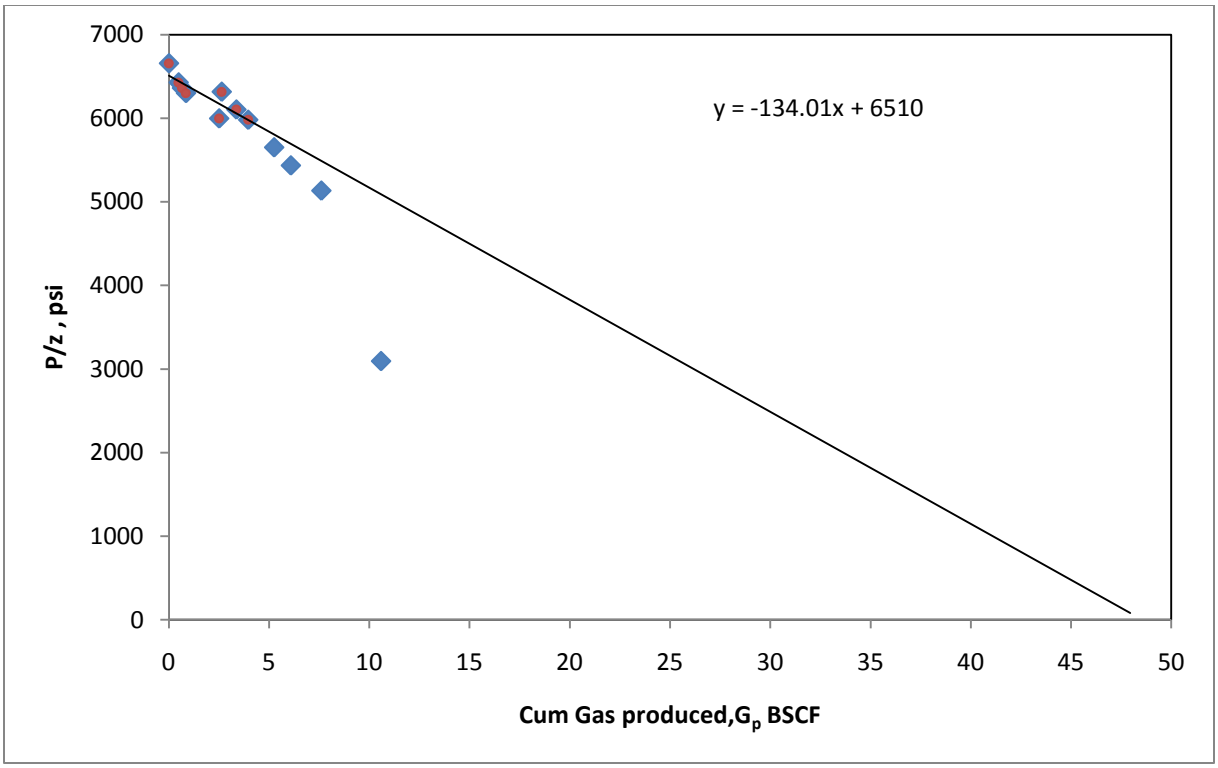

Figure 4.3 P/z vs Gp plot for the Miocene reservoir showing extrapolation of early data

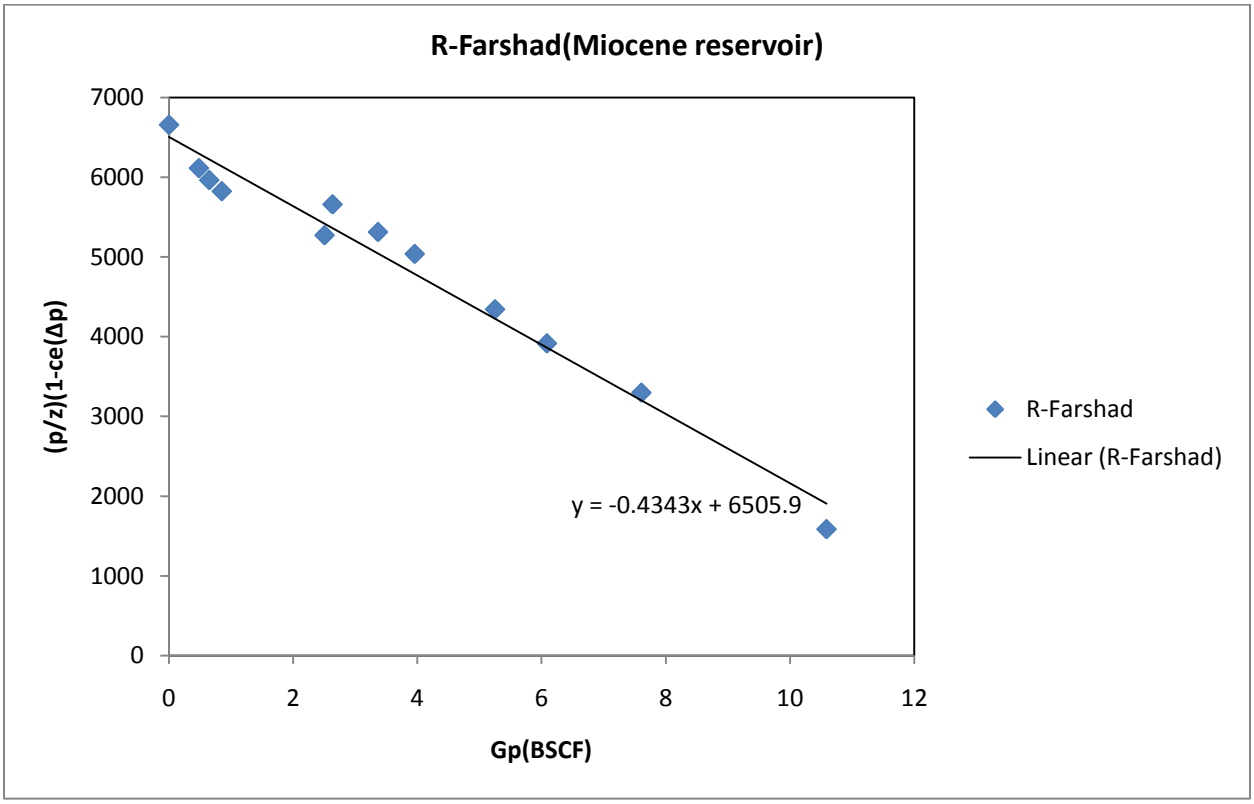

Figure 4.4 Ramagost-Farshad plot for Miocene reservoir

The equation of the straight line is $y = -0.4343x + 6505.9$

The slope = $-\frac{P_i}{z_i G} = -0.4343 = -(6505.9)x\frac{1}{G}$

This yields a value of **G = 15 BSCF**

Table 4.4 Material Balance Results for the Miocene reservoir (Volumetric estimate = 16 BSCF)

Authors	IGIP (BSCF)	Assumptions	Production Mechanism
Ramagost & Farshad	15		assume rock collapse
Roach	20		
Hammerlindl	--		
Bernard	25		
Fetkovich et al	--		
Ambastha	--		
Becerra-Arteaga	15		
Elsharkawy	11.8		Water to reservoir vol = 8.13
Havlena & Odeh	--		
Begland and Whitehead	--		
Bourgoyne et al	16	Shale properties, Csh, ksh	Shale water influx

N.B: '--' NOT AVAILABLE

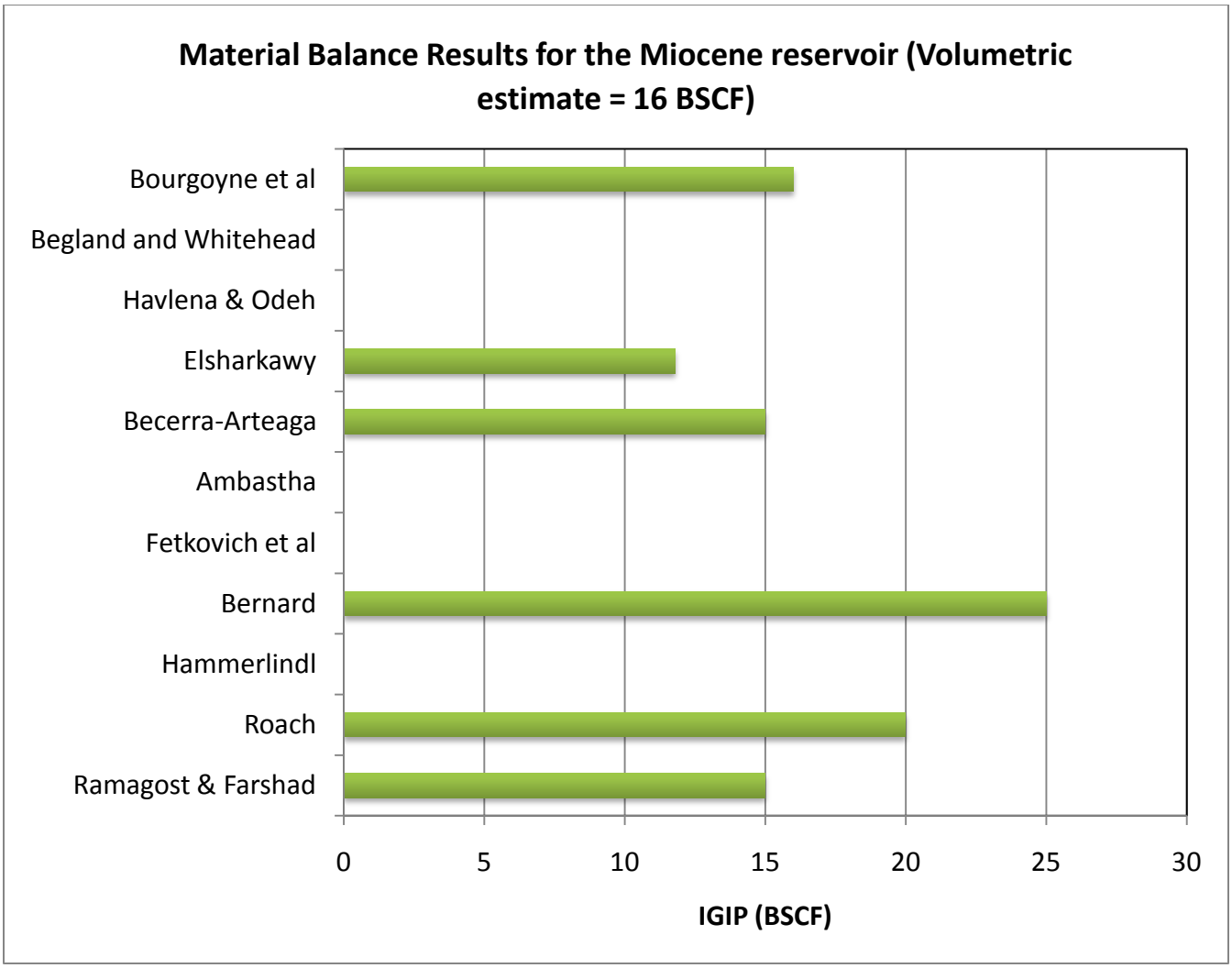

Figure 4.5 Comparative Analysis of different MB models for the Miocene reservoir case

CAJUN FIELD – Louisiana Offshore Gas Reservoir

This is a Louisiana offshore gas reservoir discovered in 1966. The reservoir has initial pressure of 11,450 psi at 13,300 ft (0.861 psi/ft). The pressure-production history was first introduced by Stelly & Farshad[29]. The complete pressure-production data was presented by Ramagost & Farshad. Volumetric estimate of IGIP is 470 BSCF based on core and log data. Many authors have studied the pressure-production history of this field. They estimated IGIP of 470 BSCF assuming abnormal formation compressibility of 20 X 10^{-6} psi^{-1}. Ambastha, however calculated IGIP between 410-760 BSCF but did not explain the reservoir mechanism. The average porosity for this reservoir is not reported and Fetkovich et al. used formation compressibility of 4 X 10^{-6} psi^{-1} to estimate IGIP of 650 BSCF and an associated water volume ratio of 0.2 using the pressure data above 6850 psi. P/z vs G_p plot of Cajun reservoir shows downward curvature. Estimation of IGIP based on early data yields IGIP of 680 BSCF which is 140% of the volumetric estimate.

Table 4.5 Pressure-production history and reservoir data for Cajun Field

P (psi)	z	P/z	G_p(BSCF)
11444	1.496	7650	0
10674	1.438	7423	10
10131	1.397	7252	29
9253	1.33	6957	54
8574	1.28	6698	78
7906	1.23	6428	101
7380	1.192	6191	120
6847	1.154	5933	145
6388	1.122	5693	161
5827	1.084	5375	187
5409	1.057	5117	198
5000	1.033	4840	216
4500	1.005	4478	236
4170	0.988	4221	246

Depth	13,300	ft
Reservoir Temperature	263	^{0}F
Gas Gravity	0.6	
Formation Compressibility, c_f	19.5	micropsi
Water Compressibility, c_w	3	micropsi
α	1.33	
Connate Water Saturation, S_{wi}	22	%

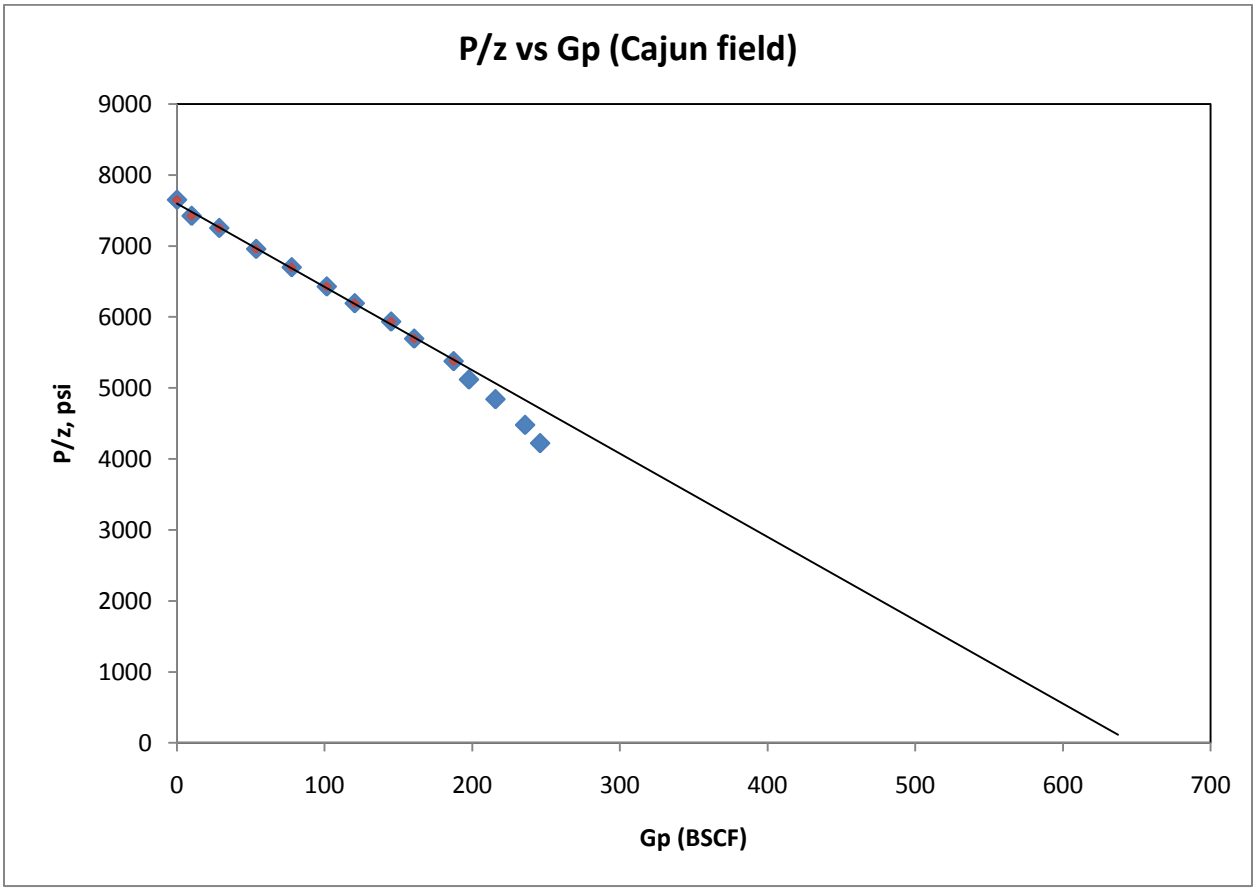

Figure 4.6 P/z vs Gp plot for the Cajun Field showing extrapolation of early data

Table 4.6 Material Balance Results for the Cajun field gas reservoir (Volumetric estimate = 470 BSCF)			
Authors	**IGIP (BSCF)**	**Assumptions**	**Production Mechanism**
Ramagost & Farshad	470	$c_f = 19 \times 10^{-6}$ psi^{-1}	assume rock collapse
Roach	522		
Stelly & Farshad	470	$c_f = 26 \times 10^{-6}$ psi^{-1}	assume rock collapse
Bernard	591		
Fetkovich et al	650	water to reservoir volume = 0.2	water influx
Ambastha	410-650	volumetric reservoir	
Becerra-Arteaga	447	α=1.33	
Elsharkawy	462		water to reservoir vol = 2.0
Havlena & Odeh	--		
Hammerlindl	433	$c_f = 19.5 \times 10^{-6}$ -6 psi^{-1}, $c_w = 3 \times 10^{-6}$ psi^{-1}	

The details of the calculations to obtain the values of the IGIP using the different techniques tabulated above can be found in the Appendix C.

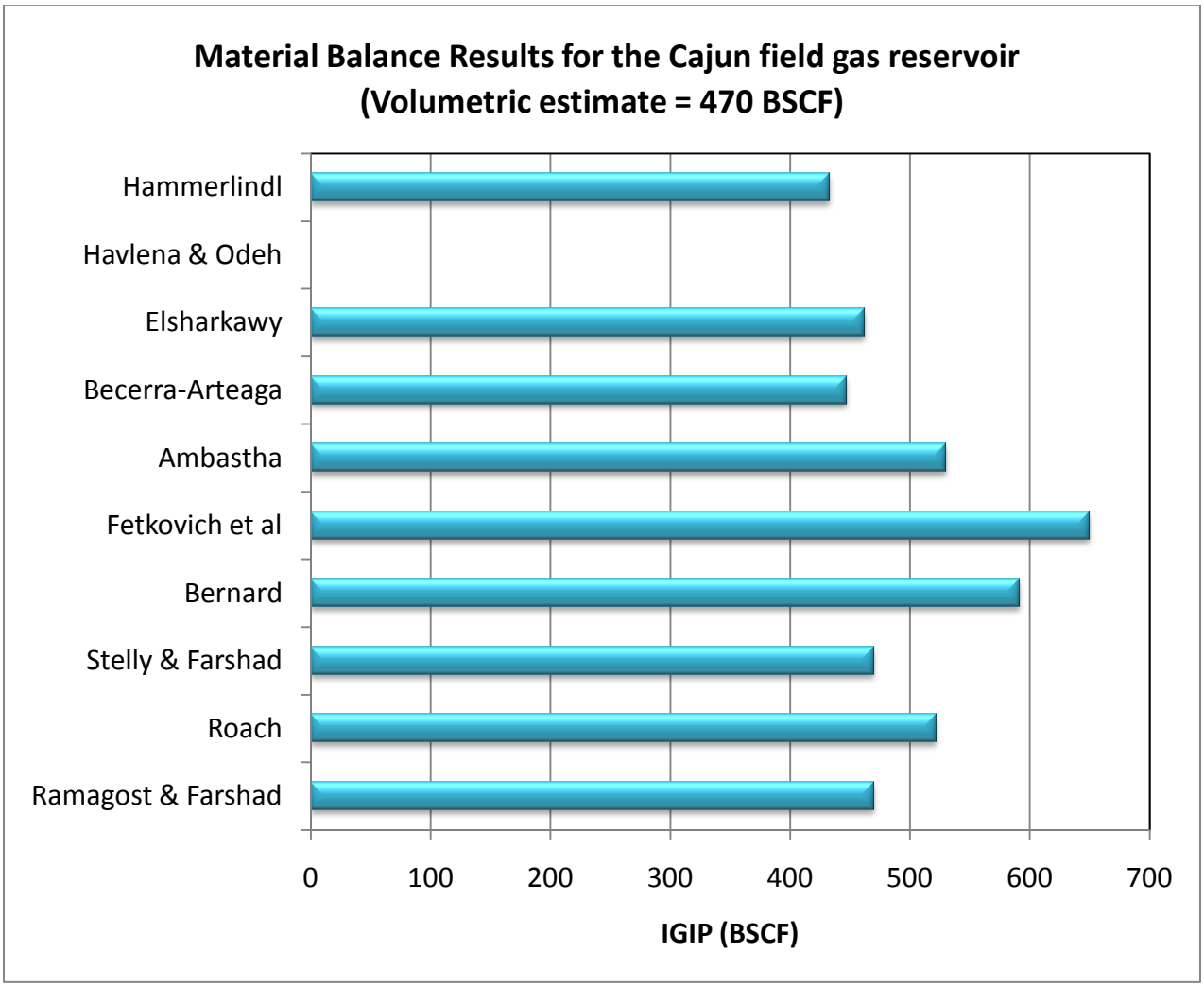

Figure 4.7 Comparative Analysis of different MB models for the Cajun reservoir case

NS2B Reservoir

The North Ossun Field, NS2B reservoir is located in Lafayette Parish, Louisiana. The reservoir was discovered in 1959. It has an initial pressure of 8921 psi at 12,500 feet (gradient of 0.714 psi/ft). The reservoir history was originally reported by Harville & Hawkins[11] and analyzed by Ramagost & Farshad[2]. Connate water saturation was reported as 34% and average porosity as 24%. The reservoir permeability is 200mD. Initial gas-in-place was calculated from good volumetric data, based on core and well logs, as 114 BSCF. Harville and Hawkins proposed that during early life, pressure was partially sustained by high rock compressibility resulting from rock failure. After the production of 20 BSCF, rock failure was essentially completed to normal rock compressibility of $6 \times 10^{-6} psi^{-1}$. However, Bourgoyne et al. proposed water influx from shale as a possible explanation of such pressure support. P/z vs G_p plot for this reservoir exhibits downward curvature indicating some pressure support as the reservoir is depleted. Extrapolation of the early data for this reservoir yields apparent gas-in-place of about 220 BSCF which is nearly twice the volumetric estimate of the IGIP. After production of 20 BSCF (17% of the IGIP) at 6500 psi (27% pressure drop), the second slope of P/z vs G_p plot started. Extrapolation of the production data from 20 to 40 BSCF yields gas-in-place of 118 BSCF which is in good agreement with the volumetric estimate. Thus, the true gas in place could not be estimated from P/z plot until 35% of the IGIP was produced. The IGIP values using various material balance techniques discussed earlier are obtained, and tabulated as shown in Table 4.8. The details of the calculations can be found in the Appendix.

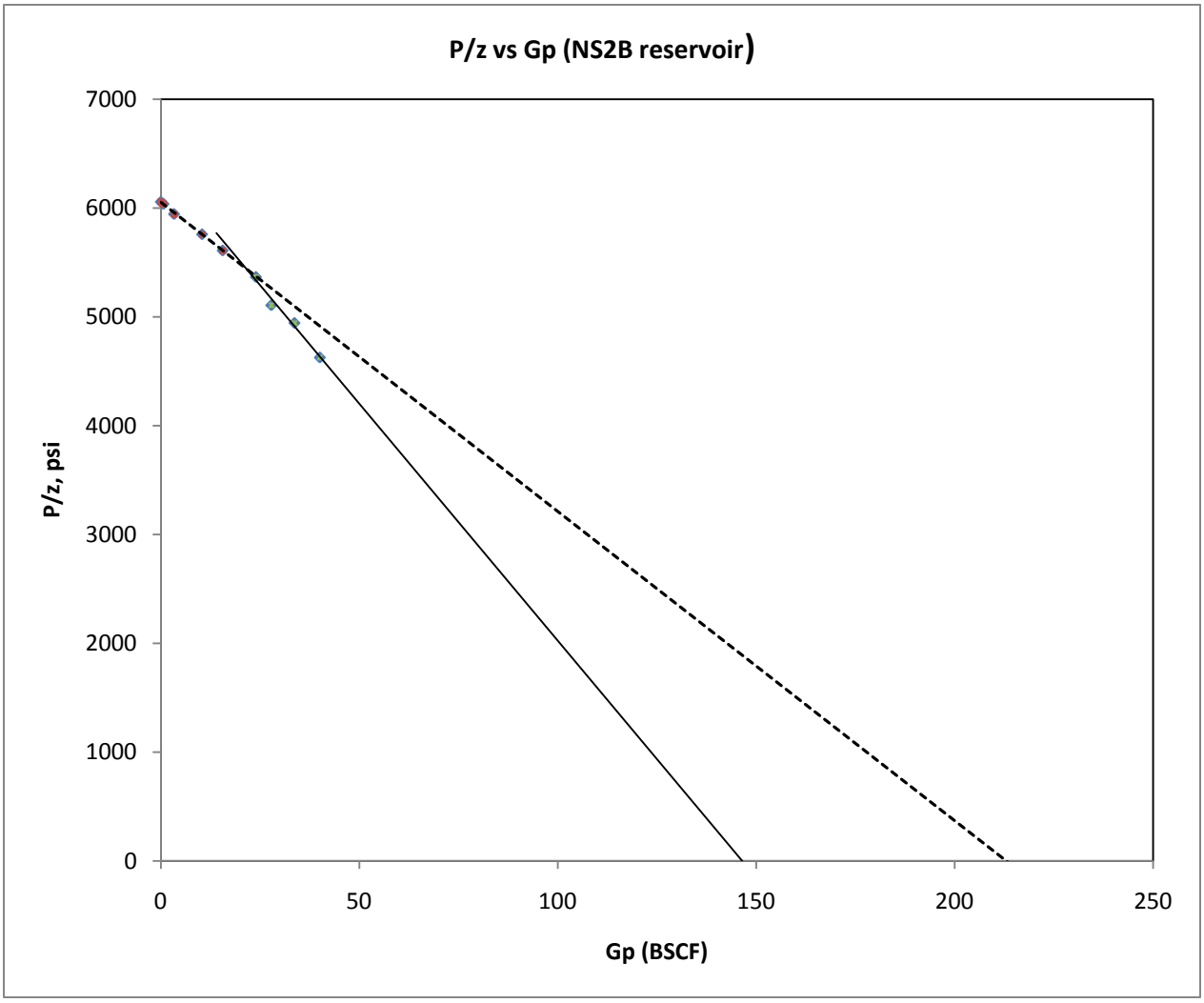

Figure 4.8 P/z vs G_p plot for the NS2B reservoir

Table 4.7 NS2B Reservoir data and Pressure-production history data

NS2B RESERVOIR PRESSURE-PRODUCTION DATA			
Pressure	z	G_p	P/z
psia		BSCF	
8921	1.473	0	6056.3
8845	1.465	0.66	6037.5
8322	1.4	3.33	5944.3
7417	1.288	10.4	5758.5
6838	1.219	15.59	5609.5
6064	1.13	23.97	5366.4
5490	1.075	27.85	5107.0
4781	0.967	33.7	4944.2
4104	0.887	40.1	4626.8

NORTH OSSUN FIELD, LAFAYETTE PARISH LOUISIANA

RESERVOIR DATA

Depth	12500	ft
Pressure	8921	psia
Gradient	0.725	psi/ft
Temperature	248	^{0}F
GWC	12580	ft
Avg Gross sand	100	ft
Porosity	24	%
Connate water	34	%
Permeability	200	mD
Producing wells	4	
Dew point pressure	6920	psia
Initial GOR	160	bbl/MMSCF
Condensate gravity	47	API
Net Bulk gas volume	2.48	BSCF
Initial z factor	1.472	
IGIP	114	Bscf
Initial gas compressibility	30	micropsi

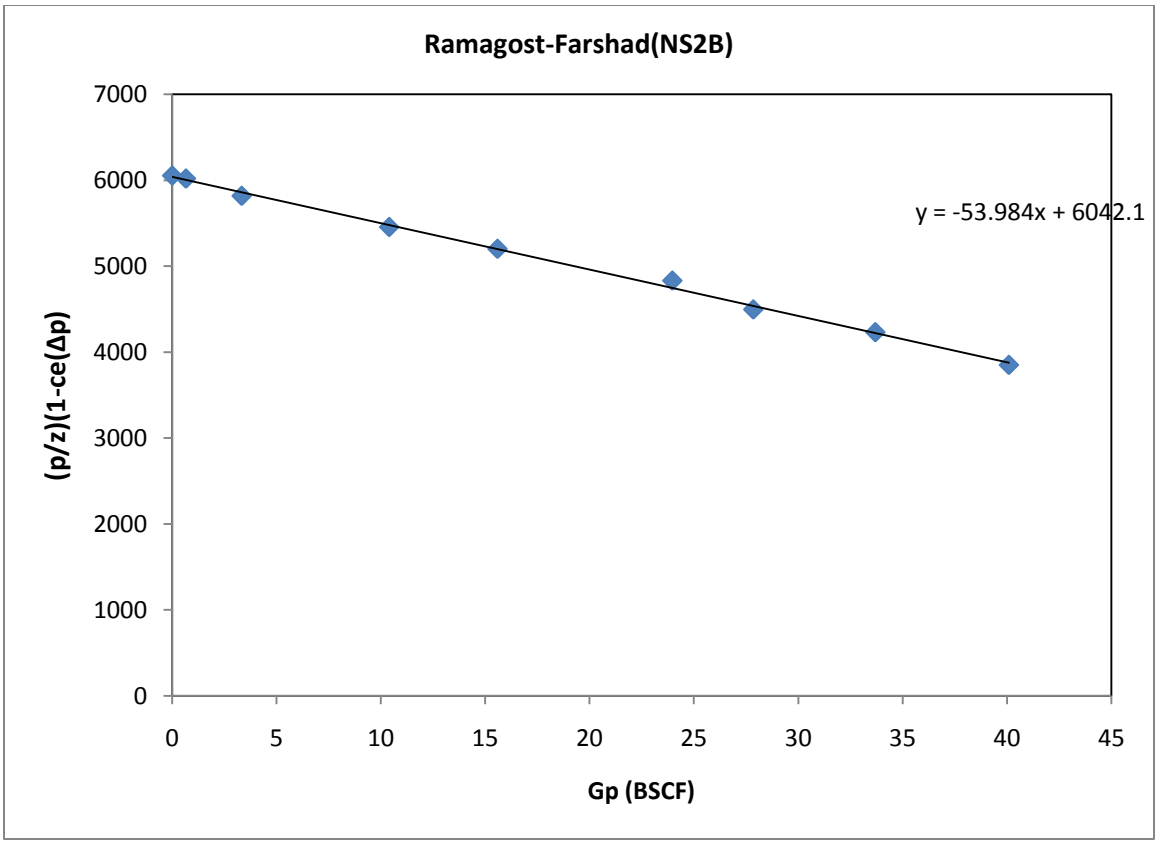

Figure 4.9 Ramagost-Farshad plot for the NS2B reservoir

Table 4.8 Material Balance Results for the NS2B reservoir (Volumetric estimate = 114 BSCF)			
Authors	**IGIP (BSCF)**	**Assumptions**	**Production Mechanism**
Ramagost & Farshad	**114**	**$c_f = 25 \times 10^{-6}$ psi^{-1}**	**assume rock collapse**
Roach	**150**		
Hammerlindl	**114**	**$c_f = 21.9 \times 10^{-6}$ psi-^{1}**	**assume absence of water influx effects**
Bernard	**154**		
Fetkovich et al	**--**		
Ambastha	**--**		
Becerra-Arteaga	**101**		
Elsharkawy	**121**	**water-to reservoir volume = 1.74**	
Harville & Hawkins	**118**	**$c_f = 28 \times 10^{-6}$ psi^{-1}**	**assume rock collapse**
Begland and Whitehead	**--**		
Bourgoyne et al	**114**	**Shale properties, C_{sh}, k_{sh}, V_{sh}**	**Shale water influx**

The details of the calculations for the values of IGIP for the NS2B reservoir using various material balance techniques can be found in the Appendix.

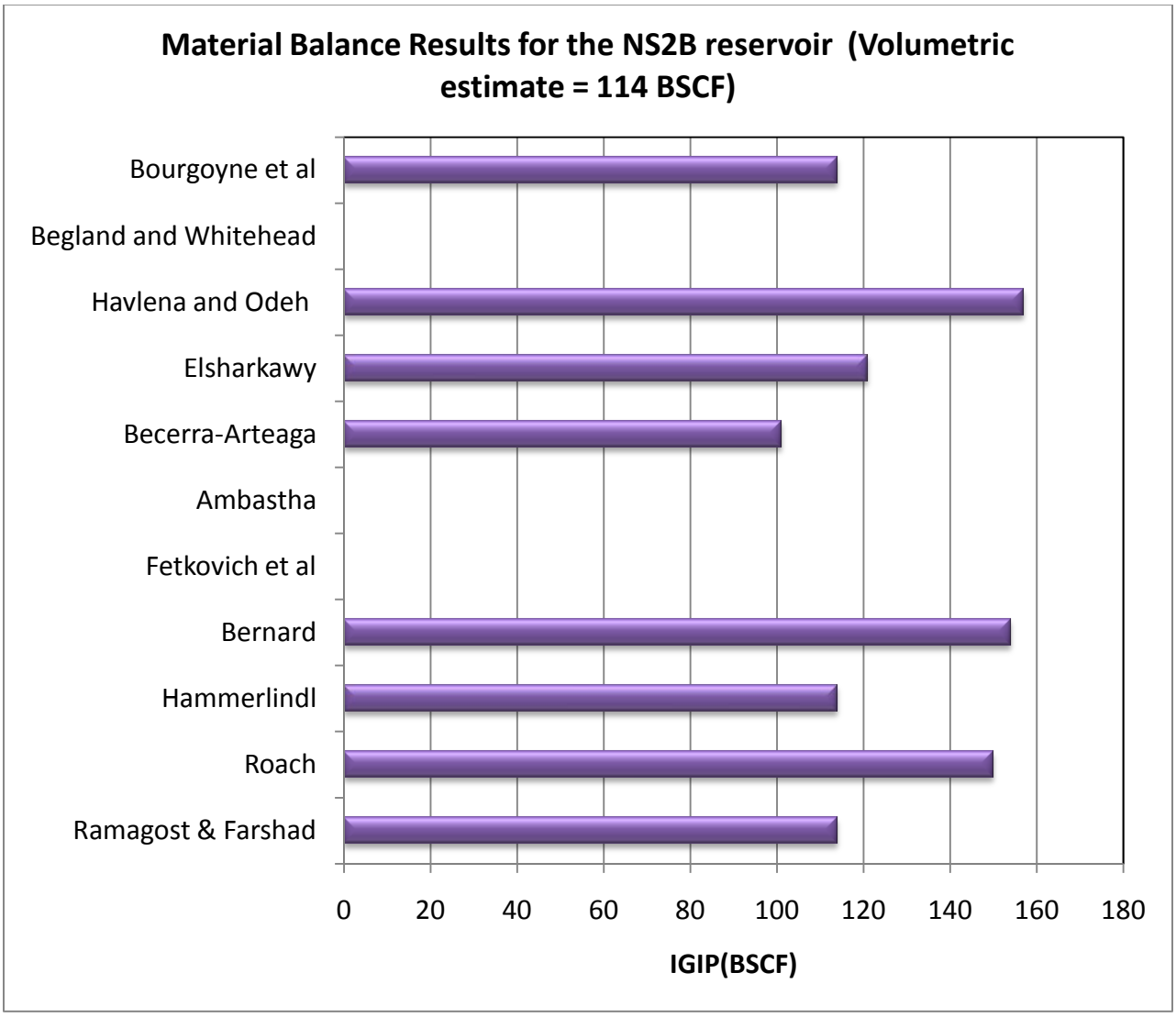

Figure 4.10 Comparative Analysis of different MB models for the NS2B reservoir case

DISCUSSION OF RESULTS

Comparing the values of the IGIP estimated using the various material balance techniques previously discussed for the four reservoir case studies, the table below displays the values of IGIP obtained.

Table 4.9 Comparison of IGIP values for the four geopressured reservoir case studies

Source/Technique	ANDERSON "L" reservoir	MIOCENE reservoir	CAJUN reservoir	NS2B reservoir
Volumetric	**70**	**16**	**470**	**114**
Early data extrapolation	**112**	**47**	**680**	**220**
Hammerlindl	**67 / 69**	**--**	**433**	**114**
Ramagost & Farshad	**70**	**15**	**470**	**114**
Roach	**75.2**	**20**	**522**	**150**
Fetkovich et al	**76**	**--**	**650**	**--**
Ambastha	**57 to 103**	**--**	**410 to 650**	**--**
Beccera-Arteaga	**75.5**	**15**	**447**	**101**
Elsharkawy	**78**	**11.8**	**462**	**121**
Havlena & Odeh	**92**	**23.6**	**680**	**157**
Begland & Whitehead	**70**	**--**	**--**	**--**
Bourgoyne et al	**--**	**16**	**--**	**114**
Bernard	**91**	**25**	**591**	**154**

Note: The values of the IGIP are in BSCF.

From the table above, it is clear that the extrapolation of the early data on P/z vs G_p plot overestimates the IGIP compared to the values obtained via the volumetric method. Hence there is a need to adjust some of the parameters used in the plot to correct for this overestimation and obtain a more accurate estimate of the IGIP. The MB techniques by Hammerlindl, Ramagost-Farshad, Becerra-Arteaga and Elsharkawy yield values of IGIP within a close range. However, the MB techniques by Roach, Fetkovich et al, Ambastha, Havlena and Odeh, and Bernard yield values of IGIP in a farther range from the volumetric estimate. These methods are highly sensitive to the values of compressibility used in the calculations of the

variables. Roach yields different values of G due to scatter in the data when plotted, and which results in not being able to get an appropriate straight line through the data points from which G can be determined.

Hammerlindl's method

Hammerlindl's method entails correcting the apparent GIP (estimated from extrapolation of early data) to actual GIP taking into consideration the effect of formation compressibility. This method can be used for reservoirs whose P/z vs G_p plots show downward curvature, and with enough data available to compute the value of the correction factor. The method could not be applied to compute G for the Miocene reservoir due to the lack of sufficient data required to compute the correction factor. This method requires prior knowledge of formation compressibility and assumes there is no water influx from aquifer or shales into the reservoir, hence not appropriate for reservoirs that are not self-depleting. The developed corrections are accurate in theory, but such required information as formation compressibility is based on limited empirical data. Hammerlindl's method underestimated the IGIP for the Anderson "L" reservoir by a negligible factor, but by a larger factor for the Cajun gas reservoir.

Ramagost- Farshad method

This method requires prior knowledge of formation compressibility which in most cases is unknown. From the results obtained for the four reservoir case studies, the Ramagost-Farshad method yields estimates that are approximately equal to the volumetric estimate. This method is best used for analyzing geopressured gas reservoirs when the pressure- and time-dependent formation compressibility values are known.

Roach's method

Roach's solution plots are used to estimate the IGIP for the four case studies, and the value obtained in each case is greater than the volumetric estimate. The NS2B reservoir solution plot shows so much scatter in the plot and it was difficult fitting a straight line, this also applies to the Miocene reservoir. Usually the straight lines in Roach's plots are fitted such that the intercept is negative. Deviations of the data from the straight line could be attributed to water

influx at a particular time in the production history of the reservoir. Roach's method is a very useful tool to simultaneously estimate the IGIP and the effective formation compressibility. The reservoir drive mechanism could be estimated from the value of the effective compressibility. Effective compressibility in the order of 18 x 10^{-6} psi^{-1} for the NS2B reservoir and 18.4 x 10^{-6} psi^{-1} for the Cajun reservoir are estimated, indicating support from water influx. The major challenge is applying this technique is that the solution plot may assume a variety of shapes. These apparent meanderings of a theoretical straight line may be unsettling to the uninitiated. Therefore, curve shapes have been correlated with specific drive mechanisms.

Bernard's method

Bernard's method is very sensitive to scatter in the data. If the data shows a little scatter, the method overestimates the IGIP. This overestimation is clearly observed in the values of IGIP obtained for the four reservoir case studies being considered. Least squares of all the data results in absurd values of IGIP, and can even result in negative compressibility values. This method is also sensitive to the initial reservoir pressure. If Bernard's method was plotted instead of the least squares, as A on the y-axis and B on the x-axis, the bad data points could be eliminated and the answer could be improved.

Fetkovich et al. method

The method of Fetkovich et al is used to estimate the IGIP for the Anderson "L" reservoir and the Cajun reservoir. For the case of the Cajun reservoir, only a portion of the data was used by the author to find the possible match. If all the data for the Cajun reservoir were used to find IGIP and $c_e(p)$, the match between $c_e(p)$ calculated and the backcalculated $c_e(p)$ for various values of IGIP would be rather difficult.

Fetkovich et al used formation compressibility of 4 x 10^{-6} psi^{-1} to estimate IGIP of 650 BSCF for the Cajun reservoir, and an associated water volume ratio of 0.2 using the pressure data above 6850 psi. For the Anderson "L" reservoir, Fetkovich et al calculated an IGIP of 76 BSCF and an associated water volume of 2.25 the reservoir volume assuming formation compressibility of 3.2 x 10^{-6} psi^{-1} by using a total compressibility match procedure.

Amabatha's method

Possible range of answers for the estimated IGIP is reported for the Anderson "L" reservoir and the Cajun reservoir. Although the method has the problem of non-uniqueness in type-curve matching, it gives possible answers for the IGIP that falls closely to the IGIP estimated by other methods considered in this study. This non-uniqueness in type-curve matching has more effect on C_D than on the IGIP.

Havlena and Odeh method

Havlena & Odeh method is used to estimate the IGIP assuming that the major drive mechanism of gas production form abnormal pressured gas reservoirs is water influx. However, if the reservoir is volumetric, the method can still be used to estimate the IGIP and the average effective compressibility. Solution plot of Havlena & Odeh method has the advantage of estimating the IGIP without prior assumption of the aquifer size and/or formation compressibility. However, the method is very sensitive to the initial pressure and early production data. The outrageous values of G obtained as shown in the table could be attributed to calculations done based on limited data, hence assuming volumetric depletion. The effect of water influx and water production was not included at all. Therefore, in using this method it is pertinent to have complete information about the reservoir such as water influx and water production in order to get reasonably accurate estimates of IGIP.

Becerra- Arteaga method

This method yields estimates of IGIP within an acceptable range compared to the values obtained via the other methods considered in this study. This method adequately predicted future performance of these geopressured gas reservoirs using early production data, and does not require the z-factor to be calculated at each pressure. It also allows us to quantify variable rock compressibility effects.

Elsharkawy's method

This method which is similar to Roach's solution plot, requires neither prior assumptions (formation compressibility, or aquifer size) nor matching procedure. Elsharkawy's method is used to simultaneously estimate the IGIP and a constant (slope) that can be used to calculate the aquifer size or non-pay sand, and predict the reservoir prevailing production mechanism. This method accounts for the downward curvature of the P/z vs Gp plot, as being caused by water influx from aquifer, water influx from shales, and formation of condensate below dew point which reduce gas permeability. The values of IGIP obtained via this method are within reasonable range when compared to the values obtained via other methods. More importantly, this method successfully estimates the IGIP after production of 15% of the IGIP and predicts the reservoir prevailing production mechanism.

SENSITIVITY ANALYSIS

This entails changing some input variables and observing the effect of the changes on the output variable, which is G in this case. In sensitivity analysis, the input parameters in forecast calculations are varied around a base value. Sensitivity analysis can be performed on any of the input variables. The usual approach is to hold all other variables in the model constant and vary every other parameter to determine the influence of these changes on the output variable. The purpose is to judge the impact of variations in variables on the base case value of the output variable. Sensitivity analysis is a deterministic modeling technique used to test or assess the impact of a change in a value of independent variable on a dependent variable.

The sensitivity analysis of the impact of some input variables like initial pressure and formation compressibility will be done with some of the Material Balance Techniques discussed previously, and the NS2B reservoir will be used as the case study.

Table 4.10	SENSITIVITY ANALYSIS OF NS2B reservoir parameters				
Input parameters					
	Base value	+5%	-5%	+10%	-10%
Pi (psi)	8921	9367	8475	9813	8029
c_f (psi^{-1})	2.19E-05	2.3E-05	0.000020805	0.00002409	0.00001971
c_w(psi^{-1})	3.00E-06	3.15E-06	0.00000285	0.0000033	0.0000027
S_{wi}	0.34	0.357	0.323	0.374	0.306
c_{gi}(psi^{-1})	3.00E-05	3.15E-05	0.0000285	0.000033	0.000027
z_i	1.473	1.54665	1.39935	1.6203	1.3257
c_e(psi^{-1})	3.47273E-05	3.65E-05	3.29909E-05	0.0000382	3.12545E-05
α	1.07	1.1235	1.0165	1.177	0.963
T(^{0}R)	710				
B_{gi}(scf/ft3)	302.71	288.29	318.64	275.19	336.34
	302.71				

Table 4.11 Sensitivity analysis of parameters in the Hammerlindl's model

Changing Input parameters		HAMMERLINDL				
		Base value	+5%	-5%	+10%	-10%
	Gapp	220	220	220	220	220
pi	Gpr	0.520	0.470	0.583	0.429	0.662
cf	Gpr	0.520	0.509	0.532	0.497	0.545
cw	Gpr	0.520	0.520	0.521	0.519	0.521
Swi	Gpr	0.520	0.513	0.527	0.506	0.534
pi	G	**114**	**103**	**128**	**94**	**146**
cf	G	**114**	**112**	**117**	**109**	**120**
cw	G	**114.5**	**114.3**	**114.6**	**114.2**	**114.7**
Swi	G	**114.5**	**112.9**	**116.0**	**111.3**	**117.5**

It is clearly seen from the values of G obtained that any small error in the value of the initial reservoir pressure will result in significant errors in the estimated value of G obtained via Hammerlindl's method. However, the change or error in values of the compressibilities and water saturation do not produce significant errors in estimated IGIP.

Table 4.12 Sensitivity Analysis of formation compressibility in the Ramagost-Farshad Model

				RAMAGOST-FARSHAD		Changing c_f			
Pressure	**z**	**Gp**	**P/z**	**Δp**	**y-variable (base value)**	**+5%**	**-5%**	**+10%**	**-10%**
psia		**BSCF**	**psia**	**pi-p**	**p/z(1-c_e(pi-p)**				
8921	1.473	0	6056	0	6056	6056	6056	6056	6056
8845	1.465	0.66	6038	76	6022	6021	6022	6020	6023
8322	1.4	3.33	5944	599	5821	5814	5827	5808	5833
7417	1.288	10.4	5759	1504	5458	5443	5473	5428	5488
6838	1.219	15.59	5610	2083	5204	5183	5224	5163	5244
6064	1.13	23.97	5366	2857	4834	4807	4861	4781	4887
5490	1.075	27.85	5107	3431	4498	4468	4529	4438	4559
4781	0.967	33.7	4944	4140	4233	4198	4269	4162	4304
4104	0.887	40.1	4627	4817	3853	3814	3892	3775	3930
				intercept	6042.1	6039.7	6044.5	6037.3	6046.8
				slope	53.985	54.963	53.007	55.941	52.029
				G(BSCF)	**112**	**110**	**114**	**108**	**116**

Table 4.13 Sensitivity analysis of changing initial pressure in the Ramagost-Farshad Model

				RAMAGOST FARSHAD		Changing P_i			
Pressure	**z**	**Gp**	**P/z**	**Δp**	**y-variable (base value)**	**+5%**	**-5%**	**10%**	**-10%**
psia		**BSCF**	**psia**	**pi-p**	**p/z(1-ce(pi-p)**				
8921	1.473	0	6056	0	6056	6359	5754	6662	5451
8845	1.465	0.66	6038	76	6022	5928	6115	5835	6209
8322	1.4	3.33	5944	599	5821	5729	5913	5636	6005
7417	1.288	10.4	5759	1504	5458	5369	5547	5279	5636
6838	1.219	15.59	5610	2083	5204	5117	5291	5030	5378
6064	1.13	23.97	5366	2857	4834	4751	4917	4668	5000
5490	1.075	27.85	5107	3431	4498	4419	4578	4340	4657
4781	0.967	33.7	4944	4140	4233	4157	4310	4080	4387
4104	0.887	40.1	4627	4817	3853	3781	3925	3710	3996
				G	**112**	**106**	**119**	**100**	**127**

Table 4.14 Changing input variables in Ramagost Farshad model

	RAMAGOST-FARSHAD MODEL			
	Effect of changing variables on IGIP (BSCF)			
		Pi	c_e	c_f
-10%	8029	**127**	**116**	116
-5%	8475	**119**	**114**	114
base value	8921	**112**	**112**	112
5%	9367	**106**	**110**	110
10%	9813	**100**	**108**	108

Table 4.15 Changing initial pressure in Roach's model

	ROACH	
Effect of changing initial pressure on IGIP		
	P_i	G
-10%	8029	**192**
-5%	8475	**182**
base value	8921	**159**
5%	9367	**175**
10%	9813	**177**

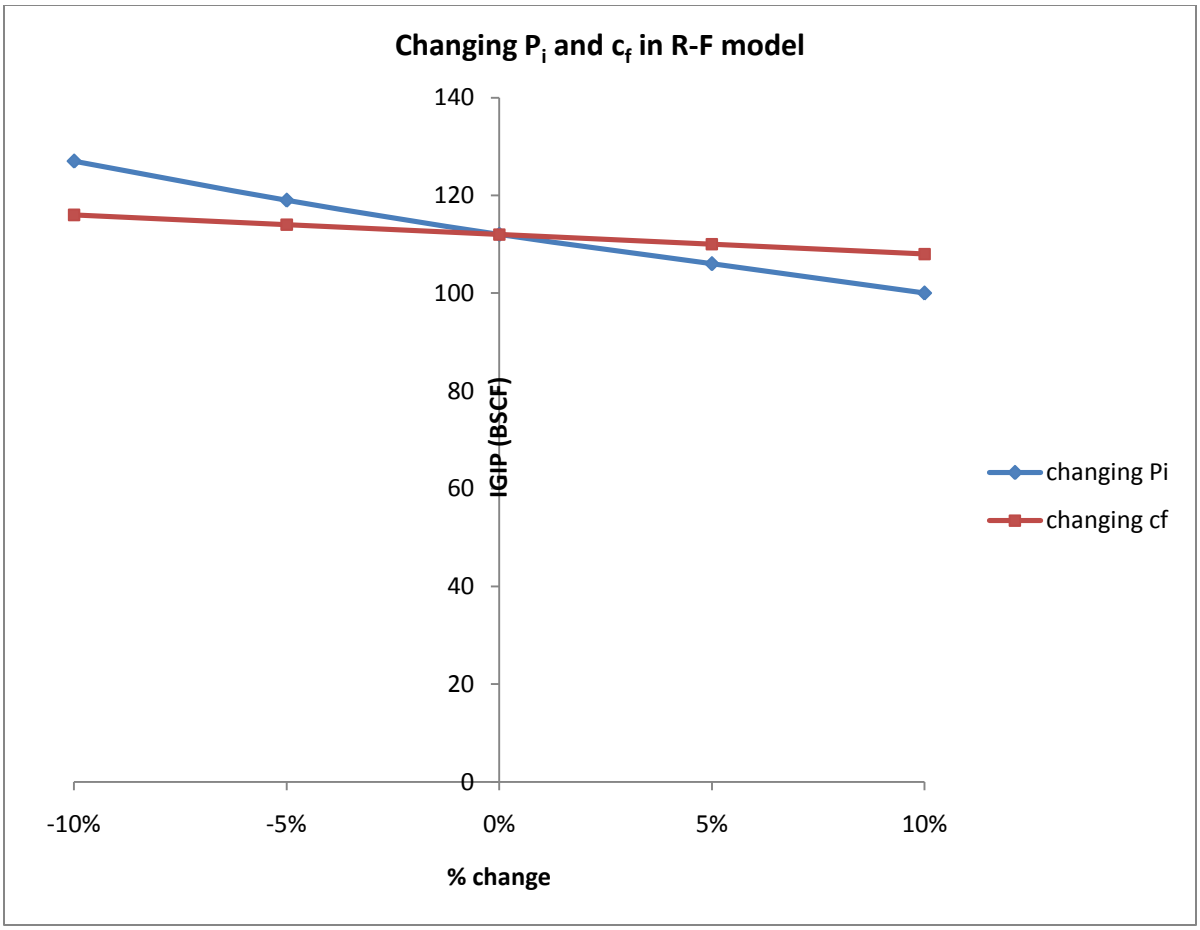

Figure 4.11 Sensitivity of initial pressure and formation compressibility on G values in Ramagost-Farshad's model

From the above plot, it is clearly observed that the value of IGIP is more sensitive to the value of initial pressures than it is to the value of formation compressibility. Hence, the petroleum engineer should ensure that the value of the initial reservoir pressure is obtained via very accurate methods, because any little error in the value of the initial reservoir pressure can result in overestimating the IGIP for overpressured gas reservoirs therefore resulting in unnecessary field development costs.

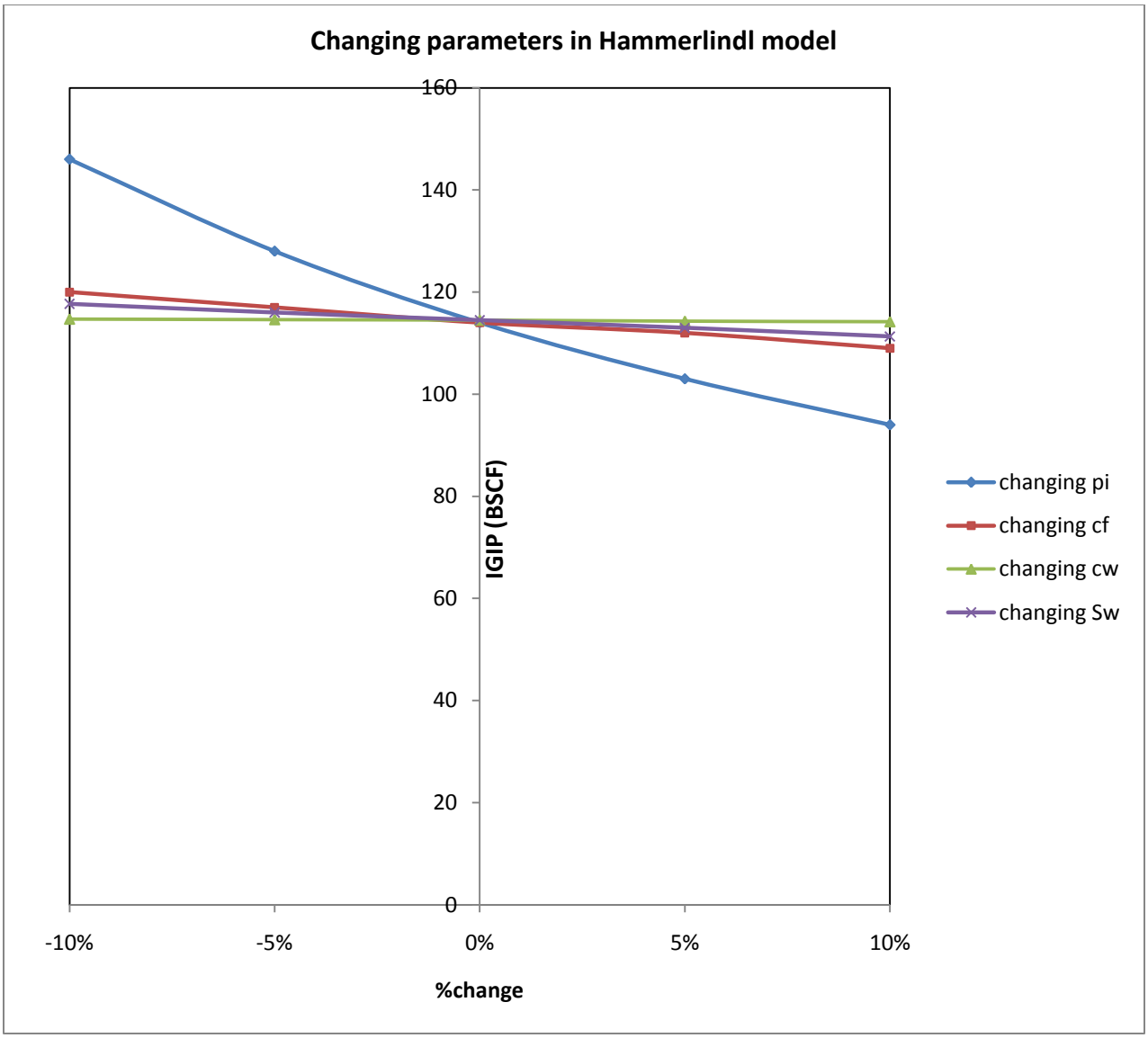

Figure 4.12 Sensitivity Analysis of input parameters in the Hammerlindl model

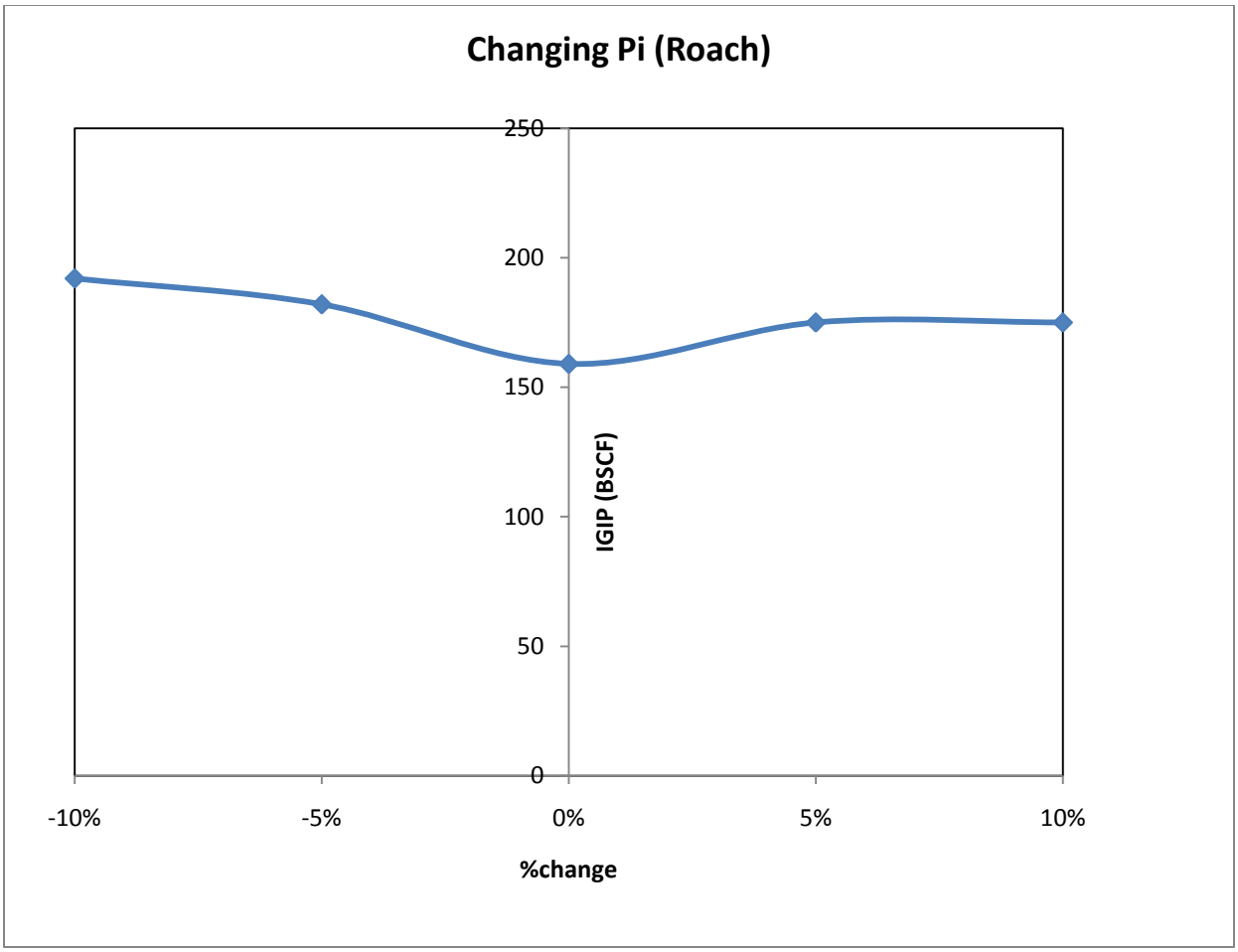

Figure 4.13 Sensitivity of initial pressure on G values in Roach's model

From the above sensitivity plot, it is observed that a little error in the value of the initial pressure, both above and below the original pressure value will result in a significant overestimation of the initial gas-in-place. This shows that the value of G obtained via Roach solution plot technique is highly sensitive to the value of the initial reservoir pressure and the early data. A small change in the value of the initial pressure or the early data would change the shape of the plot to concave upward and hence the value of G.

CHAPTER 5 - SUMMARY

The following conclusions may be drawn from this study of MB reserves determination techniques of overpressured gas reservoirs.

- Accurate estimation of the initial gas-in-place (IGIP) plays an essential role in the evaluation, analysis, prediction of future performance, and making economic decisions regarding development of gas reservoirs. Estimation of IGIP is also needed for planning long term gas contracts and commitment to supply gas to users.
- Accurate determination of the IGIP for geopressured gas reservoirs is quite often difficult because of the effect of formation compressibility and the uncertain presence of water influx from small, associated aquifer or adjacent shales.
- In the process of generating a traditional P/z plot, the well is shut-in at several points along its producing life and the average reservoir pressure is obtained for each point from a properly conducted buildup test and interpretation. The duration of the shut-in is often not long enough to directly measure current average reservoir pressure. As a result, problems with testing and interpretation comprise some of the key causes of erratic pressure data often observed in material balance plots, and this result in a scatter plot for some of the MB techniques making it difficult to fit a straight line through the data points.
- Elsharkawy's method for estimating IGIP in overpressured gas reservoirs requires no prior assumptions about the formation compressibility, aquifer size, or volume of the adjacent shales, and the method can successfully estimate the IGIP after production of 15% of the IGIP for an overpressured gas reservoir and also predict the prevailing production mechanism.
- Hammerlindl's, and Ramagost & Farshad method are valid means to predict the IGIP from early data provided the P/z vs G_p plot exhibit downward curvature and the reservoir is volumetric.
- Solution plot of Havlena and Odeh method is very useful tool to estimate the IGIP for abnormal pressure gas reservoirs without prior knowledge or assumptions about the

aquifer size or the formation compressibility. The catch-all slope from the plot can be used to calculate the effective reservoir compressibility assuming the reservoir is volumetric or the aquifer size assuming normal formation compressibility. However, the method is very sensitive to the initial pressure and early production data. The outrageous values of G obtained as observed in the four case studies could be attributed to calculations done based on limited data, hence assuming volumetric depletion. The effect of water influx and water production was not included at all. Therefore, in using this method it is pertinent to have complete information about the reservoir such as water influx and water production in order to get reasonably accurate estimates of IGIP.

- Roach's plots of most of the cases considered in this study yielded outrageous values of the IGIP and the formation compressibility compared to the other methods. This method is very sensitive to the value of the initial pressure and the early data. A small change in the value of the initial pressure or the early data would change the shape of the plot and could even lead to so much scatter in the plot that result in absurd values of IGIP. The solution plot method allows the estimation of IGIP in volumetric gas reservoirs as well as water-drive gas reservoirs. The curved nature of the P/z plot is usually due to the effects of water influx.
- The use of Bernard's method of least squares technique will only yield meaningful results after non-linearity of the P/z plot begins. It is important to have good data. Using this method on scattered data will sometimes yield absurd results, as was the case in the IGIP estimates for the four geopressured gas reservoirs considered in this study. Bernard's method is very sensitive to the error in the initial reservoir pressure and the scatter in the early data. Since most petroleum engineers are not looking for in-depth investigation of the scatter in the data, one recommends that Bernard's equation be plotted, instead of the least square, as A on the y-axis and B on the x-axis. The graphical solution in this case would eliminate the bad data and the answer would be improved.

- Fetkovich's method is very sensitive to the value of the initial pressure, the type of the data, and the assumed value of the initial pressure. In this study, it was impossible to estimate the IGIP for three cases.
- Although Ambatha's method has the problem of non-uniqueness in type-curve matching, the methods predicted range of the IGIP fall closely to the IGIP estimated by the other methods. This non-uniqueness in type-curve matching has more effect on C_D than on the IGIP.
- Most of the methods analyzed in this study produce unreliable estimate of the IGIP based on early data only. Unfortunately, this is the time when reliable estimate of the IGIP is vital for economic decision regarding the development of such gas reservoirs.
- If the production performance data from an abnormally-pressured gas reservoir are analyzed by including the effects of formation and water compressibility terms and ignoring other drive mechanisms, such as shale water influx, it is possible to infer high "apparent" formation compressibility. Thus, a reliable knowledge of reservoir drive mechanisms and formation compressibility at high pressures is important to analyze production performance data for abnormally-pressured gas reservoirs.
- Non-uniqueness problem in analyzing production performance of abnormally-pressured gas reservoirs have been demonstrated.

CHAPTER 6 - CONCLUSIONS

1. As a result of the present study, it is recommended that several techniques be considered for the best estimate of the IGIP and analysis of the possible driving mechanism of abnormally pressured gas reservoirs.
2. Sensitivity analysis shows that a small error in the value if the initial reservoir pressure can result in a large error in the estimated value of IGIP, hence unnecessary field development costs.
3. The use of a particular material balance technique is dependent on the data available at the time the IGIP and reserves is being estimated. It also depends on the primary drive mechanism of the reservoir, because some techniques can only be applied to volumetric-depleting overpressured gas reservoirs while others can be applied to water-drive gas reservoirs.
4. The dual error in mistaking both the drive mechanism and the IGIP is one that has been pointed to frequently in literature but obviously the warning has not been stated forcibly enough because the error is still of frequent occurrence in the industry.
5. Incorrect estimate of G will result in investment that was never needed. Hence the engineer must be articulate in the process used in estimating G.

NOMENCLATURE

P = pressure, psi

z = gas deviation factor

G_p = cumulative gas produced, BSCF or MMSCF

G_a = apparent gas-in-place, BSCF or MMSCF

G_o = overestimate of IGIP, BSCF or MMSCF

G_u = underestimate of IGIP, BSCF or MMSCF

G_r = volume of gas remaining at latter conditions, BSCF or MMSCF

G or IGIP = Initial gas-in-place, BSCF or MMSCF

ft = feet

c_w = water compressibility, psi^{-1}

c_g = gas compressibility, psi^{-1}

c_{gr} = rock-grain compressibility , psi^{-1}

c_f = formation compressibility, psi^{-1}

c_B = bulk compressibility, psi^{-1}

n = no of moles

V = volume, scf or ft^3

BHP = Bottom-hole pressure, psi

A = area, Acres

S_{gi} = initial gas saturation

S_{wi} = initial/connate water saturation

B_g = gas formation volume factor, bbl/scf

Φ = porosity

GIP = gas in place

P/z = pressure/ gas deviation factor

i = initial

V_p = pore volume of the reservoir

V_w = volume of water at reservoir conditions

V_g = volume of gas at reservoir conditions

G_{pr} = ratio of conventional material balance equation to the material balance equation with formation compressibility and water expansion terms or correction factor

ΔV = change in gas volume due to rock and water compressibility

W_{en} = net water influx, STB

W_e = water influx, bbl

B_w = water formation volume factor, bbl/scf

W_p = produced water from the reservoir, bbl

W_{sh} = water influx from shales, STB

R_s = solution gas-oil ratio

f(p,t) = pressure-/time- dependent potential function

α = aquifer constant

β = constant of proportionality

E_g= gas expansion factor

R_{sw} = solution gas-/oil- ratio of connate water, scf/STB

M = total associated water volume ratio in aquifer or non-pay

C_{tw} = total compressibility of water, psi^{-1}

$\bar{c_e}$ = average effective compressibility, psi^{-1}

G_{pD} = dimensionless cumulative gas produced

C_s = compressibility of shale, psi^{-1}

C_a = compressibility of aquifer, psi^{-1}

V_a = volume of aquifer

G_{LP} = cumulative volume of condensate produced, bbl

REFERENCES

1. Ambastha A.K: “Analysis of Material-Balance Equations for Gas Reservoirs”, paper CIM/SPE 90-36 presented at the 1990 Petroleum Society of CIM/SPE International Technical Meeting, Calgary, 10-13 June
2. Azari, M.: “Material Balance Equation in Geopressured Reservoirs”, paper presented at the Annual Geothermal Resources Council Meeting, Sparks, NV, October 11-14, 1987.
3. Aziz, R.M: “Deliverability Projection Model for Overpressured Gas-Condensate Reservoirs”, SPE Paper 13706, presented at the 4th Society of Petroleum Engineers of AIME Middle East Oil Technical Conference, Bahrain, March 11-14, 1985.
4. Becerra-Arteaga, T.: “Analysis of Abnormally Pressured Gas Reservoirs,” PhD dissertation, Texas A&M U., College Station, TX (December 1991)
5. Begland, T.F and Whitehead, W.R : “Depletion Performance of Volumetric High-Pressured Gas Reservoirs,” SPERE (August 1989)279; Trans., AIME, 287
6. Bernard W.J, : Gulf Coast Geopressured Gas Reservoirs: Drive Mechanism and Performance prediction,” paper SPE 14362 presented at the 1985 SPE Annual Technical Conference Exhibition, Las Vegas, Nevada, 22-25 September 1985
7. Bernard W.J,: “Reserves Estimation and Performance Prediction for Geopressured Gas Reservoirs”, Journal of Petroleum Science and Engineering, (August 1987)
8. Bourgoyne, A.T, Hawkins, M.F, Lavaquial F.P and Wickenhauser T.L: “Shale Water as a Pressure Support Mechanism in Superpressure Reservoirs”, paper SPE 3851
9. Dickinson,G.: “Geological Aspects of Abnormal Reservoir Pressures in Gulf Coast Louisiana,” AAPG Bull (Feb 1953) 37, No 2, 410
10. Donson,C.R. and Standing, M.B., 1944; “PVT and Solubility Relations for Natural Gas-Water Mixtures,” Drill.and Prod. Prac., API, 173
11. Dranchuk,P and Abdou-Kazeem, J.H,: “Calculations of z-factor for Natural Gases Using Equation of State,” JPT (July-Sept 1975), 34-36
12. Duggan, J.O : “The Anderson ‘L’ : An Abnormally-Pressured Gas Reservoir in South Texas”, Jour. Pet. Tech (Feb 1971) 132-138

13. Elsharkawy, A.M.: “Analytical and Numerical Solutions for Estimating the Gas-in-place for Abnormal Pressure Reservoirs”, SPE paper No 29934, 1995.
14. Elsharkawy, A.M.: “MB solution for High Pressure Gas Reservoirs”, SPE paper No 35589, 1996.
15. Fetkovich M.J, Resse D.E and Whitson C.H : “Application of a General Material Balance for High-Pressure Gas Reservoirs”, paper SPE 22921 presented at the 1991 SPE Annual Technical Conference and Exhibition, Dallas 6-9 October
16. Geer, E.C and Sharer, J.C: “Unconventional Geopressured Gas Recovery, Economics and Research”, paper presented at the 7th Energy Technology Conference, Washington, D.C, March 24-26, 1980
17. Hammerlindl, D.J. “Predicting Gas Reserves in Abnormally Pressured Reservoirs,” paper SPE 3479 presented at the 1971 SPE annual meeting, New Orleans, 3-6 October.
18. Harville, D.W and Hawkins, M.F: “Rock Compressibility and Failure as Reservoir Mechanisms in Geopressured Gas Reservoirs”, J. Pet Tech. (Dec 1969) 1528-1530
19. Havlena,D and Odeh, A.S: “The Material Balance Equation as an Equation of Straight Line,” JPT (August 1963), 896-900
20. Lowery, J.D, : “Reservoir Engineering Study: Geopressured Gas Reservoirs”, SPE of AIME Unsolicited Paper 13417, November 1984.
21. Mattar,L., McNeil, R ., The ‘Flowing’ Gas Material Balance; Journal of JCPT, Vol 37 #2, 1998.
22. Perry D.R Jr. : “Statistical Study of Geopressures Reservoirs in South West Louisiana”, paper SPE 3888 prepared for presentation for the Abnormal Subsurface pressure Symposium of the SPE, 1972
23. Poston S.W and Chen H.Y : “The Simultaneous Determination of Formation Compressibility and Gas-in-Place in Abnormally Pressured Reservoirs,” paper SPE 16227 presented at the 1987 SPE Production Operations Symposium, Oklahoma City, Oklahoma, 8-10 March

24. Poston S.W, Chen H.Y and Akhtar M.J: “Differentiating between Formation Compressibility and Water-Influx effects in Overpressured Reservoirs”, SPERE (August 1994)
25. Prasad R.K and Rogers, L.A : “Superpressured Gas Reservoirs : Case Studies and a Generalized Tank Model”, paper SPE 16861 presented at the 62nd Annual Meeting of SPE of AIME, Dallas, TX (Sept 27-30, 1987).
26. Raghavan, R., Scorer J.D T, and Miller F.G : “An Investigation by Numerical Methods of the Effect of Pressure-Dependent Rock and Fluid Properties on Well Flow Tests”, Society of Petroleum Engineers Journal (June 1972)
27. Ramagost, B.P and Farshad F.F: “P/z Abnormally pressured Gas Reservoirs”, paper SPE 10125 presented at the 1981 SPE Fall meeting, San Antonio, Texas, 5-7 October
28. Roach R.H: “Analyzing Geopressured Reservoirs- A Material-Balance Technique,” paper SPE 9968 available from SPE, Richardson, Texas (1981)
29. Samaniego F, and Cinco-Ley H, : “On the Determination of the Pressure-Dependent Characteristics of a Reservoir Through Transient Pressure Testing.” SPE Paper 197774, presented at the 64th Annual Technical Conference and Exhibition of the Society of Petroleum Engineers, San Antonio, TX, October 8-11, 1989
30. Stelly, O.V, & Farshad, F.F.: “Predicting Gas in Place in Abnormal Reservoirs,” Pet Eng. Int. June 1981
31. Steven W. Poston and Robert R. Berg, *Overpressured Gas Reservoirs*, Society of Petroleum Engineers Textbook series, Texas, 1997
32. Vu, T., Chen, H.Y and Poston, S.W.: “Using Short-Term Pressure Tests to Calculate Gas Reserves,” paper SPE 20111 presented at 1990 SPE Permian Basin Oil and Gas Recovery Conference, Midland Texas, 8-9 March
33. Walter H.F and Donald J.T. : “Parameters for Identification of Overpressured Formations”, paper SPE 3223 presented at SPE meeting in Dallas Texas, 1971
34. Wang, B and Teasdale T.S: “GASWAT-PC: A Microcomputer program for Gas Material Balance with Water Influx,” paper SPE 16484 ,presented at the 1987 SPE Petroleum Industry Application of Microcomputers, Montgomery, Texas, 23-26 June 1987

APPENDIX A

Calculation of IGIP for the Anderson "L" reservoir using different MB Techniques

Hammerlindl's method

For the Anderson "L" reservoir, extrapolation of the early data to the Gp axis yields an apparent gas-in-place of 112 BSCF as shown in figure (4.1)

From equation (3.17)

$G = G_a G_{pr}$

Where $G_a = 112\ BSCF$

and $G_{pr} = \frac{B_{gi} - B_{g2}}{B_{gi} - B_{g2} + \frac{B_{g2}(P_i - P_2)(c_f + c_w S_{wi})}{1 - S_{wi}}}$

where $B_g = \frac{0.00504\ zT}{P}$

at initial pressure of 9507 psi and a later pressure of 7002 psi

$$B_{gi} = \frac{0.00504\ z_i T}{P_i} = \frac{0.00504(1.44)(266 + 460)}{9507} = 5.542x10^{-4} bbl/scf$$

$$B_{g2} = \frac{0.00504\ z_2 T}{P_2} = \frac{0.00504(1.176)(266 + 460)}{7002} = 6.145x10^{-4} bbl/scf$$

Step 2: Solve for G_{pr}

$$G_{pr} = \frac{B_{gi} - B_{g2}}{B_{gi} - B_{g2} + \frac{B_{g2}(P_i - P_2)(c_f + c_w S_{wi})}{1 - S_{wi}}}$$

$$= \frac{5.542x10^{-4} - 6.145x10^{-4}}{5.542x10^{-4} - 6.145x10^{-4} + \frac{6.145x10^{-4}(9507 - 7702)(19.5x10^{-6} + (3.4x0.35x10^{-6})}{1 - 0.35}}$$

$$= 0.616$$

Step 3: Calculate actual G

$$G = G_a G_{pr}$$

$$G = 112x0.616 = \mathbf{69\ BSCF}$$

The second method entails the use of average system compressibility

From equation (3.13)

$$Actual\ GIP, G = \frac{apparent\ GIP, G_a}{F_c} = \frac{112}{F_c}$$

Where $F_c = \frac{\bar{c}_e}{\bar{c}_g} = \frac{\left[\frac{c_{ei}}{c_{gi}} + \frac{c_{en}}{c_{gn}}\right]}{2}$ and $c_e = \frac{c_{gi} S_{gi} + c_w S_{wi} + c_f}{1 - S_{wi}}$

The values of $S_{wi} = 0.35, c_f = 19.5\ x\ 10^{-6} psi^{-1}$ and $c_w = 3.4\ x\ 10^{-6} psi^{-1}$ yields a value of $c_e = 31.9\ x\ 10^{-6} psi^{-1}$

And $F_c = \frac{\bar{c}_e}{\bar{c}_g} = \frac{\left[\frac{c_{ei}}{c_{gi}} + \frac{c_{en}}{c_{gn}}\right]}{2} = 1.66$

$$G = \frac{112}{F_c} = \frac{112}{1.66} = 67.45\ BSCF$$

Ramagost-Farshad method

Sample calculations for obtaining the y-variables for the Ramagost Farshad method has been demonstrated in Chapter 3. The values obtained are tabulated and a plot is made. From a plot of $\frac{P}{z}(1 - c_e(p_i - p)$ vs Gp, the intercept is $\frac{P_i}{Z_i}$ and the slope = $-\frac{P_i}{z_i G}$ and by changing the subject of the formula, G can be obtained.

$$G = \frac{intercept}{slope}$$

For the Anderson "L" reservoir case as shown in figure 3.5, this yields a value of **70BSCF**.

Roach Solution plot

The y-variable is defined as

$$Y = \frac{1}{p_i - p}(\frac{p_i z}{p z_i} - 1)$$

And the x-variable as

$$X = \frac{G_p}{p_i - p}(\frac{p_i z}{p z_i})$$

A table of values is generated for each value of pressure and the plot of Y vs X yields an approximate straight line whose $slope = \frac{1}{G}$ and intercept = ($-c_e + W_{en}$).

For the Anderson "L" reservoir, this yields an IGIP of 78.5 BSCF as seen in figure 3.6. Detailed calculations can be seen in chapter 3.

Becerra-Arteaga Method

For this method, the first thing to do is to obtain the value of α. Thereafter the y-variables can be obtained using the following equation

$$y_{variable} = \frac{p_i}{z_i}\left[\frac{\alpha p}{\alpha p + (p_i - p)}\right]$$

The values are tabulated and plotted against Gp. The slope = $-\left(\frac{p_i}{z_i G}\right)$ and G can therefore be obtained.

The second method entails calculating G values for each data point using the following equation

$$G = G_p\left[1 + \frac{\alpha p}{p_i - p}\right]$$

Then the values of calculated G are plotted against Gp and the best average value is obtained as the IGIP.

Table A1 – Calculated values of the variables used to obtain G for the Anderson "L" reservoir using Ramagost-Farshad, Roach and Becerra-Arteaga methods

ANDERSON "L" PRESSURE-PRODUCTION HISTORY						Ramagost Farshad	Roach		Becerra-Arteaga	
BHP	Z Factor	P/Z	CUM. GAS	CONDENSATE	∆p= pi - p	y variable	y-variable	x-variable	Method 1 -- y-variable	Method 2 -- OGIP
(psia)			MMCF	MBBL	psi	(p/z)(1-ce(Δp)	(1/∆p)((piz/pzi)-1)	(Gp/Δp)(piz/pzi)		
9507	1.44	6602	0	0	0	6602			6602	
9292	1.418	6553	392.5	29.9	215	6508	3.49	1.84	6528	35.00
8970	1.387	6467	1642.2	122.9	537	6356	3.88	3.12	6414	57.60
8595	1.344	6395	3225.8	240.9	912	6209	3.55	3.65	6276	65.24
8332	1.316	6331	4260.3	317.1	1175	6094	3.64	3.78	6175	65.89
8009	1.282	6247	5503.5	406.9	1498	5949	3.79	3.88	6048	65.53
7603	1.239	6136	7538.1	561.2	1904	5764	3.99	4.26	5880	68.94
7406	1.218	6080	8749.2	650.8	2101	5673	4.08	4.52	5796	71.66
7002	1.176	5954	10509.3	776.7	2505	5478	4.34	4.65	5617	70.44
6721	1.147	5860	11758.9	864.3	2786	5339	4.55	4.76	5487	69.63
6535	1.127	5799	12789.2	939.5	2972	5249	4.66	4.90	5398	70.16
5764	1.048	5500	17262.5	1255.3	3743	4843	5.35	5.54	5008	71.49
4766	0.977	4878	22890.8	1615.8	4741	4140	7.45	6.53	4438	69.83
4295	0.928	4628	28144.6	1913.4	5212	3859	8.18	7.70	4140	75.46
3750	0.891	4209	32566.7	2136	5757	3436	9.88	8.87	3767	75.84
3247	0.854	3802	36819.9	2307.8	6260	3043	11.76	10.21	3394	75.78

Bernard's method

The first step is to calculate the values of A and B as follows:

$$A = \frac{\frac{P}{Z} - \frac{P_i}{Z_i}}{\Delta p(P/Z)}$$

For example, at the 8970 –psia time-step,

$$A = \frac{\frac{P}{Z} - \frac{P_i}{Z_i}}{\Delta p(P/Z)} = \frac{6467 - 6602}{537(6467)} = -3.9x10^{-5}$$

$$B = \frac{\frac{P_i}{Z_i} G_p}{\Delta p(P/Z)} = \frac{6602(1.642)}{537(6467)} = 3.122$$

These set of calculations is carried out for each data point and the value of G is computed as follows:

$$G = \frac{\sum B \sum(\frac{B}{n}) - \sum(B^2)}{\sum(AB) - \sum A \sum(\frac{B}{n})}$$

For the Anderson "L" reservoir case, the value of G using this method is **91 BSCF**.

Table A2 – Calculated values of the variables used to obtain G for the Anderson "L" reservoir using Bernard's method

ANDERSON "L" PRESSURE-PRODUCTION HISTORY					BERNARD'S METHOD					
BHP	Z Factor	P/Z	CUM. GAS		A	B	AB	B^2	A/n	B/n
(psia)			MMCF	$\Delta p = pi - p$	(p/z)-pi/zi)/Δp(p/z)					
9507	1.44	6602	0	0						
9292	1.418	6553	392.5	215	-3.5E-05	1.839	-6.42E-05	3.383	-2.182E-06	0.211
8970	1.387	6467	1642.2	537	-3.9E-05	3.122	-1.21E-04	9.746	-2.428E-06	0.609
8595	1.344	6395	3225.8	912	-3.5E-05	3.652	-1.30E-04	13.334	-2.218E-06	0.833
8332	1.316	6331	4260.3	1175	-3.6E-05	3.781	-1.38E-04	14.295	-2.275E-06	0.893
8009	1.282	6247	5503.5	1498	-3.8E-05	3.883	-1.47E-04	15.074	-2.370E-06	0.942
7603	1.239	6136	7538.1	1904	-4E-05	4.260	-1.70E-04	18.144	-2.491E-06	1.134
7406	1.218	6080	8749.2	2101	-4.1E-05	4.522	-1.85E-04	20.444	-2.552E-06	1.278
7002	1.176	5954	10509.3	2505	-4.3E-05	4.652	-2.02E-04	21.640	-2.715E-06	1.353
6721	1.147	5860	11758.9	2786	-4.5E-05	4.755	-2.16E-04	22.615	-2.842E-06	1.413
6535	1.127	5799	12789.2	2972	-4.7E-05	4.900	-2.28E-04	24.005	-2.914E-06	1.500
5764	1.048	5500	17262.5	3743	-5.4E-05	5.536	-2.96E-04	30.648	-3.346E-06	1.916
4766	0.977	4878	22890.8	4741	-7.5E-05	6.535	-4.87E-04	42.700	-4.659E-06	2.669
4295	0.928	4628	28144.6	5212	-8.2E-05	7.703	-6.30E-04	59.335	-5.114E-06	3.708
3750	0.891	4209	32566.7	5757	-9.9E-05	8.874	-8.77E-04	78.743	-6.174E-06	4.921
3247	0.854	3802	36819.9	6260	-0.00012	10.213	-1.20E-03	104.311	-7.353E-06	6.519
Σ					**-0.00083**	**78.22465**	**-0.00509**	**478.41723**	**-0.00005**	**29.9011**

Elsharkawy's method

The first step is to compute the formation volume factor for each data point and the corresponding x and y variables as proposed by his technique.

For example, at the 8009 psia time-step,

$$Y = \frac{(G_p + G_{LP})B_g + W_p B_w}{(B_g - B_{gi})} = \frac{(5503.5 + 0.4069)0.5857 + 0}{(0.5857 - 0.5542)} = 102{,}412.3MMSCF$$

$$X = \left(\frac{p_i - p}{B_g - B_{gi}}\right) = \frac{9507 - 8009}{0.5857 - 0.5542} = 47590.17\text{psi/bbl/MMSCF}$$

Plotting Y against X yields the intercept as the value of the IGIP. The plot of Y vs X as shown in figure 3.9 yields an IGIP of **78BSCF.**

Table A3 – Calculated values of the variables used to obtain G for the Anderson "L" reservoir using Elsharkawy's method

ANDERSON "L" PRESSURE-PRODUCTION HISTORY					ELSHARKAWY				
BHP	Z Factor	P/Z	CUM. GAS	CONDENSATE	CONDENSATE, GLP	Bg			
(psia)			MMCF	MBBL	MMBBL	bbl/MMCF	Bg-Bgi	X	Y
9507	1.44	6602	0	0	0	0.55423	0		
9292	1.418	6553	392.5	29.9	0.0299	0.55839	0.0042	51676.293	52681.7
8970	1.387	6467	1642.2	122.9	0.1229	0.56578	0.0116	46454.84	80383.41
8595	1.344	6395	3225.8	240.9	0.2409	0.57216	0.0179	50839.051	102894.7
8332	1.316	6331	4260.3	317.1	0.3171	0.57793	0.0237	49571.763	103882.6
8009	1.282	6247	5503.5	406.9	0.4069	0.58570	0.0315	47590.017	102412.3
7603	1.239	6136	7538.1	561.2	0.5612	0.59628	0.0421	45269.331	106877.1
7406	1.218	6080	8749.2	650.8	0.6508	0.60177	0.0475	44189.503	110745.1
7002	1.176	5954	10509.3	776.7	0.7767	0.61454	0.0603	41529.836	107080.6
6721	1.147	5860	11758.9	864.3	0.8643	0.62445	0.0702	39673.317	104571.3
6535	1.127	5799	12789.2	939.5	0.9395	0.63102	0.0768	38698.738	105091.8
5764	1.048	5500	17262.5	1255.3	1.2553	0.66528	0.1111	33704.037	103419.4
4766	0.977	4878	22890.8	1615.8	1.6158	0.75008	0.1959	24206.67	87672.7
4295	0.928	4628	28144.6	1913.4	1.9134	0.79059	0.2364	22050.537	94143.72
3750	0.891	4209	32566.7	2136	2.136	0.86939	0.3152	18266.747	89842.29
3247	0.854	3802	36819.9	2307.8	2.3078	0.96237	0.4081	15337.633	86823.36

Table A4 – Calculated values of the variables used to obtain G for the Anderson "L" reservoir using Havlena and Odeh's method

ANDERSON "L" RESERVOIR -- - HAVLENA & ODEH

BHP	Z Factor	P/Z	CUM. GAS	CONDENSATE						
(psia)			MMCF	MBBL	∆p= pi - p	Bg	Eg	F	F/Eg	(Pi-P)/Eg
9507	1.44	6602	0	0	0	0.0005542	0	0		
9292	1.418	6553	392.5	29.9	215	0.0005584	4.2E-06	219166	52677.7	51.68
8970	1.387	6467	1642.2	122.9	537	0.0005658	1.2E-05	929132	80377.4	46.45
8595	1.344	6395	3225.8	240.9	912	0.0005722	1.8E-05	2E+06	102887	50.84
8332	1.316	6331	4260.3	317.1	1175	0.0005779	2.4E-05	2E+06	103875	49.57
8009	1.282	6247	5503.5	406.9	1498	0.0005857	3.1E-05	3E+06	102405	47.59
7603	1.239	6136	7538.1	561.2	1904	0.0005963	4.2E-05	4E+06	106869	45.27
7406	1.218	6080	8749.2	650.8	2101	0.0006018	4.8E-05	5E+06	110737	44.19
7002	1.176	5954	10509.3	776.7	2505	0.0006145	6E-05	6E+06	107073	41.53
6721	1.147	5860	11758.9	864.3	2786	0.0006244	7E-05	7E+06	104564	39.67
6535	1.127	5799	12789.2	939.5	2972	0.000631	7.7E-05	8E+06	105084	38.70
5764	1.048	5500	17262.5	1255.3	3743	0.0006653	0.00011	1E+07	103412	33.70
4766	0.977	4878	22890.8	1615.8	4741	0.0007501	0.0002	2E+07	87666.5	24.21
4295	0.928	4628	28144.6	1913.4	5212	0.0007906	0.00024	2E+07	94137.3	22.05
3750	0.891	4209	32566.7	2136	5757	0.0008694	0.00032	3E+07	89836.4	18.27
3247	0.854	3802	36819.9	2307.8	6260	0.0009624	0.00041	4E+07	86817.9	15.34

APPENDIX B

Calculation of IGIP for the Miocene reservoir using different MB Techniques

Table B1 – Calculated values of the variables used to obtain G for the Miocene reservoir using Ramagost-Farshad, Roach and Becerra-Arteaga methods

Pressure-production history for Miocene Reservoir						**Ramagost-Farshad**	**Roach**		**Becerra-Arteaga**
Pressure	z	Gp	Gp	P/z		**y variable**	**y-variable**	**x-variable**	**y-variable**
psi		MMSCF	BScf		**∆p= pi - p**	**(p/z)(1-ce(Δp)**	**(1/∆p)((piz/pzi)-1)**	**(Gp/Δp)(piz/pzi)**	
10984	1.65	0	0	6657	0	6657			
10156	1.58	482	0.482	6428	828	6113	4.3E-05	0.000603	6364
9924	1.56	648	0.648	6362	1060	5963	4.38E-05	0.00064	6278
9703	1.54	850	0.85	6301	1281	5824	4.41E-05	0.000701	6195
8936	1.49	2505	2.505	5997	2048	5271	5.37E-05	0.001358	5894
9222	1.46	2634	2.634	6316	1762	5659	3.06E-05	0.001575	6008
8789	1.44	3366	3.366	6103	2195	5312	4.13E-05	0.001673	5834
8313	1.39	3957	3.957	5981	2671	5037	4.23E-05	0.001649	5634
7064	1.25	5251	5.251	5651	3920	4342	4.54E-05	0.001578	5068
6250	1.15	6086	6.086	5435	4734	3914	4.75E-05	0.001575	4662
4928	0.96	7608	7.608	5133	6056	3296	4.9E-05	0.001629	3929
2723	0.88	10589	10.589	3094	8261	1584	0.000139	0.002758	2453

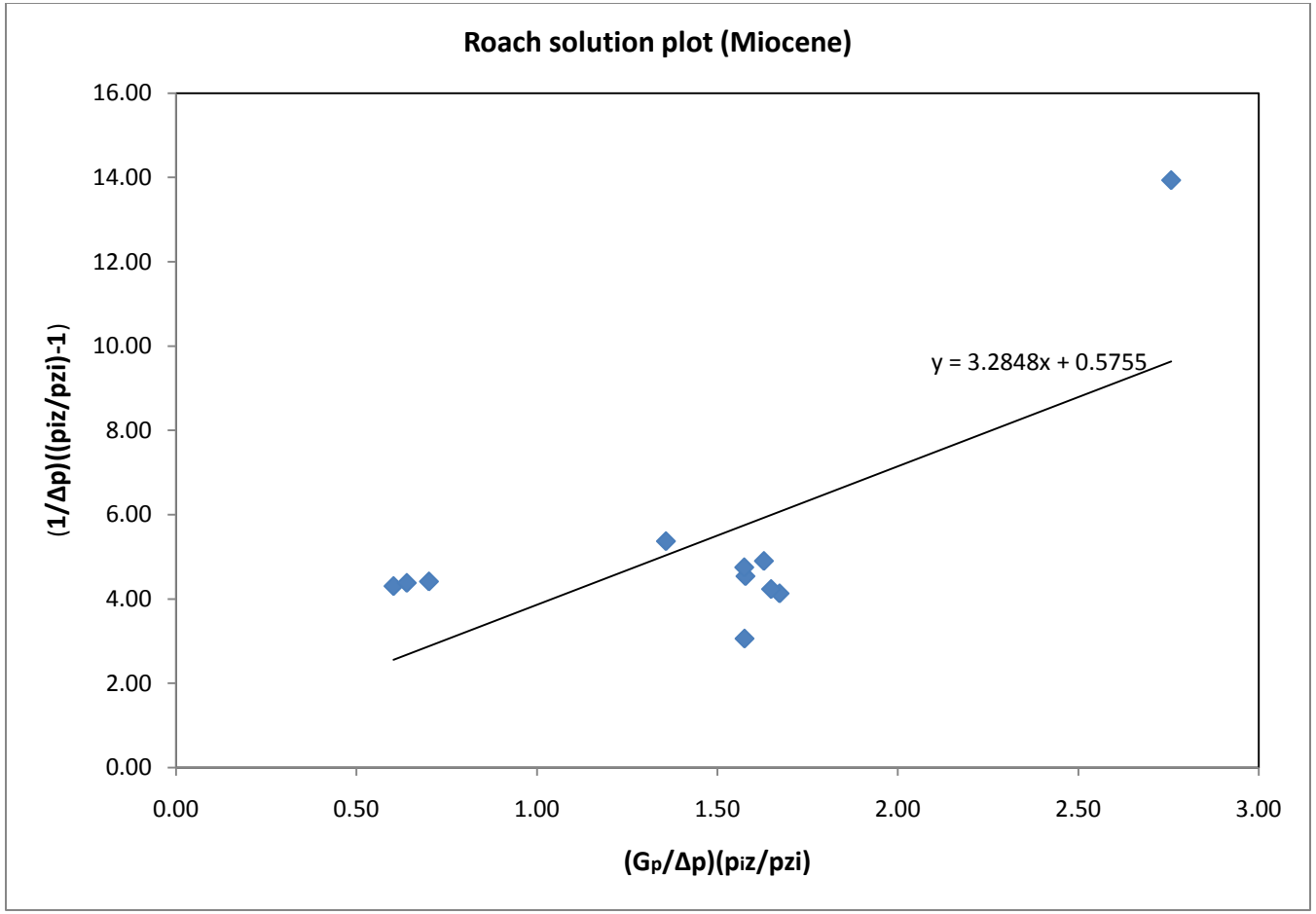

Figure B.1 Roach's solution plot for the Miocene reservoir

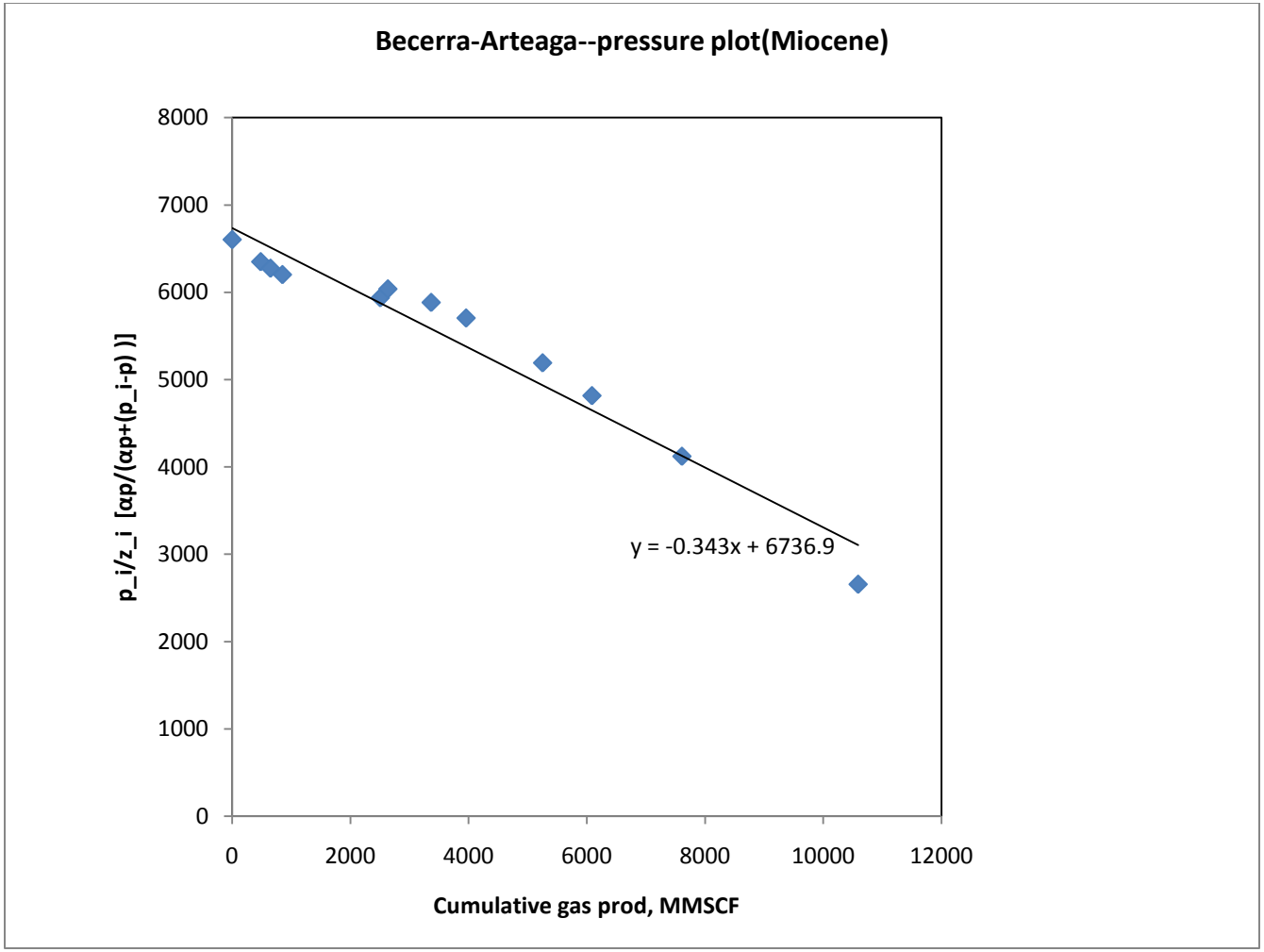

Figure B.2 Becerra-Arteaga's plot for the Miocene reservoir

Table B2 – Calculated values of the variables used to obtain G for the Miocene reservoir using Bernard's method

MIOCENE RESERVOIR PRESSURE-PRODUCTION HISTORY						BERNARD'S METHOD				
BHP	Z Factor	P/Z	CUM. GAS		A	B	AB	B^2	A/n	B/n
(psia)			MMCF	∆p= pi - p	(p/z)-pi/zi)/Δp(p/z)					
10984	1.65	6657	0	0						
10156	1.58	6428	482	828	-4.3E-05	0.603	-2.60E-05	0.363	-3.587E-06	0.030
9924	1.56	6362	648	1060	-4.4E-05	0.640	-2.80E-05	0.409	-3.651E-06	0.034
9703	1.54	6301	850	1281	-4.4E-05	0.701	-3.10E-05	0.491	-3.679E-06	0.041
8936	1.49	5997	2505	2048	-5.4E-05	1.358	-7.29E-05	1.843	-4.476E-06	0.154
9222	1.46	6316	2634	1762	-3.1E-05	1.575	-4.82E-05	2.482	-2.550E-06	0.207
8789	1.44	6103	3366	2195	-4.1E-05	1.673	-6.91E-05	2.797	-3.443E-06	0.233
8313	1.39	5981	3957	2671	-4.2E-05	1.649	-6.98E-05	2.719	-3.529E-06	0.227
7064	1.25	5651	5251	3920	-4.5E-05	1.578	-7.16E-05	2.490	-3.783E-06	0.207
6250	1.15	5435	6086	4734	-4.8E-05	1.575	-7.48E-05	2.480	-3.959E-06	0.207
4928	0.96	5133	7608	6056	-4.9E-05	1.629	-7.98E-05	2.654	-4.084E-06	0.221
2723	0.88	3094	10589	8261	-0.00014	2.758	-3.84E-04	7.604	-1.161E-05	0.634

APPENDIX C

Calculation of IGIP for the Cajun reservoir using different MB Techniques

Table C1 – Calculated values of the variables used to obtain G for the Cajun reservoir using Ramagost-Farshad, Roach and Becerra-Arteaga methods

CAJUN PRESSURE-PRODUCTION HISTORY						Ramagost-Farshad	Roach	Becerra-Arteaga	
BHP	Z Factor	P/Z	CUM. GAS		y variable	y-variable	x-variable	Method 1 -- y-variable	Method 2 --OGIP
(psia)			MMSCF	∆p= pi - p	(p/z)(1-ce(Δp)	(1/∆p)((piz/pzi)-1)	(Gp/Δp)(piz/pzi)		
11444	1.496	7650	0	0	7650			7650	
10674	1.438	7423	9920	770	7275	3.97	13.277	7256	192.814
10131	1.397	7252	28620	1313	7006	4.18	22.993	6970	322.323
9253	1.33	6957	53600	2191	6563	4.54	26.899	6494	354.662
8574	1.28	6698	77670	2870	6202	4.95	30.906	6112	386.278
7906	1.23	6428	101420	3538	5840	5.37	34.116	5724	402.842
7380	1.192	6191	120360	4064	5541	5.80	36.593	5410	411.054
6847	1.154	5933	145010	4597	5228	6.29	40.670	5084	432.270
6388	1.122	5693	160630	5056	4949	6.80	42.687	4796	430.551
5827	1.084	5375	187340	5617	4595	7.53	47.463	4435	445.818
5409	1.057	5117	197730	6035	4319	8.20	48.978	4160	433.432
5000	1.033	4840	215660	6444	4034	9.01	52.892	3885	438.214
4500	1.005	4478	235740	6944	3674	10.20	57.999	3541	438.923
4170	0.988	4221	245900	7274	3427	11.17	61.271	3309	433.388

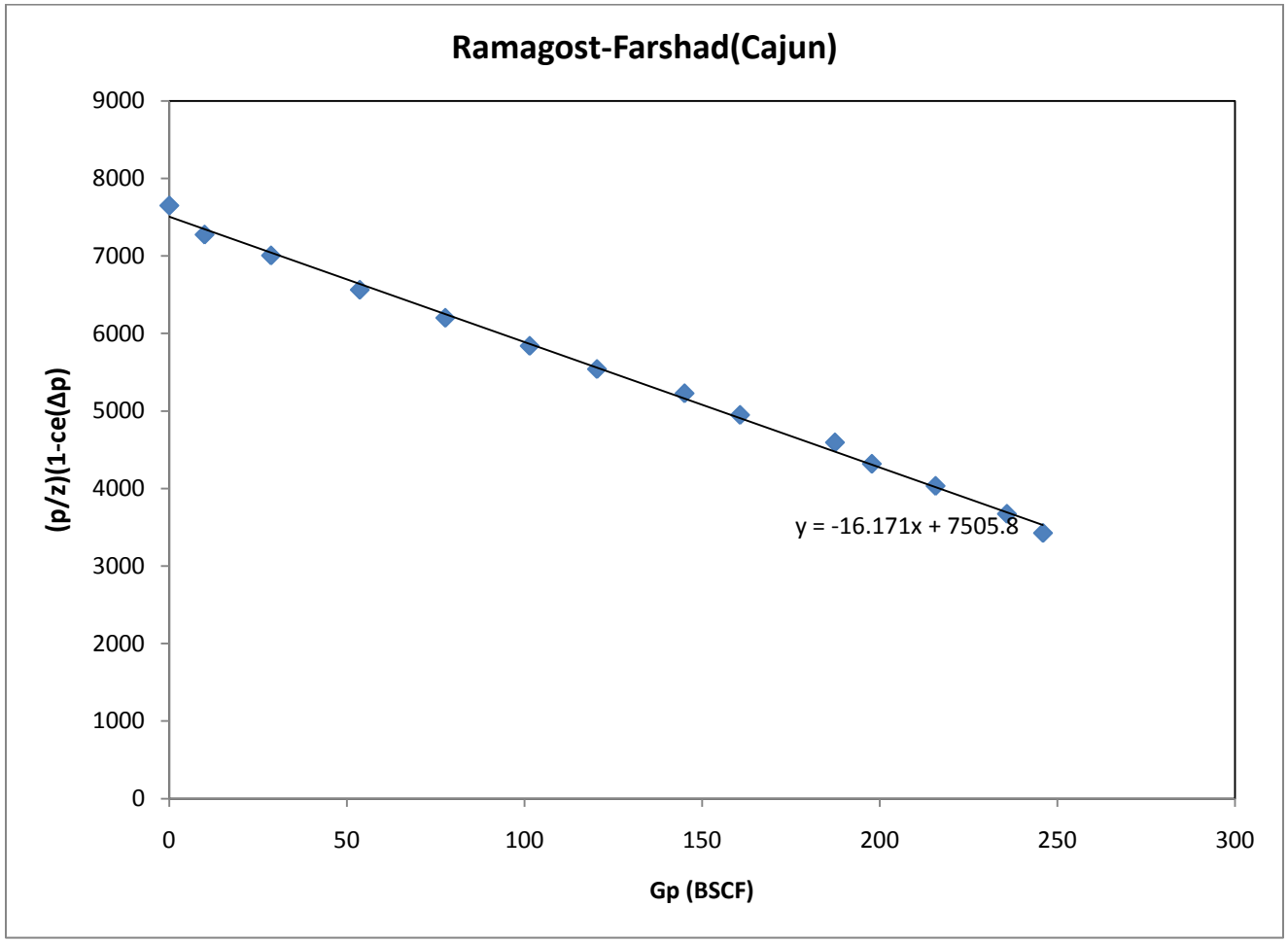

Figure C.1 Ramagost-Farshad's plot for the Cajun reservoir

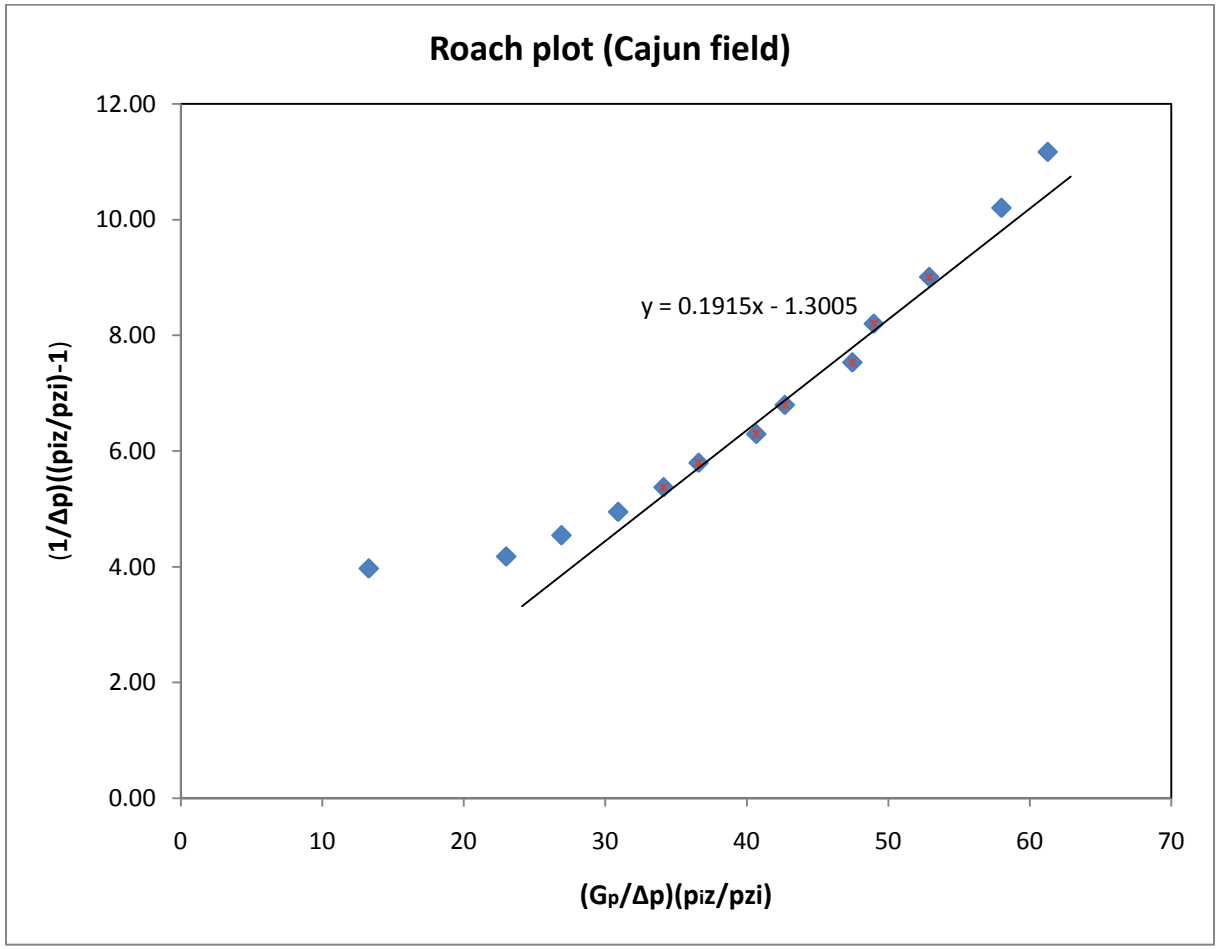

Figure C.2 Roach's plot for the Cajun reservoir

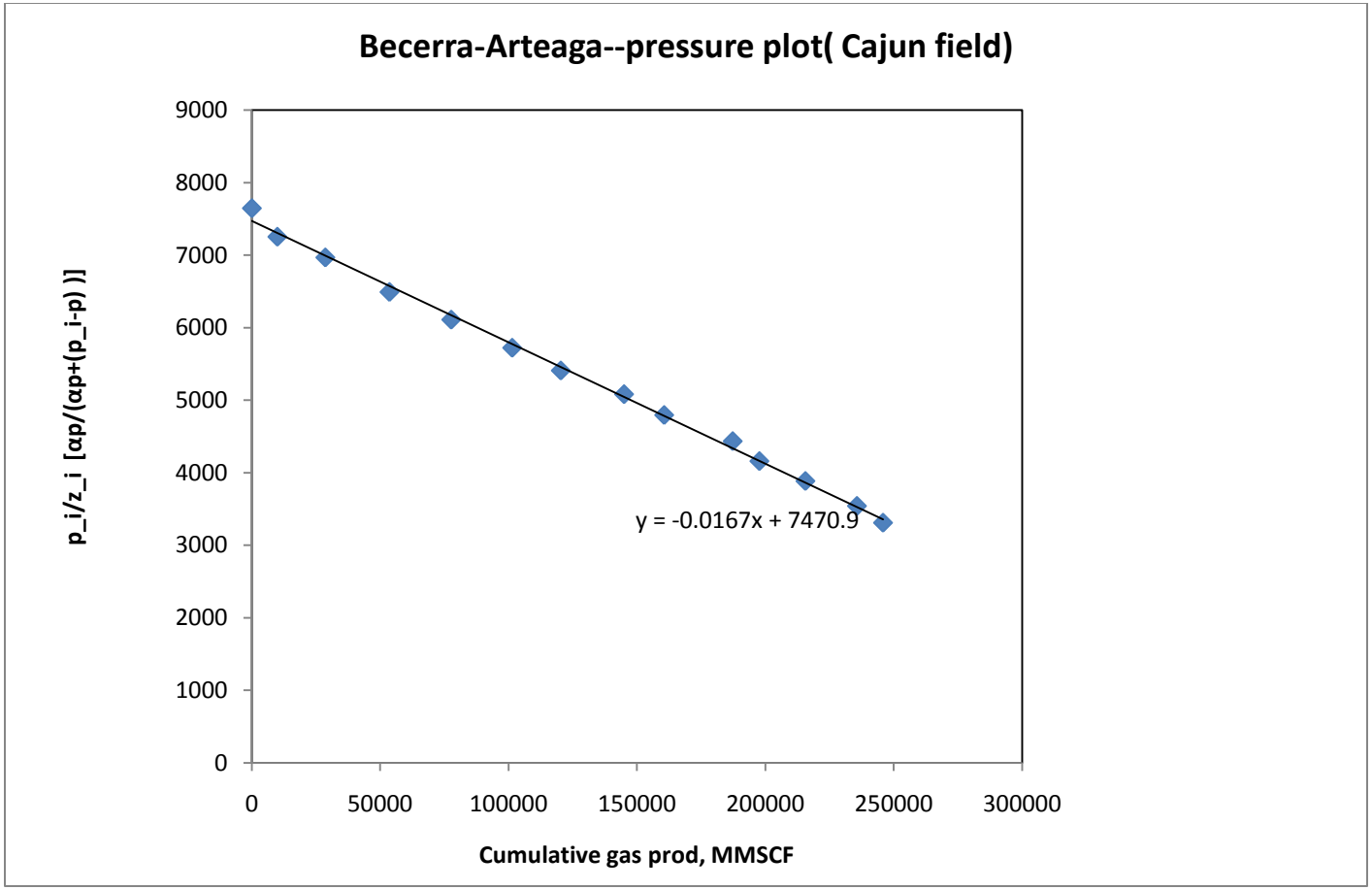

Figure C.3 Becerra-Arteaga's plot for the Cajun reservoir

Table C2 – Calculated values of the variables used to obtain G for the Cajun reservoir using Bernard's method

CAJUN RESERVOIR PRESSURE-PRODUCTION HISTORY					BERNARD'S METHOD					
BHP	Z Factor	P/Z	CUM. GAS		A	B	AB	B^2	A/n	B/n
(psia)			MMCF	∆p= pi - p	(p/z)-pi/zi)/Δp(p/z)					
11444	1.496	7650	0	0						
10674	1.438	7423	10	770	-4E-05	0.013	-5.27E-07	0.000	-2.836E-06	0.00001
10131	1.397	7252	29	1313	-4.2E-05	0.023	-9.61E-07	0.001	-2.984E-06	0.00004
9253	1.33	6957	54	2191	-4.5E-05	0.027	-1.22E-06	0.001	-3.245E-06	0.00005
8574	1.28	6698	78	2870	-4.9E-05	0.031	-1.53E-06	0.001	-3.535E-06	0.00007
7906	1.23	6428	101	3538	-5.4E-05	0.034	-1.83E-06	0.001	-3.839E-06	0.00008
7380	1.192	6191	120	4064	-5.8E-05	0.037	-2.12E-06	0.001	-4.140E-06	0.00010
6847	1.154	5933	145	4597	-6.3E-05	0.041	-2.56E-06	0.002	-4.495E-06	0.00012
6388	1.122	5693	161	5056	-6.8E-05	0.043	-2.90E-06	0.002	-4.854E-06	0.00013
5827	1.084	5375	187	5617	-7.5E-05	0.047	-3.58E-06	0.002	-5.380E-06	0.00016
5409	1.057	5117	198	6035	-8.2E-05	0.049	-4.02E-06	0.002	-5.857E-06	0.00017
5000	1.033	4840	216	6444	-9E-05	0.053	-4.76E-06	0.003	-6.434E-06	0.00020
4500	1.005	4478	236	6944	-0.0001	0.058	-5.92E-06	0.003	-7.287E-06	0.00024
4170	0.988	4221	246	7274	-0.00011	0.061	-6.84E-06	0.004	-7.978E-06	0.00027

APPENDIX D

Calculation of IGIP for the NS2B reservoir using different MB Techniques

Table D1 – Calculated values of the variables used to obtain G for the NS2B reservoir using Ramagost-Farshad, Roach and Becerra-Arteaga methods

NS2B RESERVOIR PRESSURE-PRODUCTION HISTORY						Ramagost-Farshad	Roach		Becerra-Arteaga	
BHP	Z Factor	P/Z	CUM. GAS	CONDENSATE		y variable	y-variable	x-variable	Method 1 -- y-variable	Method 2 --OGIP
(psia)			BSCF	MBBL	$\Delta p = pi - p$	(p/z)(1-ce(Δp)	(1/Δp)((piz/pzi)-1)	(Gp/Δp)(piz/pzi)		
8921	1.473	6056	0		0	6056			6056	
8845	1.465	6038	0.66		76	6022	4.10	0.0087	6026	1972.58
8322	1.4	5944	3.33		599	5821	3.15	0.0057	5810	704.58
7417	1.288	5759	10.4		1504	5458	3.44	0.0073	5411	502.96
6838	1.219	5610	15.59		2083	5204	3.82	0.0081	5136	511.12
6064	1.13	5366	23.97		2857	4834	4.50	0.0095	4742	467.37
5490	1.075	5107	27.85		3431	4498	5.42	0.0096	4428	447.76
4781	0.967	4944	33.7		4140	4233	5.43	0.0100	4013	429.70
4104	0.887	4627	40.1		4817	3853	6.41	0.0109	3583	393.28

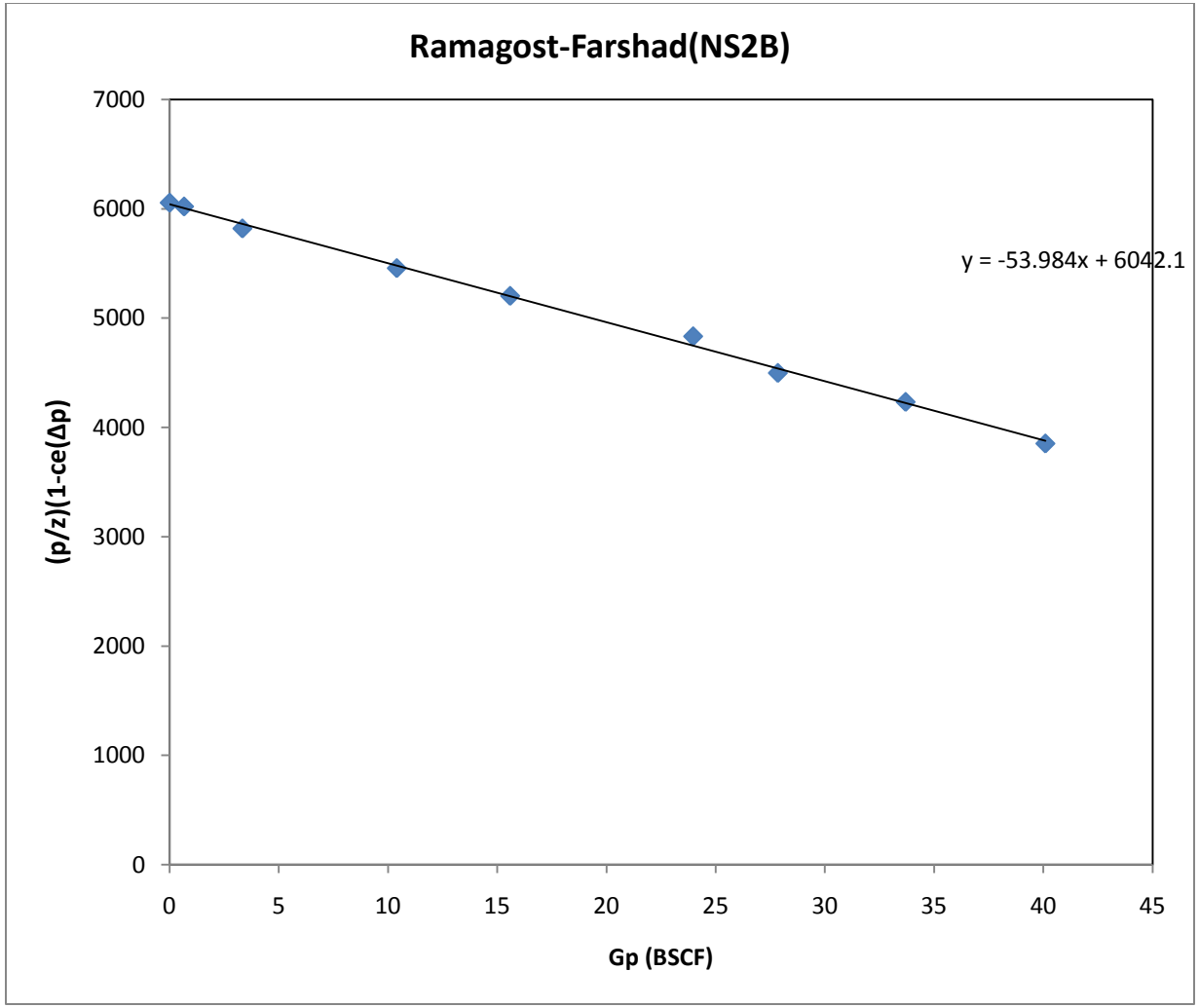

Figure D.1 Ramagost-Farshad's plot for the NS2B reservoir

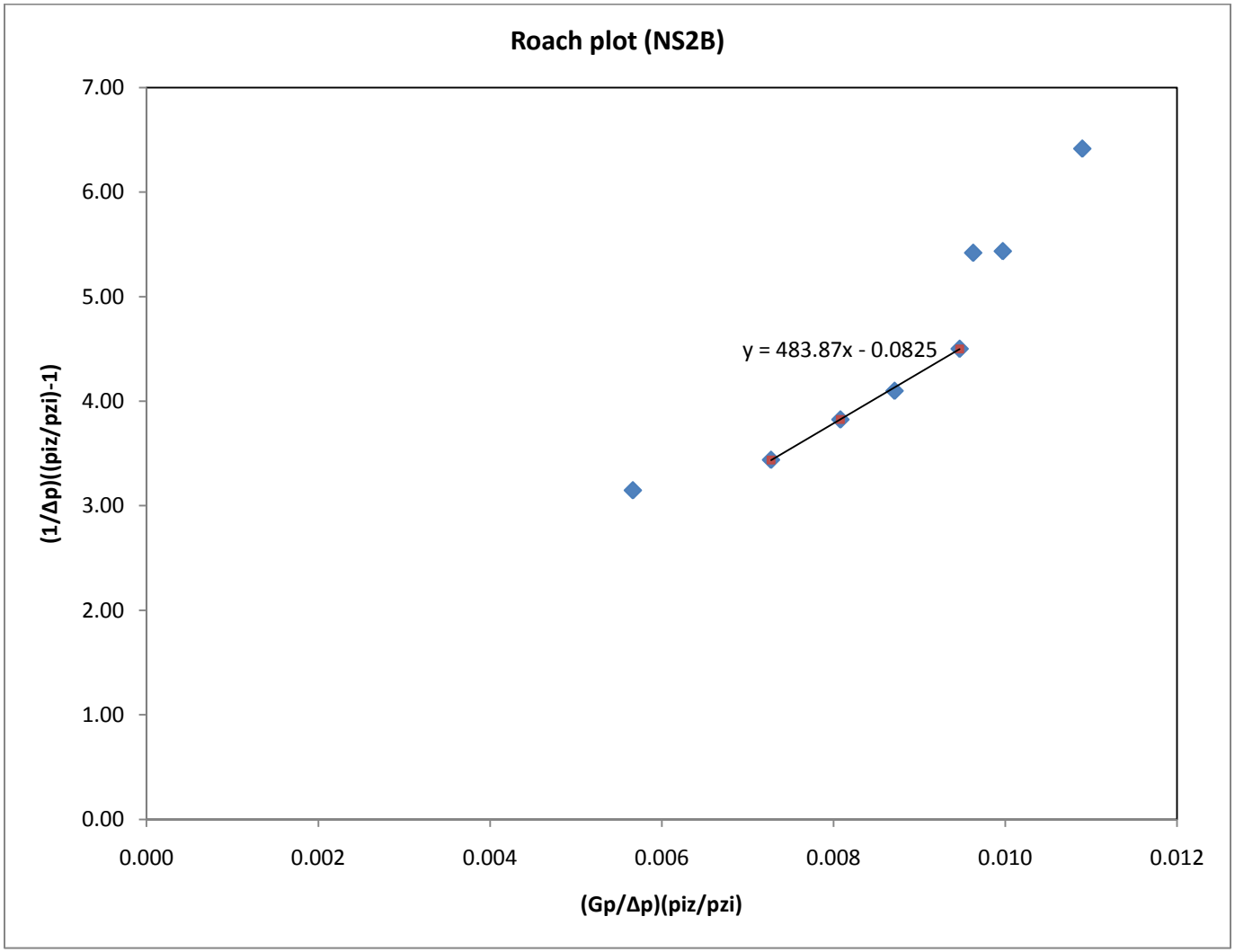

Figure D.2 Roach's plot for the NS2B reservoir

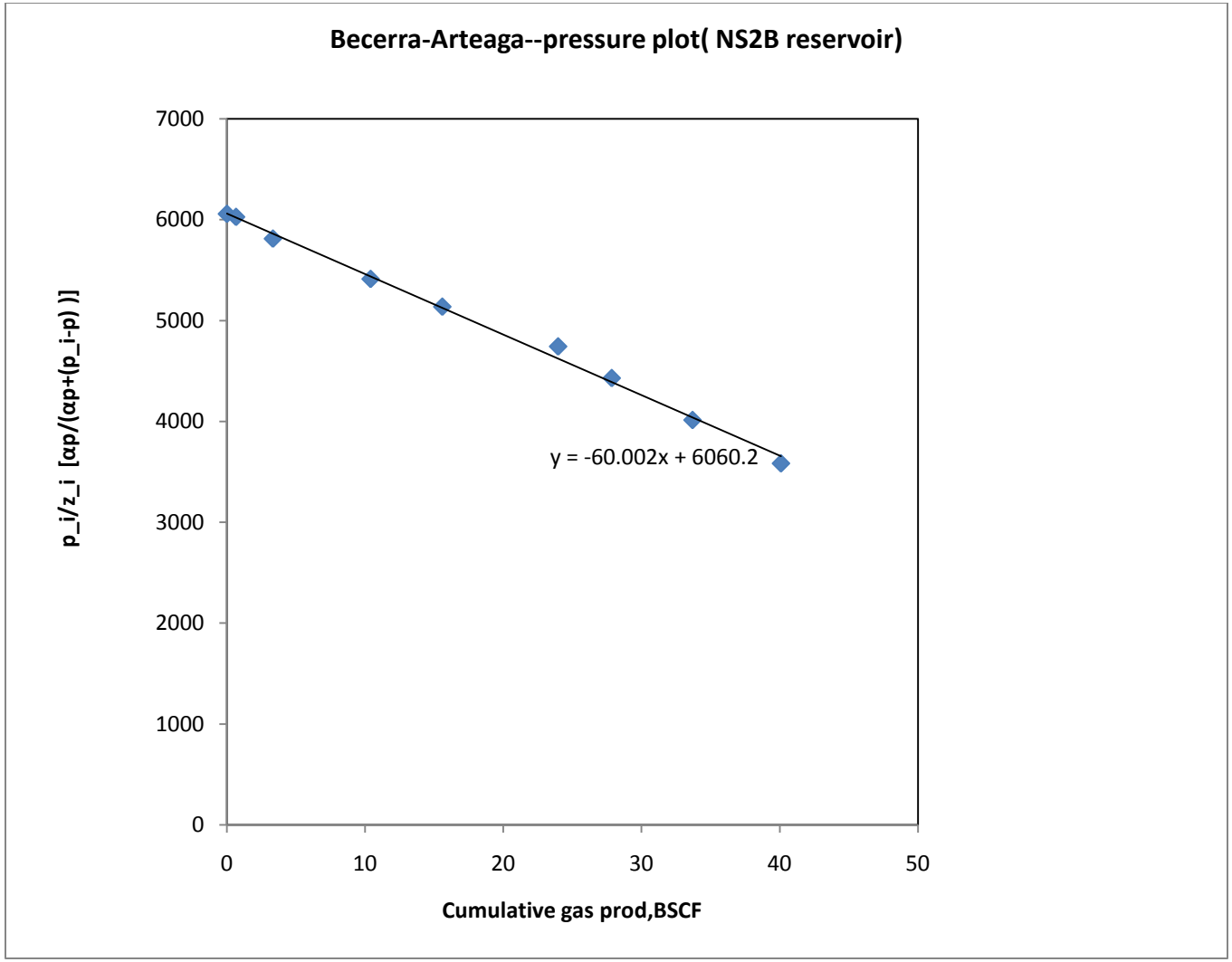

Figure D.3 Becerra-Arteaga's plot for the NS2B reservoir

Table D2 – Calculated values of the variables used to obtain G for the NS2B reservoir using Bernard's method

NS2B RESERVOIR PRESSURE-PRODUCTION HISTORY					BERNARD'S METHOD					
BHP	z Factor	P/Z	CUM. GAS		A	B	AB	B^2	A/n	B/n
(psia)			BSCF	$\Delta p = pi - p$	(p/z)-pi/zi)/Δp(p/z)					
8921	1.473	6056	0	0						
8845	1.465	6038	0.66	76	-4.1E-05	0.009	-3.57E-07	7.59E-05	-4.554E-06	8.43E-06
8322	1.4	5944	3.33	599	-3.1E-05	0.006	-1.78E-07	3.21E-05	-3.497E-06	3.56E-06
7417	1.288	5759	10.4	1504	-3.4E-05	0.007	-2.50E-07	5.29E-05	-3.821E-06	5.88E-06
6838	1.219	5610	15.59	2083	-3.8E-05	0.008	-3.09E-07	6.53E-05	-4.249E-06	7.26E-06
6064	1.13	5366	23.97	2857	-4.5E-05	0.009	-4.26E-07	8.97E-05	-5.000E-06	9.96E-06
5490	1.075	5107	27.85	3431	-5.4E-05	0.010	-5.22E-07	9.27E-05	-6.020E-06	1.03E-05
4781	0.967	4944	33.7	4140	-5.4E-05	0.010	-5.42E-07	9.94E-05	-6.037E-06	1.10E-05
4104	0.887	4627	40.1	4817	-6.4E-05	0.011	-6.99E-07	1.19E-04	-7.127E-06	1.32E-05